

8-28-2012

In vitro cytotoxicity and skin irritation testing of antimicrobial conjugated electrolytes : interactions with mammalian cells

Kristin N. Wilde

Follow this and additional works at: https://digitalrepository.unm.edu/cbe_etds

Recommended Citation

Wilde, Kristin N.. "In vitro cytotoxicity and skin irritation testing of antimicrobial conjugated electrolytes : interactions with mammalian cells." (2012). https://digitalrepository.unm.edu/cbe_etds/17

This Dissertation is brought to you for free and open access by the Engineering ETDs at UNM Digital Repository. It has been accepted for inclusion in Chemical and Biological Engineering ETDs by an authorized administrator of UNM Digital Repository. For more information, please contact disc@unm.edu.

Kristin N. Wilde

Candidate

Chemical and Nuclear Engineering

Department

This dissertation is approved, and it is acceptable in quality and form for publication:

Approved by the Dissertation Committee:

Heather E. Canavan, Chairperson

David G. Whitten

Diane S. Lidke

Deborah G. Evans

**IN VITRO CYTOTOXICITY AND SKIN IRRITATION
TESTING OF ANTIMICROBIAL CONJUGATED
ELECTROLYTES: INTERACTIONS WITH MAMMALIAN
CELLS**

by

KRISTIN N. WILDE

B.S., Chemical and Fuels Engineering, University of Utah, 2001
M.Ch.E., Chemical Engineering, Auburn University, 2007

DISSERTATION

*Submitted in Partial Fulfillment of the
Requirements for the Degree of*

**Doctor of Philosophy
Engineering**

The University of New Mexico
Albuquerque, New Mexico

July, 2012

DEDICATION

to Justin

ACKNOWLEDGMENTS

I would like to give my heartfelt thanks to my committee chair, Prof. Heather E. Canvan, for her ongoing encouragement, patience, and willingness to see me through this process. I would also like to express my sincere gratitude to my committee. Thank you, Prof. David Whitten, for welcoming me into your truly international group. Thank you, Prof. Diane Lidke, for your example of world-class interdisciplinary research. Thank you, Prof. Debi Evans, for showing me that not all experiments occur in a flask or beaker, and encouraging me to try something new. Collectively, you have been to six of the seven continents during your time on my committee.

Without the help of many people, my research would not have been possible. Thank you to Prof. Diane Lidke for your assistance in data collection, specifically your many Tuesday afternoons operating the microscopes. I would like to thank members of the Whitten and Schanze Groups, especially Prof. Liping Ding, Dr. Eunkyung Ji, Dr. Katsu Ogawa, Dr. Anand Parthasarath, Dr. Yanli Tang, Ying Wang, and Dr. Zhijun Zhou, for synthesizing test compounds and providing powders and solutions on request. Thank you to Kirsten Cicotte for making the electrospun mats, and Prof. Tom Corbitt for cutting them to size.

I would like to thank the entire Canavan Group, past and present, for helpful discussions and constructive criticism. I would specifically like to thank Dr. Jamie Reed for her support and encouragement during her last year at UNM and since. You are an inspiration to me, and many others. Thank you also to Marta Cooperstein, my lunchtime running partner, for your patience and encouragement during my final year at UNM. I would also like to thank several undergraduates (some now graduates, with their own students) for their work on specific projects related to my research: Daniel Cox, Blake Bluestein, and KaLia Burnette. I would also like to thank the entire Whitten Group for their support.

I am very grateful to Prof. Tom Corbitt, Prof. Linnea Ista, and Dr. Patrick Burton for providing extra motivation and encouragement these last few months. Thank you to Dr. Jamie Reed, Alex Leonard, and Blake Bluestein for reading various drafts of my work. Thank you to the UNM Graduate Resource Center, especially Anna Cabrera, for providing well-organized boot camps that were instrumental in getting my dissertation written. Thank you to my friends, lab neighbors, and fellow students in the Center for Biomedical Engineering, the Department of Chemical and Nuclear Engineering, and the Nanoscience and Microsystems Program for your support, especially Dr. Akinbayowa Falase, Ulises Martinez, Kirsten Cicotte, Alex Leonard, Matt Rush, and Kevin Cushing.

I would like to acknowledge the following individuals for teaching me how to use specific equipment or perform certain techniques: Dr. Jamie Reed (tissue culture), Adrienne Lucero (goniometer, plasma reactor), Mary Anne Raymond-Stintz (TEM), Rachel Grattan (antibody labeling on coverslips), Ulises Martinez and Dr. Akinbayowa Falase (epifluorescent microscopy), Anne Hellebust

(live/dead assay), Marta Cooperstein (MTS assay), Ying Wang (plate reader), Prof. Linnea Ista (confocal microscopy), Travis Woods and Prof. Tom Corbitt (flow cytometry), and Prof. Jim Freyer (Coulter counter).

I would like to acknowledge the funding that made this work possible: the U.S. National Science Foundation (NSF) Partnerships for Research and Education in Materials (UNM/Harvard PREM, DMR-0611616), the NSF Integrative Graduate Education and Research Traineeship (IGERT) in Nanoscience and Microsystems (DGE-0504276), the U.S. Defense Threat Reduction Agency, the New Mexico Spatiotemporal Modeling Center (P50GMO852673, for support of Prof. Diane Lidke), and the NSF Research Experience for Undergraduates in Nanoscience and Microsystems (DMR-1005217, for support of Daniel Cox and KaLia Burnette).

I would like to especially thank the principal investigators for the PREM and IGERT grants: Prof. Gabriel Lopez, Prof. Julia Fulghum, Prof. Heather Canavan, Prof. Dimiter Petsev, and Prof. Elizabeth Hedberg-Dirk (PREM); and Prof. Abhaya Datye (IGERT). Thank you to Isela Roeder and Heather Armstrong for your help with graduate assistantships and travel. I would also like to thank Prof. Tim Ward (Department Chair), Cheryl Brozena, Jocelyn White, Geoff Courtin, and Ken Carpenter of the UNM Chemical and Nuclear Engineering Department for keeping things running smoothly in the department. Thank you to Stephanie Sanchez and Anne Trabaldo of the Center for Biomedical Engineering for keeping things running smoothly in the center (Who knew you could receive skin via FedEx?).

Last but not least, I would like to thank my family and friends for their love and support. Thank you Dr. Justin Wilde, my loving husband, who knew firsthand the hurdles I would face in pursuing a PhD and encouraged me to be stubborn. Thank you to my parents, who always encourage me to pursue my dreams and taught me to eat an elephant one bite at a time. I would like to thank my brother, my grandparents, and my Wilde family for their love.

Thank you to Dr. Terry Ring at the University of Utah for instilling my love of research and encouraging me to pursue graduate school. Thank you to all my friends, especially those in Utah and New Mexico, for your support. Thank you to the best neighbors ever, the Greenfelders, for countless shared meals, computer tech support, and crayon drawings.

**IN VITRO CYTOTOXICITY AND SKIN IRRITATION TESTING OF
ANTIMICROBIAL CONJUGATED ELECTROLYTES:
INTERACTIONS WITH MAMMALIAN CELLS**

by

Kristin N. Wilde

B.S., Chemical and Fuels Engineering, University of Utah, 2001

M.Ch.E., Chemical Engineering, Auburn University, 2007

Ph. D., Engineering, University of New Mexico, 2012

ABSTRACT

An estimated 19,000 deaths and \$3-4 billion in health care costs per year in the U.S. are attributed to methicillin-resistant *Staphylococcus aureus* (MRSA) infections. Certain cationic phenylene ethynylene (CPE)-based polymers (PPEs) and oligomers (OPEs) have been demonstrated to exhibit dark and light-activated antimicrobial activity. Envisioned applications of these CPEs include the fabrication of antimicrobial surfaces to reduce or prevent the spread of potentially untreatable strains of bacteria.

Until recently, it was unknown if the polymers or oligomers would exhibit similar biocidal activity toward mammalian cells. This work examines the toxicity of CPEs to mammalian cells at three levels: cytotoxicity testing of cell monolayers, skin irritation testing of tissues, and intracellular co-localization. Eight CPEs, two PPEs and six OPEs, were selected for these studies based on biocidal activity and diversity of repeat unit number and functional groups.

In the cytotoxicity studies, two cell types were exposed to eight CPEs at concentrations from 1-100 µg/mL for 24 hours. As expected, concentration plays the largest role in determining viability. At intermediate concentrations (~5-10 µg/mL), the interplay between light and the light-activated compounds is very important.

To mimic skin exposure in vitro, eight CPEs and two types of electrospun mats were selected for skin irritation testing using tissues derived from human epidermal keratinocytes. PPE-DABCO and PPE-Th were non-irritants up to the highest tested concentrations, 924 µg/mL and 100 µg/mL, respectively. The lack of skin irritation for all substances, as measured by two endpoints, alleviates initial safety concerns for products based on these polymers and oligomers, both in solution and as electrospun mats.

In the localization studies, three compounds (one polymer and two oligomers) were included in growth media above epithelial cell monolayers for 1-4 hours, stained to localize the nearest membrane or organelle, and viewed using fluorescence microscopy. The three compounds were successfully localized to two distinct locations within the cell, indicating that at least two modes of action are possible for these compounds. In all cases, the addition of light changed the effects of the compounds on the mammalian cells. The modes of action of these compounds appear to be governed primarily by length.

For applications below cytotoxic concentrations, these compounds are safe for mammalian cells. The concentrations at which the longer S-OPEs and the DABCO-containing compounds are cytotoxic are much higher than for the

shortest S-OPE, PPE-Th, and the remaining two EO-OPEs, thus these compounds have the widest range of concentrations available for potential applications. Although the more aggressive EO-OPEs may find limited applicability for antimicrobial agents, they may find promise for other applications, such as live-cell imaging, intracellular drug delivery, and as anti-cancer agents.

TABLE OF CONTENTS

CHAPTER 1	1
1.1 Introduction	1
1.2 Background and Literature Review.....	2
1.2.1 <i>Novel biocides</i>	<i>2</i>
1.2.2 <i>Biophysical studies of novel biocides</i>	<i>6</i>
1.2.3 <i>Phenylene ethynylenes.....</i>	<i>7</i>
1.2.4 <i>Biocidal activity of phenylene ethynylenes</i>	<i>11</i>
1.4 Research Goals	13
CHAPTER 2 – CYTOTOXICITY TESTING.....	17
2.1 Introduction	17
2.2 Materials and Methods.....	19
2.2.1 <i>Routine cell culture.....</i>	<i>19</i>
2.2.2 <i>Cell culture for MTS assay</i>	<i>19</i>
2.2.3 <i>Cell treatment with polymer/oligomer solutions</i>	<i>19</i>
2.2.4 <i>Light exposure</i>	<i>20</i>
2.2.5 <i>MTS assay.....</i>	<i>21</i>
2.3 Results and Discussion.....	21
2.3.1 <i>Effect of concentration on viability</i>	<i>21</i>
2.3.2 <i>Effect of light on viability</i>	<i>24</i>
2.3.3 <i>Comparison between cell types.....</i>	<i>25</i>
2.3.4 <i>Comparison among individual compounds</i>	<i>29</i>
2.3.5 <i>Comparison among families based on chemical structure.....</i>	<i>31</i>
2.4 Summary	36
CHAPTER 3 - SKIN IRRITATION TESTING	38
3.1 Introduction	38
3.1.1 <i>Background.....</i>	<i>38</i>
3.1.2 <i>Description of test methods.....</i>	<i>39</i>
3.1.3 <i>Description of test system.....</i>	<i>42</i>
3.2 Materials and Methods.....	45

3.2.1	<i>Sample preparation</i>	45
3.2.2	<i>Skin irritation test</i>	47
3.2.3	<i>Cytokine analysis</i>	52
3.3	Results and Discussion	54
3.3.1	<i>Skin irritation criteria</i>	54
3.3.2	<i>MTT assay</i>	54
3.3.3	<i>Cytokine assay</i>	60
3.4	Summary	64
	CHAPTER 4 – INTRACELLULAR LOCALIZATION	66
4.1	Introduction	66
4.2	Materials and Methods	70
4.2.1	<i>Cell culture</i>	70
4.2.2	<i>Cell treatment with polymer/oligomer solutions</i>	70
4.2.3	<i>Cell staining</i>	71
4.2.4	<i>Microscopy</i>	71
4.3	Results and Discussion	73
4.3.1	<i>Co-localization of polymer and plasma membrane</i>	73
4.3.2	<i>Co-localization of oligomers and endoplasmic reticulum</i>	77
4.3.3	<i>Comparison of different cell types</i>	80
4.4	Summary	82
	CHAPTER 5 – CONCLUSIONS AND FUTURE DIRECTIONS	84
5.1	Conclusions	84
5.1.1	<i>Review of experimental methods</i>	84
5.1.2	<i>Conclusions from cytotoxicity testing of cell monolayers</i>	85
5.1.3	<i>Conclusions from skin irritation testing of tissues</i>	86
5.1.4	<i>Conclusions from intracellular co-localization studies</i>	87
5.2	Future Directions	88
5.2.1	<i>Refining the mode of action</i>	88
5.2.2	<i>Product safety</i>	92
5.2.3	<i>New application</i>	95
	APPENDIX	97

A.1	Terminology	97
A.2	Development of Antibiotics	97
A.3	Antibiotic Resistance	99
A.4	Conventional Biocides	101
A.5	Preliminary Results	106
A.6	Interference with MTT Assay.....	107
A.7	MTT Assay Acceptance Criteria	109
	REFERENCES	111

CHAPTER 1

1.1 Introduction

An estimated 19,000 deaths and \$3-4 billion in health care costs per year in the U.S. are attributed to methicillin-resistant *Staphylococcus aureus* (MRSA) infections.¹ Antibiotic resistance is not only a problem in developed countries. Multidrug-resistant *Mycobacterium tuberculosis* is on the rise in developing countries, and infection from this bacterium requires two years of treatment with antibiotics.¹ *Clostridium difficile* and vancomycin-resistant enterococci also are of clinical importance.² Though less common, multidrug-resistant strains of Gram-negative bacteria such as *Acinetobacter baumannii*, *Escherichia coli*, *Klebsiella pneumonia*, and *Pseudomonas aeruginosa* also exist. These strains are particularly problematic because the outer membrane of Gram-negative bacteria poses a challenge to developing new antibiotics for these bacteria.³ Figure 1 illustrates the fundamental differences between Gram-positive and Gram-negative bacteria. Refer to Sections A.1 - A.3 for helpful terminology and information about the development of antibiotics and antibiotic resistance.

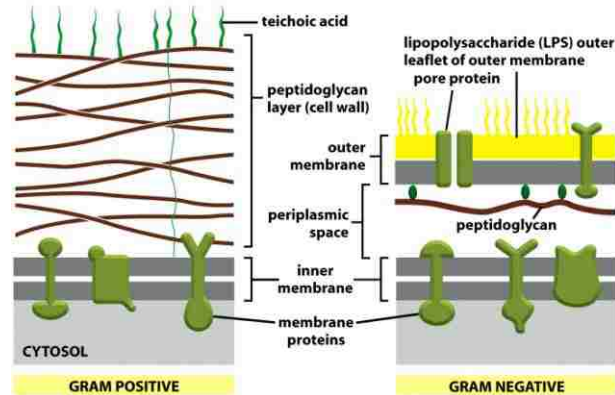


Figure 1-1. Comparison of the outer layers of Gram-positive and Gram-negative bacteria (from Alberts 2008). Gram-positive bacteria have a thick peptidoglycan layer above an inner membrane. Gram-negative bacteria have two sets of lipid bilayers separated by a much thinner peptidoglycan layer.

In a clinical setting, individuals with bacterial infections are likely to contact a wide variety of surfaces; therefore, making these surfaces antimicrobial would reduce or prevent the spread of potentially untreatable strains of bacteria. Although a number of sterilization techniques are already in place in any modern hospital (refer to Section A.4 for details), these techniques are not applicable to all surfaces, and require vigilance on the part of medical and support staff to maintain sterility.

1.2 Background and Literature Review

1.2.1 *Novel biocides*

Antimicrobial peptides, also called host-defense peptides, were first discovered by Zasloff in 1987 in the skin of an African frog⁴ and represent an important parallel research area in terms of methods of study and proposed mechanisms of action. These natural polymers are generally short peptides (10-50 amino acids), have a net positive charge (+2 to +9), and have a significant

($\geq 30\%$) fraction of residues that are hydrophobic.⁵ Antimicrobial peptides are found in a wide variety of organisms (e.g. bacteria, insects, plants, and vertebrates), and constitute a defense against environmental microbes in organisms lacking a more specific antibody-based response.⁶⁻⁷ As of 2004, 895 antimicrobial peptides had been identified in eukaryotes alone.⁸

In an effort to increase the stability of these antimicrobial peptides while retaining their biocidal activity, a number of peptidomimetics have been developed, including α -peptides, β -peptides, peptoids (oligo-*N*-substituted glycines), and cyclic peptides. See Table 1-1 for a summary of structures and research groups working on these peptidomimetics and other novel biocides. A common strategy for making peptidomimetics is to replace naturally-occurring L enantiomers with D enantiomers.⁵ Like natural peptides, synthetic α -peptides have a helical conformation and β -peptides have a sheet conformation.

The so-called ‘facially-amphiphilic’ polymers and oligomers have only one feature of the antimicrobial peptides, yet retain their biocidal action.⁹⁻¹⁰ Many antimicrobial peptides have both hydrophobic and hydrophilic regions within one repeat unit, where the hydrophobic region tends to become soluble in the hydrophobic tails of the phospholipid bilayer. See Figure 1-2 for an illustration of distinct hydrophobic and hydrophilic regions on two representative AMPs. This amphiphilicity imparts membrane permeability to the peptide. Facially-amphiphilic arylamide oligomers, phenylene ethylenes, polynorbornenes, and polymethacrylates have been produced (refer to Table 1-1 for structures). As will

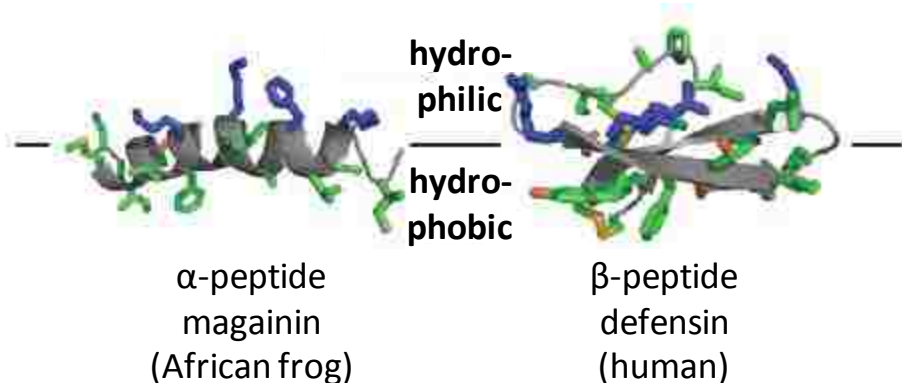
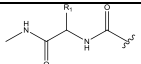
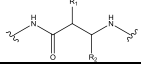
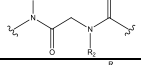
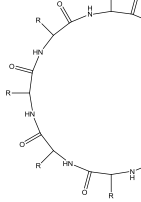
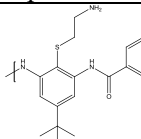
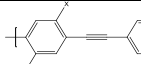
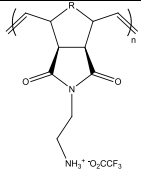
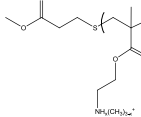
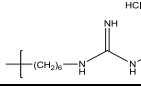
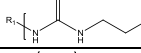
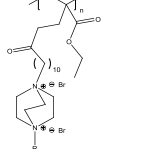


Figure 1-2. Illustration of facially-amphiphilic antimicrobial peptides magainin and defensin (adapted from Tew 2010). Hydrophilic residues lie above an imaginary plane through the peptides, and hydrophobic residues lie below the plane.

be discussed in greater detail in Section 1.2.2, the phenylene ethynylene polymers and oligomers produced by the Whitten and Schanze Groups are facially-symmetric rather than facially-amphiphilic. However, the Tew Group has synthesized and tested a number of facially-amphiphilic phenylene ethynylenes¹¹⁻¹⁹ which may provide data upon which assumptions about the Whitten and Schanze polymers and oligomers can be based.

The last category of novel biocides to be discussed here is cationic polymers. These polymers are not based on peptides at all, but rely on functional groups common to or similar to conventional disinfectants. Polymers with biguanides, oligoguanidines, and polymers with quaternary ammoniums fall into this category. The polymer backbone is believed to aid in the orientation of these functional groups relative to the phospholipid bilayer. The cationic polymers are attracted to bacterial cell membranes, which have a net negative charge.

Table 1-1. Antimicrobial macromolecules, categorized by chemical structure (adapted from Gabriel 2007).

Chemical structure	Example(s)	Research Group(s)
<i>Antimicrobial peptidomimetics</i>		
α -peptides		Shai, ²⁰ Zasloff ²¹
β -peptides		DeGrado, ²² Gellman, ²³ Seebach ²⁴
Peptoids (oligo-N-substituted glycines)		Barron, ²⁵ Winter ²⁶
Cyclic peptides		Ghadiri ²⁷
<i>Facially amphiphilic antimicrobial polymers and oligomers</i>		
Arylamide oligomers and analogs		DeGrado ²⁸
Phenylene ethynylenes		Whitten and Schanze, ²⁹⁻³⁴ Tew ^{11-12, 14}
Polynorbornenes		Tew ³⁵
Polymethacrylates		DeGrado ³⁶
<i>Biocidal cationic polymers</i>		
Polymers with biguanides		Tazuke, ³⁷ Zhang ³⁸
Oligoguanidines		Honig ³⁹
Polymers containing quaternary ammoniums		Mathias ⁴⁰

1.2.2 Biophysical studies of novel biocides

A 2007 review by Gabriel and co-workers⁴¹ provides a top-level overview of biophysical studies of the novel biocides discussed in Section 1.2.1. As shown in Table 1-2 below, very little mammalian tissue culture work has been done. Instead, research tends to focus on either simple (i.e. membranes and red blood cells) or complex (e.g. in vivo toxicity) studies. The in vivo studies include toxicity testing as a pre-cursor for efficacy studies. Several peptidomimetics have undergone clinical trials, with only four reaching Phase 3 clinical efficacy trials – namely PexigananTM, IsegananTM, NeuprexTM, and OmigananTM.⁵ These four peptidomimetics are derived from antimicrobial peptides found in frogs, pigs, humans, and cattle, respectively.

Table 1-2. Biophysical techniques used to study interactions between novel biocides and membranes, cells, tissues, and animals (adapted from ⁴¹).

Technique	Biocide(s)
Spectroscopy (i.e. solid-state NMR, vibrational spectroscopy, circular dichroism, fluorescence, neutron reflection, ATR/FTIR)	cyclic peptides
	arylamide oligomers and analogs
X-ray (i.e. GIXD, SAXS)	<i>phenylene ethynylenes</i>
Calorimetry (i.e. ITC, DSC)	β -peptides
	polymers with biguanides
Vesicle leakage and flip-flop assays (membranes)	β -peptides
	cyclic peptides
	<i>phenylene ethynylenes</i>
Hemolysis assays (cells)	peptoids
	cyclic peptides
	<i>phenylene ethynylenes</i>
	polynorbornenes
<i>In vitro cytotoxicity (tissues)</i>	<i>phenylene ethynylenes</i>
In vivo toxicity (animals)	α -peptides
	β -peptides
	peptoids
	cyclic peptides
<i>Microscopy</i> (i.e. AFM, SEM, TEM, confocal, fluorescence)	β -peptides
	polymethacrylates

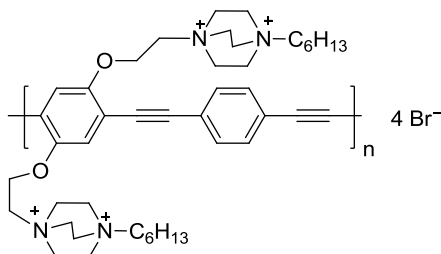
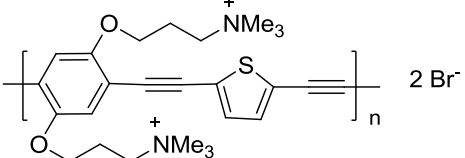
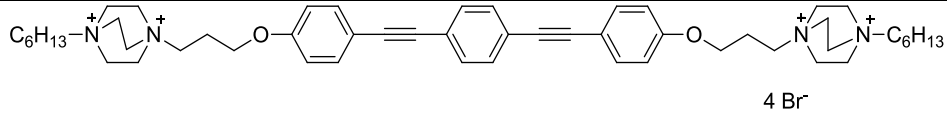
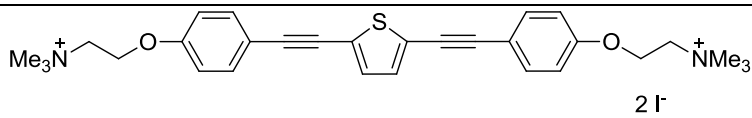
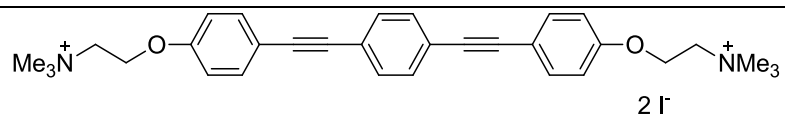
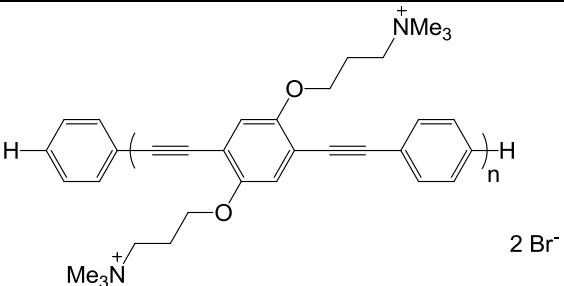
AFM, atomic force microscopy; ATR, attenuated total reflection; DSC, differential scanning calorimetry; FTIR, Fourier transform infrared spectroscopy; GIXD, grazing incidence X-ray diffraction; ITC, isothermal titration calorimetry; SEM, scanning electron microscopy TEM, transmission electron microscopy.

1.2.3 *Phenylene ethynylenes*

In collaboration with the Schanze Group at the University of Florida, the Whitten Group at the University of New Mexico synthesizes, characterizes, and develops applications for conjugated phenylene ethynylene (CPE)-based polymers and oligomers.^{30-34, 42-58} For a recent review of the group's work, see Ji et al.⁵⁹ All of these polymers and oligomers are conjugated electrolytes, i.e., they have double or triple bonds separated by a single bond, and form ions in solution. All are fluorescent and soluble in water to some extent. Specific structures of the polymers and oligomers to be discussed in this work are presented in Table 1-3 below.

The oligomers can be divided into three families: the oligomeric phenylene ethynylenes (OPEs), the symmetric oligomeric phenylene ethynylenes (S-OPEs), and the end-only oligomeric phenylene ethynylenes (EO-OPEs). The oligomers are chemically similar to PPEs, but have fewer repeat units (usually $n < 10$). OPEs have a carboxyester headgroup, a phenyl tailgroup, and quaternary ammonium pendant side chains. S-OPEs are similar to OPEs, but are symmetric in that they have the same group for both the headgroup and the tailgroup. S-OPEs synthesized to date include those with H, COO-, and COOEt end groups. EO-OPEs are symmetric like the S-OPEs, but lack side chains and have cationic end groups instead.

Table 1-3. Chemical structures of phenylene ethynylene polymers and oligomers, categorized by family.

Family	Structure	#	Name
PPEs		1	PPE-DABCO
		2	PPE-Th
EO-OPEs		3	EO-OPE-1-DABCO
		4	EO-OPE-1-Th
		5	EO-OPE-1-C ₂
S-OPEs		6-8	S-OPE-n(H) 6: n = 1 7: n = 2 8: n = 3

PPEs = Poly(phenylene ethynylene)s

EO-OPEs = End-Only Oligo(phenylene ethynylene)s

S-OPEs = Symmetric Oligo(phenylene ethynylene)s

DABCO = 1,4-diazabicyclo[2.2.2]octane; Me = methyl group, CH₃; Th = thiophene

The aromatic component of the repeat units of the polymers and oligomers may be exclusively phenyl rings, or, alternately, a thiophene may be substituted for a phenyl ring. Thiophene substitutions, end groups, and pendant side chains give each phenylene ethynylene-based compound its unique character. If a polymer or oligomer has two phenyl rings in its repeat unit, the second phenyl ring may or may not have a pendant side chain. Key features of the eight compounds discussed in this work are summarized in Table 1-4 below.

Table 1-4. Comparison of chemical structures among compounds.

Compound	n	Side chain	End group	Linker	Thiophene?
PPE-DABCO	---	DABCO	H	C2	no
PPE-Th	---	NMe ₃	H	C3	yes
S-OPE-1(H)	1	NMe ₃	H	C3	no
S-OPE-2(H)	2	NMe ₃	H	C3	no
S-OPE-3(H)	3	NMe ₃	H	C3	no
EO-OPE-1-DABCO	1	N/A	DABCO	C3	no
EO-OPE-1-Th	1	N/A	NMe ₃	C2	yes
EO-OPE-1-C2	1	N/A	NMe ₃	C2	no

The chemical and photophysical properties of the PPEs, S-OPEs, and some of the EO-OPEs are relatively well characterized.^{31, 34, 46} Characterization is underway for the remainder of the recently-synthesized EO-OPEs. As shown in Table 1-5, PPEs absorb light in the visible region of the electromagnetic spectrum, while EO-OPEs and S-OPEs absorb light in the ultraviolet region of the spectrum.

Table 1-5. Absorption and fluorescence maxima of CPE-based compounds in this work.

Compound	$\lambda_{\max}^{\text{abs}}$ (nm) in MeOH	$\lambda_{\max}^{\text{fl}}$ (nm) in MeOH	$\lambda_{\max}^{\text{abs}}$ (nm) in H ₂ O	$\lambda_{\max}^{\text{fl}}$ (nm) in H ₂ O
PPE-DABCO	422	441	394	436
PPE-Th	422	475, 502	432	475, 502
EO-OPE-1-DABCO	---	---	---	---
EO-OPE-1-Th(C2)	355*	390*	---	---
EO-OPE-1-C2	326	355	---	---
S-OPE-1(H)	302, 348	392	303, 348	398
S-OPE-2(H)	318, 374	420	318, 370	454
S-OPE-3(H)	320, 384	432	320, 380	438

*These maxima are for a closely related compound, EO-OPE-1-Th(C3).

All of the phenylene ethynylenes discussed so far have been *para*-phenylene ethynylenes – that is, the two substituents are positioned directly opposite each other on the benzene ring. However, a summary of phenylene ethynylenes would not be complete without a brief discussion of the *meta*-phenylene ethynylenes. The Tew Group at the University of Massachusetts has synthesized and extensively tested *m*-phenylene ethynylenes.¹¹⁻¹⁹ The Tew Group has also studied one *p*-phenylene ethynylene.¹¹

1.2.4 Biocidal activity of phenylene ethynylenes

Previous research has demonstrated that PPEs have light-activated biocidal activity against Gram-positive *Bacillus anthracis* spores and *Bacillus atrophaeus* and Gram-negative *Escherichia coli*, *Cobetia marina* (a marine bacterium), and *Pseudomonas aeruginosa* strain PAO1 (a model pathogen).^{42, 44-45, 57} Light-activated biocidal activity has been observed for OPEs, S-OPEs, and EO-OPEs against *Staphylococcus aureus*, *Staphylococcus epidermidis*, and *E. coli*.^{31, 52} Representative data for four oligomers against *S. aureus* are presented in Table 1-6 below. It is worth noting that the oligomer concentration for the

light-activated biocidal activity shown in Table 1-7 is at least 400 times less than that for the dark activity (0.01 vs. 4-5 $\mu\text{g}/\text{mL}$). In general, the CPE-based polymers and oligomers are activated by visible and UV light, respectively, which corresponds to their wavelengths of maximum absorption (refer to Table 1-5 above).

Table 1-6. Biocidal activity (percentage dead) of select oligomers against *S. aureus*. (Zhou 2010 and Tang 2011)

Oligomer	30 minutes		60 minutes	
	dark [†]	light [‡]	dark [†]	light [‡]
EO-OPE-1(C2)	17	38.7	38.8	93.1
S-OPE-1(H)	7.71	32.15	11.88	68.66
S-OPE-2(H)	22.36	13.35	13.89	38.47
S-OPE-3(H)	37.64	19.18	51.92	33.63

[†]4-5 $\mu\text{g}/\text{mL}$, [‡]0.01 $\mu\text{g}/\text{mL}$

The proposed biocidal mechanism involves: a) adsorption of the cationic CPE to the negatively-charged surface of the bacterial membrane; b) irradiation of the polymer, which causes singlet oxygen production at the CPE/membrane interface; and c) bacterial death due to the presence of the singlet oxygen or subsequently-produced reactive oxygen species.⁵⁹ This mechanism is depicted in Figure 1-3 below. This light-activated biocidal activity is correlated to aerobic conditions (e.g. presence of oxygen).⁴⁴ Singlet oxygen is known to kill bacterial and mammalian cells.⁶⁰⁻⁶² The proposed mechanism may have a dark (light-independent) component as well. For example, a thiophene-containing PPE exhibits dark biocidal activity and a diazabicyclooctane (DABCO)-containing PPE demonstrates strong light-activated biocidal activity.⁴⁷ Studies of these two polymers in model bacterial membrane systems – including liposomes, bilayer-

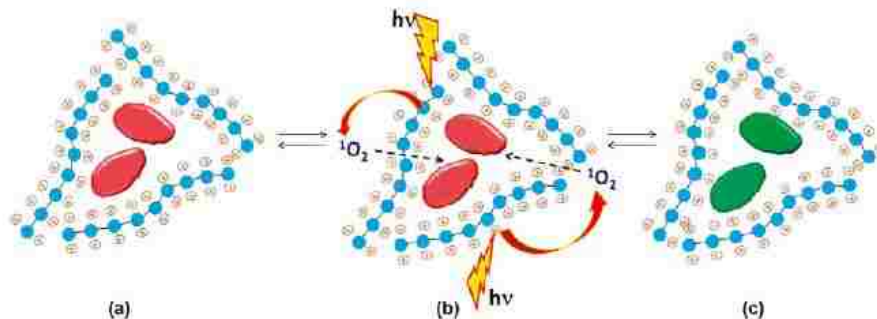


Figure 1-3. Proposed mechanism of biocidal action: (a) The cationic CPE adsorbs to the bacterial membrane, (b) irradiation of the CPE produces singlet oxygen at the CPE/membrane interface, and (c) singlet oxygen or subsequently-produced reactive oxygen species kill bacteria. (Ji et al. 2011) Live bacteria are shown in red, and dead bacteria are green.

coated microspheres, and monolayers at an air-water interface – suggest that both PPEs associate with the lipid membrane, but incorporate into the membrane to different extents.⁴⁷ Additional studies of these two polymers, and ten other phenylene ethynylene compounds, with liposomes verified disruption of bacterial membrane mimics (DOPG/DOPE 20/80) with ten of the twelve compounds.⁵⁰ The compounds that did not disrupt the bacterial membrane mimics (anionic PPE-SO₃ and OPE-1) are not included in this work.

1.4 Research Goals

From the previous discussion, it is clear that novel biocides like phenylene ethynylenes have great promise in many applications. Because bacteria and other pathogens are found in virtually every environment on earth, the possible applications for biocides are almost unlimited. However, in developing a specific application, responsible researchers must consider both desired and undesired effects of the intended application from synthesis to final disposal. Any potential application is likely to come in contact with humans at some point during the

product lifecycle, even if the product is never intended to be applied to skin, ingested, inhaled, or otherwise internalized. Establishing relative toxicity data is important to understand how an active ingredient may affect humans. With complex regulatory environments present in many countries, establishing such data seems to be a daunting task. Fortunately, researchers are guided by relevant international standards⁶³ and a large body of published work on analogous compounds, particularly antimicrobial peptides.

In practice, toxicity is determined using *in vitro* and *in vivo* methods. Because animal testing is very specific to the end application, the work described here will focus on *in vitro* methods. As described in this chapter, phenylene ethynylene polymers and oligomers are effective light-activated biocides. However, their applications have been limited until more information is known about potential human toxicity. This work determines whether or not select phenylene ethynylene polymers and oligomers are likely to be harmful to humans at concentrations envisioned in potential applications. This work focuses entirely on *in vitro* responses of mammalian cells to the phenylene ethynylene polymers and oligomers and is therefore an important first step in developing applications for these compounds.

This work examines toxicity to mammalian cells at three levels. Initially, the polymers and oligomers were included in growth media above endothelial cell monolayers for 24 hours and the resulting cell viability was assayed. To better approximate external (e.g. skin) exposure, epithelial cells were treated in the

same manner. Eight different compounds with promising biocidal activity (refer to Table 1-3) were included in these initial studies.

To further mimic skin exposure in the closest possible manner in vitro, multi-layer human keratinocyte tissues were obtained and polymer or oligomer solutions were applied directly to the tissue surface for a one-hour period. Following an established protocol for skin irritation testing, growth media samples were taken from the tissues 24 hours following exposure and viability of the tissues was assayed 42 hours following exposure. The media samples were later tested for cytokines, proteins produced in response to tissue irritation. The eight compounds assayed in the cytotoxicity studies (as well as electrospun mats based on one of the EO-OPEs) were included in the skin irritation testing.

Based on the results of the cytotoxicity studies and complementary techniques performed by other group members (e.g., TEM of bacterial membrane lysis), three of the eight compounds (one PPE and two EO-OPEs) were chosen for additional study with co-localization. Due to their inherent fluorescence, accumulated polymers or oligomers are visible via fluorescence microscopy. The compounds were included in growth media above epithelial cell monolayers stained with membrane- or organelle-specific dyes to co-localize the CPE and the nearest membrane or organelle. The three compounds were successfully localized to two distinct locations within the cell, indicating that at least two modes of action are possible for these compounds.

The three studies span distances from hundreds of nanometers at the intracellular level to tissue constructs almost 10 mm in size consisting of more

than a million cells. An overview of the three studies, cytotoxicity testing of cell monolayers, skin irritation testing of tissues, and intracellular co-localization, and how they are presented in this document is shown in Table 1-7 below.

Detailed methods and results will be presented in the following three chapters.

The final chapter combines and summarizes the results, and suggests possible future directions for these interesting and unique antimicrobial compounds.

Table 1-7. Overview of studies included in this work and chapter organization.

Chapter Number and Name	Compounds Included (Refer to Table 1-3)	Cell Type(s)
2. Cytotoxicity Testing of Cell Monolayers	1. PPE-DABCO 2. PPE-Th 3. EO-OPE-1-DABCO 4. EO-OPE-1-Th 5. EO-OPE-1-C2 6. S-OPE-1(H) 7. S-OPE-2(H) 8. S-OPE-3(H)	Bovine aortic endothelial cells Vero (monkey epithelial) cells
3. Skin Irritation Testing of Tissues	1. PPE-DABCO 2. PPE-Th 3. EO-OPE-1-DABCO 4. EO-OPE-1-Th 5. EO-OPE-1-C2 6. S-OPE-1(H) 7. S-OPE-2(H) 8. S-OPE-3(H) <i>Electrospun (ES) mats:</i> Control ES mat 4. EO-OPE-1-Th ES mat	Human keratinocytes
4. Intracellular Co-Localization	2. PPE-Th 4. EO-OPE-1-Th 5. EO-OPE-1-C2	Bovine aortic endothelial cells Vero (monkey epithelial) cells

CHAPTER 2 – CYTOTOXICITY TESTING

2.1 Introduction

As discussed in Chapter 1, antimicrobial conjugated electrolytes (specifically phenylene ethynylene polymers and oligomers) are effective at killing Gram-positive, Gram-negative bacteria, and viruses, and may be readily attached to surfaces or incorporated into fibers. These traits make them ideally suited for biomedical devices or other applications. However, prior to use in such applications, the polymers and oligomers must be tested for toxicity toward mammals.

Cytotoxicity data are traditionally determined from cell monolayers grown in culture. In brief, mammalian cell culture involves obtaining a small number of cells from an animal, placing those cells in aqueous medium containing the nutrients necessary for growth, and allowing the cells to proliferate either on a surface (e.g. tissue culture polystyrene) or in suspension in a controlled environment (typically 37° C, 5% CO₂, and 90% relative humidity). When the cells have almost outgrown their initial container, they are split (passaged) into secondary containers as needed, usually within a few days. In this manner, large numbers of cells are available every few days on a continuous basis. Depending on the nature of the original tissue sample, cells may be passaged for several weeks ('regular' cell lines) or indefinitely ('immortal' cell lines) prior to transforming, that is, losing traits of the original population (i.e. contact inhibition, chromosome count, morphology, etc.).⁶⁴⁻⁶⁵ With good aseptic

technique, these cells can provide consistent results over an extended period of time, especially if early passages of cells are cryogenically preserved.

To improve reproducibility, established cell lines from recognized cell repositories are recommended for cytotoxicity testing. ISO 10993-5 provides detailed guidelines as to how to best perform cytotoxicity testing.⁶⁶ Cells are seeded uniformly on multi-well plates, exposed to antimicrobial agents (e.g. in growth medium) at varying concentrations for a fixed length of time, and then assessed either qualitatively or quantitatively. Qualitative evaluation is based on observation of morphological changes. Quantitative assays may be based on cell death, inhibition of cell growth, or cell proliferation. Three of the most common quantitative cytotoxicity assays – MTT, XTT, and neutral red uptake – are based on a color change that is directly related to the number of living cells.⁶⁷⁻⁶⁹

In this work, two cell types were exposed to eight compounds at concentrations from 1-100 µg/mL for 24 hours. During the last 50 minutes of the 24-hour exposure period, half of the cells were irradiated with either visible or ultraviolet light, depending on the compound. Following irradiation, the cells were assayed for viability relative to untreated cells. Relative viability was then compared among compounds with respect to light or dark conditions and concentration. Three runs of each set of conditions, all with triplicate samples, were performed on separate days.

2.2 Materials and Methods

2.2.1 Routine cell culture

Bovine aortic endothelial cells (BAECs) were obtained from Genlantis (San Diego, CA). Vero cells were obtained from ATCC (Manassas, VA). Cells were grown in DMEM-based medium *with* phenol red (HyClone, Logan, UT) to approximately 70-80% confluence (monolayer surface coverage) in tissue culture polystyrene (TCPS) flasks. Cells were provided with fresh growth medium every 2 days and upon reaching 70-80% confluence, were trypsinized with 0.25% trypsin/EDTA (Gibco, Grand Island, NY) and passaged into new TCPS flasks. Growth medium was supplemented with 10% FBS (HyClone, Logan, UT), 1% MEM NEAA (for endothelial cells only; Gibco, Grand Island, NY), and 1% penicillin/streptomycin (HyClone, Logan, UT). Cells were incubated at 37° C, 5% CO₂, and ~90% relative humidity.

2.2.2 Cell culture for MTS assay

At ~80% confluence, cells were trypsinized, diluted in growth medium without phenol red, and counted via Coulter counter (Beckman Coulter, Fullerton, CA). Cell solution was diluted to a concentration of 100,000 cells/mL with DMEM-based medium *without* phenol red. Cells were seeded in 96-well plates at a density of 10,000 cells per well and placed in an incubator (37° C, 5% CO₂, and ~90% RH).

2.2.3 Cell treatment with polymer/oligomer solutions

After 24 hours, the medium was exchanged for 1:1 DMEM/F-12-based medium. For each compound tested, three wells each at concentrations of 0

(negative control), 1, 5, 10, 50, and 100 $\mu\text{g}/\text{mL}$ polymer or oligomer were prepared and three wells were left as-is (containing DMEM-based medium without phenol red). To facilitate testing in light and dark conditions, a second plate was prepared in an identical manner. Following medium exchange, the plates were returned to the incubator.

Solutions were prepared from polymers and oligomers synthesized as previously described.²⁹⁻³⁴ Polymer test solutions were prepared by diluting aqueous stock solutions to the desired test concentration by adding sterile 1:1 DMEM/F-12 medium (HyClone, Logan, UT). Stock solutions of the oligomers were prepared by weighing the oligomers, dissolving them in 100 μL DMSO (assisted by vortex mixing), adding 900 μL ultrapure water, and vortex mixing. The oligomer test solutions were prepared by diluting stock solutions to the desired test concentration by adding sterile 1:1 DMEM/F-12 medium. Polymer and oligomer test solutions were prepared within a day of the medium exchange.

2.2.4 Light exposure

After 23 hours in the incubator, the plates were removed from the incubator and allowed to cool for 10 minutes (to prevent later overheating above 39.5° C, when cells are adversely affected by temperature),⁶⁴ uncovered in a biosafety cabinet in the dark. Following this brief cooling period, the “dark” plate was covered in foil and the “light” plate was exposed to light for 50 minutes. Light plates containing polymer solutions were placed on a light box (Mini Light Box, Bel-Art Products, Pequannock, NJ) emitting visible light. Light plates containing oligomer solutions were placed beneath a 365-nm UV lamp (Model

EA-140, 4 Watt, Spectroline, Westbury, NY) supported by two empty tissue culture flasks.

2.2.5 MTS assay

Immediately following light exposure (for a total of 24 hours of exposure to polymer or oligomer solutions), an MTS assay was conducted. 20 μ L of MTS solution (Promega, Madison, WI), previously thawed for ~1 hour, was added to each sample well on the two plates. Following addition of the MTS solution, the plates were returned to the incubator for one hour. After exactly one hour, the wells were quickly checked for bubbles, any bubbles were eliminated, and absorbance readings at 570 nm were measured on a microplate reader (Molecular Devices, Sunnyvale, CA) after a 10-second pre-mix. The plate reader was set to 37° C and allowed to warm up prior to use. Absorbance readings were measured one plate at a time in the order in which MTS solution was added to the plates.

2.3 Results and Discussion

2.3.1 Effect of concentration on viability

In general, we found that viability decreases with increasing concentration. The decrease in viability with increasing concentration is consistent in dark and light conditions. This decrease in viability is also consistent in both cell types. Table 2-1 lists relative viabilities of *endothelial* cells after 24-hour exposure to eight test compounds in both light and dark conditions at five concentrations: 1, 5, 10, 50, and 100 μ g/mL. Table 2-2 lists relative viabilities of *epithelial* cells tested similarly. The decrease in viability with

concentration occurs with all compounds tested. There is one exception to this trend. Endothelial cells exposed to PPE-DABCO appear to have a higher viability at 100 µg/mL than 50 µg/mL (refer to red box in Table 2-1). Because this trend does not occur with epithelial cells exposed to the same concentrations of the same polymer, the apparent increase is most likely due to aggregation of the polymer in solution with the endothelial cells. Aggregation of polymer would affect the absorbance readings on which the viabilities are based.

In cell-based assays, the onset of cytotoxicity for a given compound for a given exposure time is defined as the concentration at which relative viability is \leq 70%. In most cases, the onset of cytotoxicity occurs between 10 and 50 µg/mL. At the lowest concentration tested, 1 µg/mL, one of the oligomers, EO-OPE-1-Th, is cytotoxic to both cell types in certain conditions. At a concentration of 5 µg/mL, two additional oligomers, S-OPE-1(H) and EO-OPE-1-C2, are cytotoxic to both cell types in certain conditions.

At a concentration of 100 µg/mL, only three of the 32 cell type/compound/condition combinations have viabilities greater than 70%: endothelial PPE-DABCO dark and PPE-DABCO light (refer to red box in Table 2-1), and endothelial EO-OPE-1-Th light (refer to green box in Table 2-1). However, these three combinations have viabilities less than 70% at concentrations less than 100 µg/mL, so the higher-than-expected viabilities at 100 µg/mL are probably not a true indicator that these compounds are non-toxic at that concentration.

Table 2-1. Relative viabilities (%) for *endothelial* cells exposed to each of eight test compounds for 24 hours, with the final 50 minutes of exposure in dark or light conditions. Viabilities $\leq 70\%$ are shown in bold type. The red, green, and blue boxes highlight specific data points discussed in Section 2.3.

Concentration ($\mu\text{g/mL}$):		1	5	10	50	100
PPE-DABCO	dark	72 \pm 14	71 \pm 8	68 \pm 13	62 \pm 23	192 \pm 24
	light	73 \pm 6	72 \pm 6	71 \pm 10	68 \pm 15	156 \pm 19
PPE-Th	dark	75 \pm 11	71 \pm 17	72 \pm 11	34 \pm 22	69 \pm 46
	light	72 \pm 10	70 \pm 13	62 \pm 15	39 \pm 10	57 \pm 43
S-OPE-1(H)	dark	85 \pm 10	87 \pm 10	81 \pm 8	60 \pm 9	56 \pm 8
	light	85 \pm 11	58 \pm 16	50 \pm 9	55 \pm 7	54 \pm 6
S-OPE-2(H)	dark	91 \pm 9	87 \pm 16	78 \pm 14	62 \pm 15	55 \pm 16
	light	89 \pm 11	84 \pm 8	52 \pm 10	40 \pm 4	43 \pm 6
S-OPE-3(H)	dark	87 \pm 7	86 \pm 10	87 \pm 13	75 \pm 10	59 \pm 14
	light	83 \pm 6	93 \pm 10	78 \pm 17	43 \pm 4	50 \pm 8
EO-OPE-1-DABCO	dark	87 \pm 17	86 \pm 12	71 \pm 12	31 \pm 3	33 \pm 6
	light	89 \pm 4	87 \pm 8	62 \pm 9	57 \pm 7	59 \pm 8
EO-OPE-1-Th	dark	85 \pm 18	89 \pm 14	91 \pm 12	40 \pm 28	29 \pm 3
	light	58 \pm 9	56 \pm 9	56 \pm 10	69 \pm 7	81 \pm 10
EO-OPE-1-C2	dark	89 \pm 18	102 \pm 15	113 \pm 18	22 \pm 6	28 \pm 3
	light	84 \pm 10	56 \pm 10	53 \pm 6	49 \pm 8	51 \pm 8

Table 2-2. Relative viabilities (%) for *epithelial* cells exposed to each of eight test compounds for 24 hours, with the final 50 minutes of exposure in dark or light conditions. Viabilities $\leq 70\%$ are shown in bold type. The blue boxes highlight specific data points discussed in Section 2.3.

Concentration ($\mu\text{g/mL}$):		1	5	10	50	100
PPE-DABCO	dark	84 \pm 7	84 \pm 6	84 \pm 6	74 \pm 20	62 \pm 12
	light	90 \pm 4	95 \pm 10	89 \pm 6	77 \pm 24	57 \pm 10
PPE-Th	dark	67 \pm 36	79 \pm 4	83 \pm 7	70 \pm 9	35 \pm 17
	light	60 \pm 39	89 \pm 8	66 \pm 16	22 \pm 6	20 \pm 11
S-OPE-1(H)	dark	91 \pm 10	82 \pm 9	89 \pm 4	63 \pm 9	47 \pm 6
	light	78 \pm 14	44 \pm 16	29 \pm 4	28 \pm 4	27 \pm 2
S-OPE-2(H)	dark	102 \pm 14	105 \pm 7	92 \pm 18	58 \pm 9	36 \pm 10
	light	81 \pm 9	64 \pm 18	29 \pm 6	24 \pm 3	24 \pm 1
S-OPE-3(H)	dark	96 \pm 11	99 \pm 7	97 \pm 19	60 \pm 13	26 \pm 5
	light	95 \pm 11	59 \pm 13	49 \pm 11	33 \pm 13	25 \pm 3
EO-OPE-1-DABCO	dark	81 \pm 5	102 \pm 17	98 \pm 9	23 \pm 14	14 \pm 1
	light	87 \pm 22	65 \pm 23	42 \pm 15	27 \pm 7	29 \pm 3
EO-OPE-1-Th	dark	85 \pm 10	92 \pm 7	101 \pm 8	33 \pm 19	12 \pm 1
	light	65 \pm 13	29 \pm 6	29 \pm 7	32 \pm 4	39 \pm 3
EO-OPE-1-C2	dark	95 \pm 7	96 \pm 5	101 \pm 11	44 \pm 24	11 \pm 2
	light	81 \pm 14	65 \pm 12	32 \pm 8	23 \pm 6	24 \pm 5

2.3.2 Effect of light on viability

In general, we find that adding light during cell exposure to the test compound decreases viability, particularly at concentrations from 5 to 10 $\mu\text{g/mL}$. At the lowest concentration tested, 1 $\mu\text{g/mL}$, the effect of light on viability is negligible for all compounds except one of the oligomers, EO-OPE-1-Th. For 1 $\mu\text{g/mL}$ EO-OPE-1-Th, viability decreases from 85 to 58% for endothelial cells (refer to blue box in Table 2-1) and 85 to 65% for epithelial cells with the addition of light (refer to blue box in Table 2-2). At 5 $\mu\text{g/mL}$, light decreases viability of both cell types exposed to EO-OPE-1-Th and two additional oligomers, S-OPE-1(H) and EO-OPE-1-C2. At 10 $\mu\text{g/mL}$, light decreases viability of both cell types exposed to all compounds tested except PPE-DABCO. At 50 $\mu\text{g/mL}$, light decreases viability of both cell types exposed to the three symmetric oligomers. At 100 $\mu\text{g/mL}$, light increases viability of both cell types exposed to the three “end-only” oligomers. The viability of cells exposed to PPE-DABCO is unaffected or slightly increased by light, except at 100 $\mu\text{g/mL}$, where a decrease in viability is observed in both cell types. The effect of light on the viability of cells exposed to PPE-Th is unclear.

2.3.3 Comparison between cell types

In general, we find that relative viability is somewhat cell-type dependent, particularly at higher polymer or oligomer concentrations. Table 2-3 compares viabilities of endothelial cells *and* viabilities of epithelial cells in the *dark*. Table 2-4 compares viabilities between the two cell types in the *light*. The instances where epithelial cell viability is less than endothelial cell viability are tabulated at the bottom of each table. Figures 2-1 - 2-4 provide graphical comparisons of relative viabilities for the two cell types. Figures 2-1 and 2-2 are for *endothelial* cells. Figures 2-3 and 2-4 are for *epithelial* cells.

For the lower concentrations, 1-10 $\mu\text{g}/\text{mL}$, epithelial cells do not have lower viabilities than endothelial cells overall (seven of the 16 compound/condition combinations for 1, 5, and 10 $\mu\text{g}/\text{mL}$). However, where viability is lower for epithelial cells than endothelial cells at lower concentrations, the majority of occurrences are in the light (five of seven, five of seven, and six of seven for 1, 5, and 10 $\mu\text{g}/\text{mL}$, respectively). At 50 $\mu\text{g}/\text{mL}$, epithelial cells have lower relative viabilities than endothelial cells for ten of the 16 compound/condition combinations. Of these ten occurrences, seven are in the light. At 100 $\mu\text{g}/\text{mL}$, epithelial cells have lower relative viabilities for 14 of the 16 compound/concentration combinations. Of these 14 occurrences, seven are in the light and seven are in the dark.

Table 2-3. Relative viabilities (%) for bovine aortic *endothelial* cells (BAECs) and Vero (*epithelial*) cells exposed to each of eight test compounds for 24 hours, with the final 50 minutes of exposure in *dark*.

Concentration (µg/mL):		1	5	10	50	100
PPE-DABCO	BAEC	72 ± 14	71 ± 8	68 ± 13	62 ± 23	192 ± 24
	Vero	84 ± 7	84 ± 6	84 ± 6	74 ± 20	62 ± 12
PPE-Th	BAEC	75 ± 11	71 ± 17	72 ± 11	34 ± 22	69 ± 46
	Vero	67 ± 36	79 ± 4	83 ± 7	70 ± 9	35 ± 17
S-OPE-1(H)	BAEC	85 ± 10	87 ± 10	81 ± 8	60 ± 9	56 ± 8
	Vero	91 ± 10	82 ± 9	89 ± 4	63 ± 9	47 ± 6
S-OPE-2(H)	BAEC	91 ± 9	87 ± 16	78 ± 14	62 ± 15	55 ± 16
	Vero	102 ± 14	105 ± 7	92 ± 18	58 ± 9	36 ± 10
S-OPE-3(H)	BAEC	87 ± 7	86 ± 10	87 ± 13	75 ± 10	59 ± 14
	Vero	96 ± 11	99 ± 7	97 ± 19	60 ± 13	26 ± 5
EO-OPE-1-DABCO	BAEC	87 ± 17	86 ± 12	71 ± 12	31 ± 3	33 ± 6
	Vero	81 ± 5	102 ± 17	98 ± 9	23 ± 14	14 ± 1
EO-OPE-1-Th	BAEC	85 ± 18	89 ± 14	91 ± 12	40 ± 28	29 ± 3
	Vero	85 ± 10	92 ± 7	101 ± 8	33 ± 19	12 ± 1
EO-OPE-1-C2	BAEC	89 ± 18	102 ± 15	113 ± 18	22 ± 6	28 ± 3
	Vero	95 ± 7	96 ± 5	101 ± 11	44 ± 24	11 ± 2
Vero < BAEC		2/8	2/8	1/8	3/8	7/8

Table 2-4. Relative viabilities (%) for bovine aortic *endothelial* cells (BAECs) and Vero (*epithelial*) cells exposed to each of eight test compounds for 24 hours, with the final 50 minutes of exposure in *light*.

Concentration (µg/mL):		1	5	10	50	100
PPE-DABCO	BAEC	73 ± 6	72 ± 6	71 ± 10	68 ± 15	156 ± 19
	Vero	90 ± 4	95 ± 10	89 ± 6	77 ± 24	57 ± 10
PPE-Th	BAEC	72 ± 10	70 ± 13	62 ± 15	39 ± 10	57 ± 43
	Vero	60 ± 39	89 ± 8	66 ± 16	22 ± 6	20 ± 11
S-OPE-1(H)	BAEC	85 ± 11	58 ± 16	50 ± 9	55 ± 7	54 ± 6
	Vero	78 ± 14	44 ± 16	29 ± 4	28 ± 4	27 ± 2
S-OPE-2(H)	BAEC	89 ± 11	84 ± 8	52 ± 10	40 ± 4	43 ± 6
	Vero	81 ± 9	64 ± 18	29 ± 6	24 ± 3	24 ± 1
S-OPE-3(H)	BAEC	83 ± 6	93 ± 10	78 ± 17	43 ± 4	50 ± 8
	Vero	95 ± 11	59 ± 13	49 ± 11	33 ± 13	25 ± 3
EO-OPE-1-DABCO	BAEC	89 ± 4	87 ± 8	62 ± 9	57 ± 7	59 ± 8
	Vero	87 ± 22	65 ± 23	42 ± 15	27 ± 7	29 ± 3
EO-OPE-1-Th	BAEC	58 ± 9	56 ± 9	56 ± 10	69 ± 7	81 ± 10
	Vero	65 ± 13	29 ± 6	29 ± 7	32 ± 4	39 ± 3
EO-OPE-1-C2	BAEC	84 ± 10	56 ± 10	53 ± 6	49 ± 8	51 ± 8
	Vero	81 ± 14	65 ± 12	32 ± 8	23 ± 6	24 ± 5
Vero < BAEC		5/8	5/8	6/8	7/8	7/8

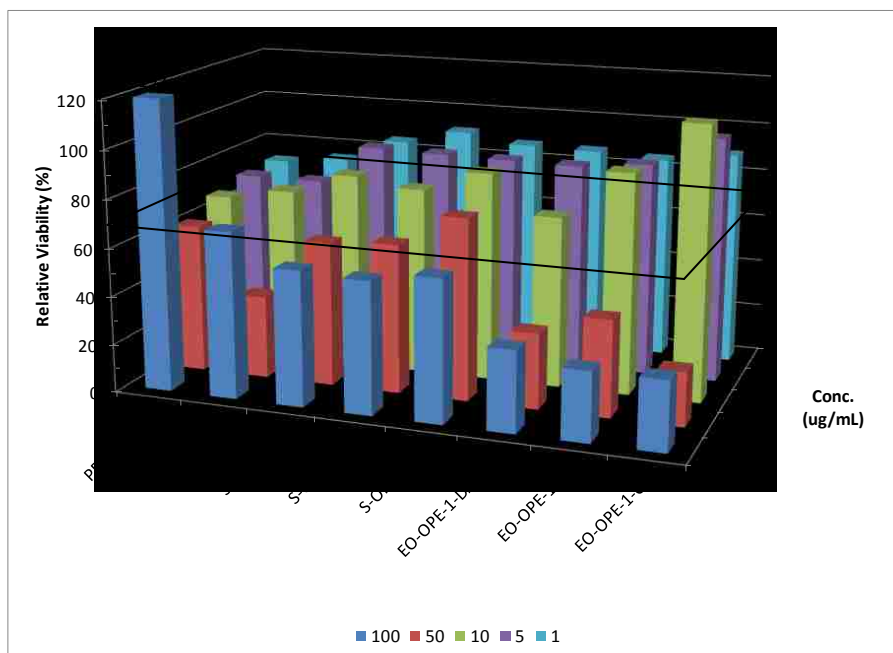


Figure 2-1. Relative viabilities (in %) of bovine aortic *endothelial* cells exposed to varying concentrations (1, 5, 10, 50, and 100 µg/mL, depth axis) of eight compounds (horizontal axis) for 24 hours in the *dark*. The shape outlined in black indicates 70% relative viability, below which the compounds are cytotoxic.

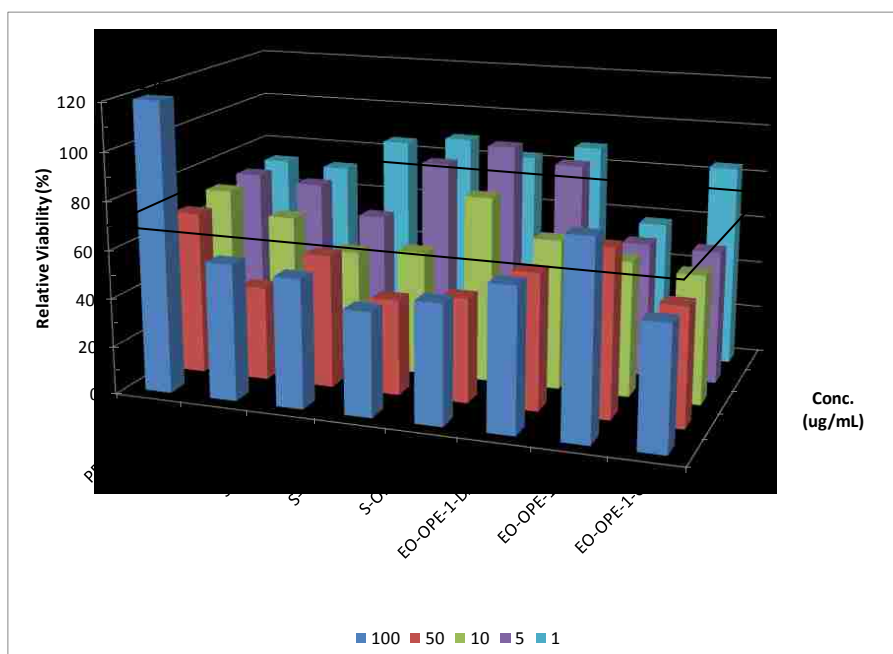


Figure 2-2. Relative viabilities (in %) of bovine aortic *endothelial* cells exposed to varying concentrations (1, 5, 10, 50, and 100 µg/mL, depth axis) of *eight compounds* (horizontal axis) for 24 hours (with final 50 minutes in visible or UV light). The shape outlined in black indicates 70% relative viability, below which the compounds are cytotoxic.

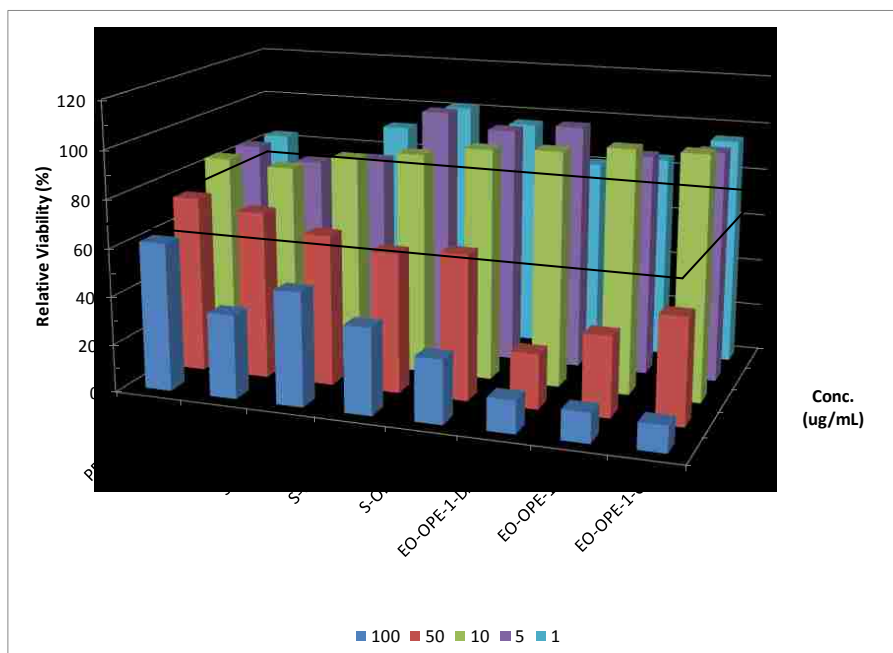


Figure 2-3. Relative viabilities (in %) of Vero (*epithelial*) cells exposed to varying concentrations (1, 5, 10, 50, and 100 µg/mL, depth axis) of eight compounds (horizontal axis) for 24 hours in the *dark*. The shape outlined in black indicates 70% relative viability, below which the compounds are cytotoxic.

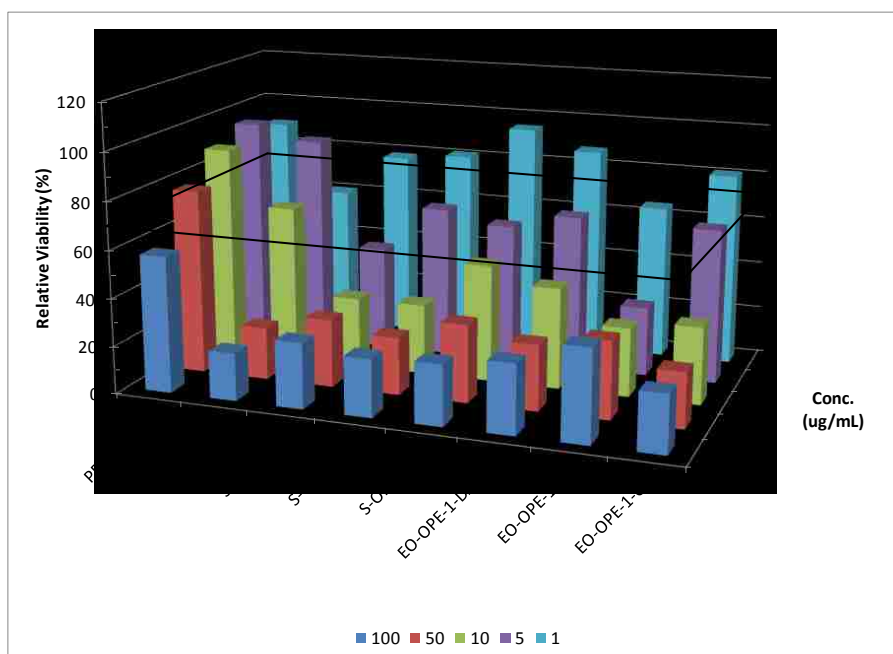


Figure 2-4. Relative viabilities (in %) of Vero (*epithelial*) cells exposed to varying concentrations (1, 5, 10, 50, and 100 µg/mL, depth axis) of *eight compounds* (horizontal axis) for 24 hours (with final 50 minutes in visible or UV *light*). The shape outlined in black indicates 70% relative viability, below which the compounds are cytotoxic.

2.3.4 Comparison among individual compounds

To better compare cytotoxicity among the different compounds, relative viabilities at the lowest two concentrations bracketing 70% were interpolated to obtain 'lethal' concentrations corresponding to 70% viability (LC₇₀). Table 2-5 gives these calculated concentrations for both endothelial cells and epithelial cells. The LC₇₀ values are of the same order of magnitude and exhibit similar trends for both cell types. LC₇₀ values for *endothelial* cells range from less than one to 66 µg/mL. LC₇₀ values for *epithelial* cells range from less than one to 68 µg/mL.

Table 2-6 more closely examines Table 2-5 by ranking the compounds in order of overall, dark, and light cytotoxicity.

Table 2-5. Calculated concentrations at which 70% of cells are viable (cytotoxic concentration) after 24-hour exposure to each of eight different compounds in dark or light conditions. Compounds are grouped by family: PPEs, S-OPEs, and EO-OPEs.

<i>Endothelial Cells</i>		LC₇₀	<i>Epithelial Cells</i>		LC₇₀
PPE-DABCO	dark	7	PPE-DABCO	dark	63
	light	27		light	68
PPE-Th	dark	13	PPE-Th	dark	<1
	light	5		light	<1
S-OPE-1(H)	dark	31	S-OPE-1(H)	dark	39
	light	3		light	2
S-OPE-2(H)	dark	30	S-OPE-2(H)	dark	36
	light	7		light	4
S-OPE-3(H)	dark	66	S-OPE-3(H)	dark	39
	light	19		light	4
EO-OPE-1-DABCO	dark	11	EO-OPE-1-DABCO	dark	25
	light	8		light	4
EO-OPE-1-Th	dark	27	EO-OPE-1-Th	dark	28
	light	<1		light	<1
EO-OPE-1-C2	dark	29	EO-OPE-1-C2	dark	32
	light	3		light	4

Table 2-6. Comparison of compounds with respect to LC₇₀ values (µg/mL) for endothelial cells and epithelial cells. Compounds are listed in order of increasing LC₇₀. Dashed lines group the compounds into high (LC₇₀ < 10), medium (10 ≤ LC₇₀ < 35), and low (LC₇₀ ≥ 35) cytotoxicity.

<i>Endothelial Cells</i>		<i>Epithelial Cells</i>	
<u>Overall (Light or Dark)</u>		<u>Overall (Light or Dark)</u>	
EO-OPE-1-Th	light <1	PPE-Th	light <1
EO-OPE-1-C2	light 3	EO-OPE-1-Th	light <1
S-OPE-1(H)	light 3	S-OPE-1(H)	light 2
PPE-Th	light 5	S-OPE-2(H)	light 4
PPE-DABCO	dark 7	EO-OPE-1-C2	light 4
S-OPE-2(H)	light 7	S-OPE-3(H)	light 4
EO-OPE-1-DABCO	light 8	EO-OPE-1-DABCO	light 4
S-OPE-3(H)	light 19	PPE-DABCO	dark 63
<u>Dark</u>		<u>Dark</u>	
PPE-DABCO	7	PPE-Th	<1
EO-OPE-1-DABCO	11	EO-OPE-1-DABCO	25
PPE-Th	13	EO-OPE-1-Th	28
EO-OPE-1-Th	27	EO-OPE-1-C2	32
EO-OPE-1-C2	29	S-OPE-2(H)	36
S-OPE-2(H)	30	S-OPE-1(H)	39
S-OPE-1(H)	31	S-OPE-3(H)	39
S-OPE-3(H)	66	PPE-DABCO	63
<u>Light</u>		<u>Light</u>	
EO-OPE-1-Th	<1	PPE-Th	<1
EO-OPE-1-C2	3	EO-OPE-1-Th	<1
S-OPE-1(H)	3	S-OPE-1(H)	2
PPE-Th	5	S-OPE-2(H)	4
S-OPE-2(H)	7	EO-OPE-1-C2	4
EO-OPE-1-DABCO	8	S-OPE-3(H)	4
S-OPE-3(H)	19	EO-OPE-1-DABCO	4
PPE-DABCO	27	PPE-DABCO	68

The DABCO polymer is unique in that it is cytotoxic at a lower concentration in the dark. All other compounds are cytotoxic at lower concentrations in the light. In the dark, the DABCO-containing polymers and oligomers are cytotoxic at the lowest concentrations, the thiophene-substituted polymers and oligomers are cytotoxic at intermediate concentrations, and oligomers with neither DABCO nor thiophene functional groups are cytotoxic at the highest concentrations. In light, the thiophene-substituted polymers and oligomers are cytotoxic at the lowest concentrations, the oligomers with neither DABCO nor thiophene functional groups are cytotoxic at intermediate concentrations, and DABCO-containing polymers and oligomers are cytotoxic at the highest concentrations. In both dark and light and with both cell types, the S-OPE-3(H) oligomer is cytotoxic at higher concentrations than its shorter analogs, S-OPE-1(H) and S-OPE-2(H).

2.3.5 Comparison among families based on chemical structure

As discussed in Chapter 1, the eight compounds tested fall into three families of phenylene ethynylenes: PPEs, S-OPEs, and EO-OPEs (refer to Tables 1-3 and 1-4). Viability data can be compared across these families to look for trends attributable to characteristic chemical structures. Figures 2-5 and 2-6 show relative viabilities after exposure to PPEs as a function of concentration. Figure 2-5 shows data for *endothelial* cells and Figure 2-6 shows data for *epithelial* cells. Neglecting the endothelial cell data for 100 $\mu\text{g}/\text{mL}$, viability after exposure to PPE-DABCO is not significantly affected by concentration or light conditions. For PPE-Th, more cells are killed in the light with increasing concentration.

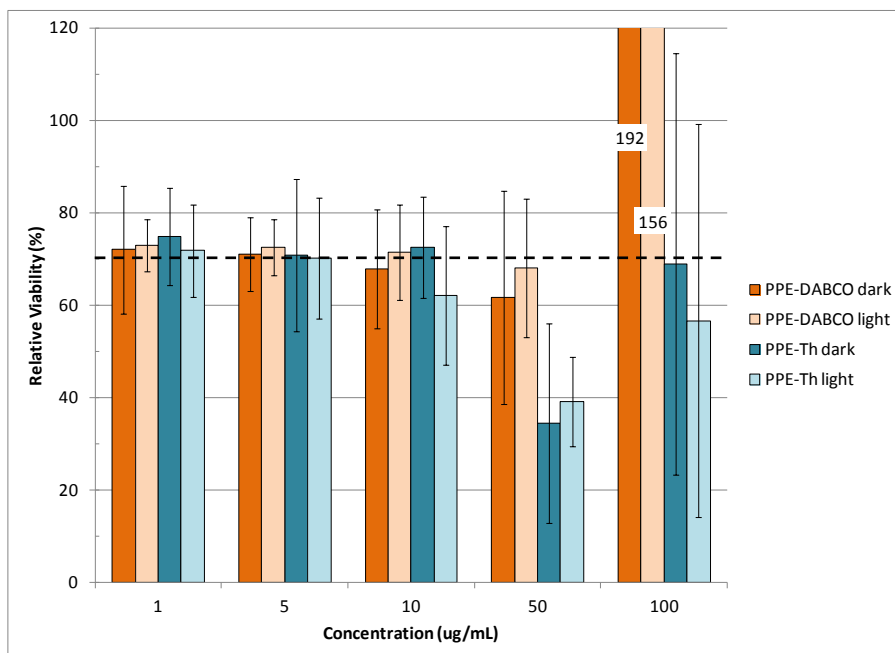


Figure 2-5. Relative viabilities (in %) of bovine aortic *endothelial* cells exposed to varying concentrations (1, 5, 10, 50, and 100 µg/mL, horizontal axis) of *two PPEs* for 24 hours (in the dark or with the final 50 minutes in light). The dashed black line indicates 70% viability, below which the compounds are considered cytotoxic.

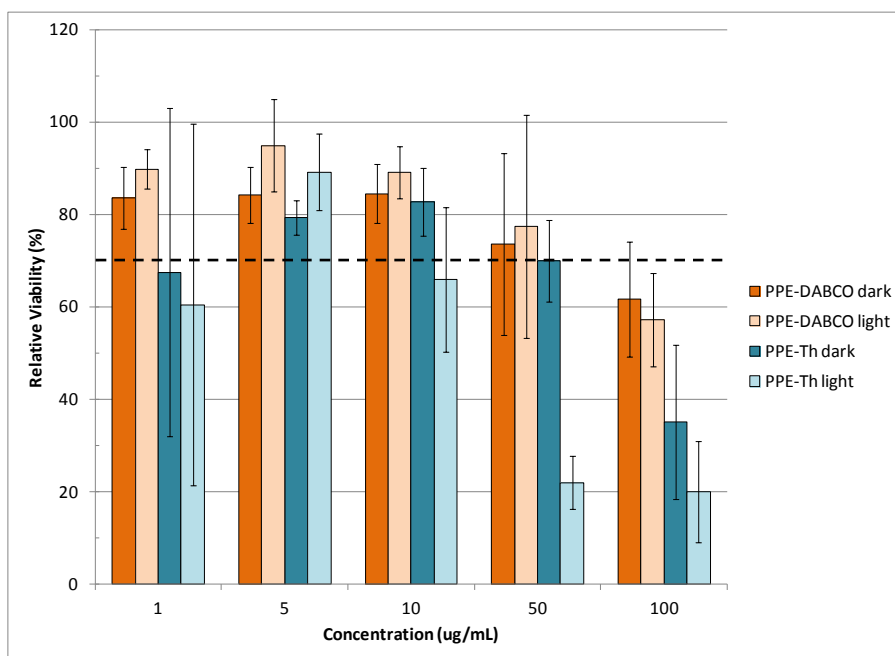


Figure 2-6. Relative viabilities (in %) of Vero (*epithelial*) cells exposed to varying concentrations (1, 5, 10, 50, and 100 µg/mL, horizontal axis) of *two PPEs* for 24 hours (in the dark or with the final 50 minutes in light). The dashed black line indicates 70% viability, below which the compounds are considered cytotoxic.

Figures 2-7 - 2-10 present similar data for the two families of oligomers. Figures 2-7 and 2-8 show relative viabilities after exposure to S-OPEs as a function of concentration. Symmetric oligomers (S-OPEs) follow a trend similar to PPE-Th. More cells are killed in the light with increasing concentration. Further, for S-OPEs, the number of repeat units factors into differences in viability with increasing concentration. Viability for S-OPE-1(H) in light is significantly lower than viability in the dark at 5 $\mu\text{g}/\text{mL}$. For S-OPE-2(H) and S-OPE-3(H) viabilities are significantly lower at 10 and 50 $\mu\text{g}/\text{mL}$, respectively. Figures 2-9 and 2-10 show relative viabilities after exposure to EO-OPEs as a function of concentration. The end-only oligomers (EO-OPEs) follow a trend opposite PPE-Th and the S-OPEs in that more cells are killed in the dark with increasing concentration.

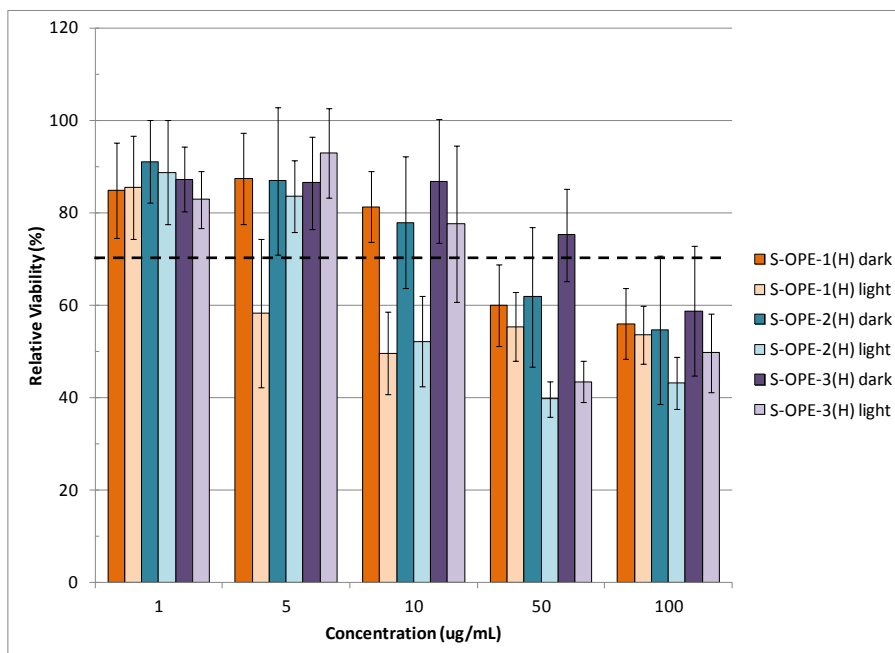


Figure 2-7. Relative viabilities (in %) of bovine aortic *endothelial* cells exposed to varying concentrations (1, 5, 10, 50, and 100 µg/mL, horizontal axis) of *three S-OPEs* for 24 hours (in the dark or with the final 50 minutes in light). The dashed black line indicates 70% viability, below which the compounds are considered cytotoxic.

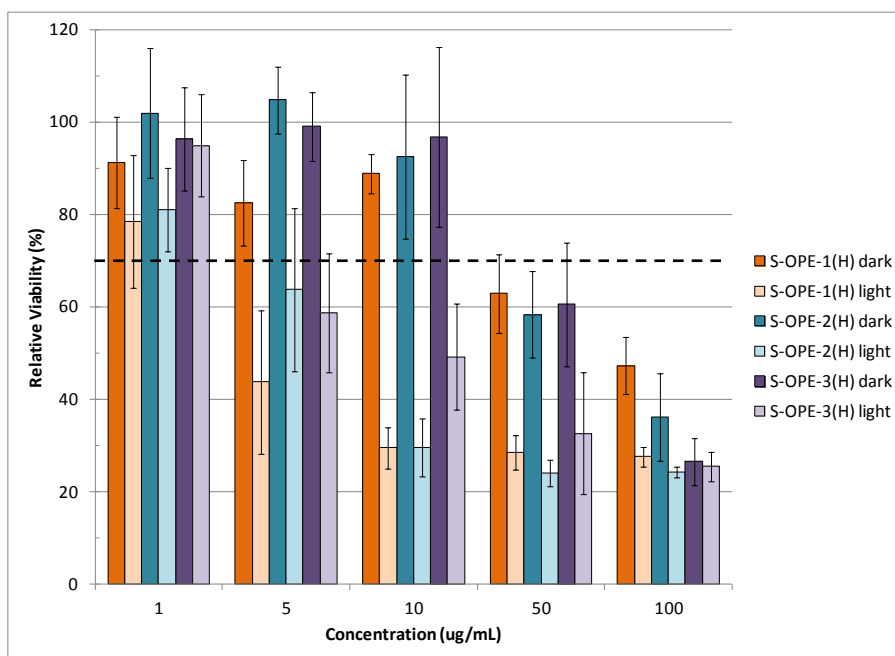


Figure 2-8. Relative viabilities (in %) of Vero (*epithelial*) cells exposed to varying concentrations (1, 5, 10, 50, and 100 µg/mL, horizontal axis) of *three S-OPEs* for 24 hours (in the dark or with the final 50 minutes in light). The dashed black line indicates 70% viability, below which the compounds are considered cytotoxic.

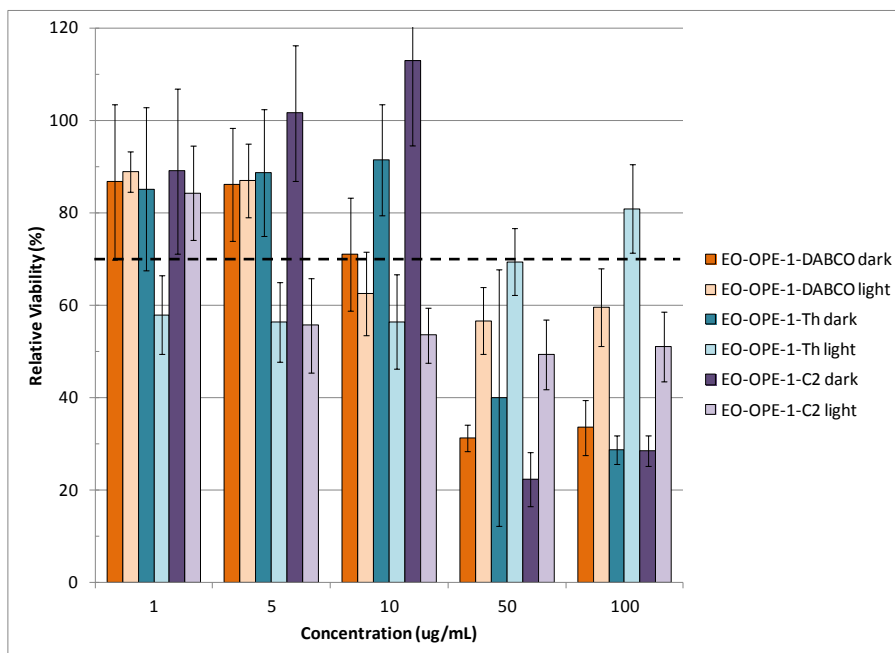


Figure 2-9. Relative viabilities (in %) of bovine aortic *endothelial* cells exposed to varying concentrations (1, 5, 10, 50, and 100 µg/mL, horizontal axis) of *three EO-OPEs* for 24 hours (in the dark or with the final 50 minutes in light). The dashed black line indicates 70% viability, below which the compounds are considered cytotoxic.

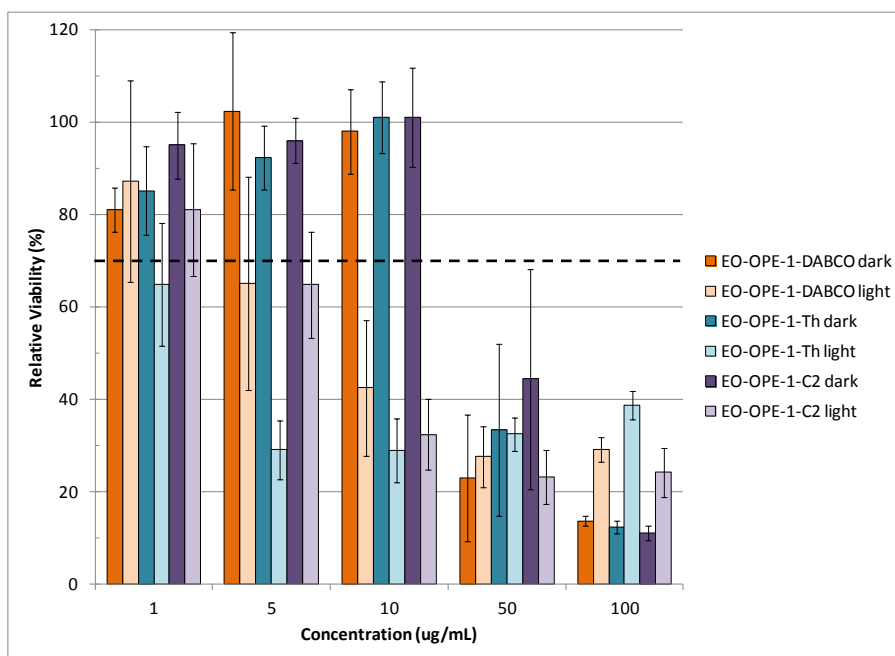


Figure 2-10. Relative viabilities (in %) of Vero (*epithelial*) cells exposed to varying concentrations (1, 5, 10, 50, and 100 µg/mL, horizontal axis) of *three EO-OPEs* for 24 hours (in the dark or with the final 50 minutes in light). The dashed black line indicates 70% viability, below which the compounds are considered cytotoxic.

2.4 Summary

Two types of mammalian cells were assayed for viability following exposure to five concentrations of eight light-activated phenylene ethynylene compounds for a period of 24 hours. Half of the cells were irradiated with visible or UV light during the last 50 minutes of the 24-hour exposure period, while the other half remained in the dark. The cytotoxicity testing described here represents a very conservative approach. Having potentially cytotoxic compounds present in growth medium is analogous to systemic (internal) exposure at a constant concentration. As all currently-envisioned applications are external to the body, receiving such constant, high-concentration exposure is unlikely. Also, any cytotoxic effects observed during these experiments are probably exaggerated because all compounds were dosed in serum-free medium. Serum, which is always present in vivo, is known to mask cytotoxic effects.⁶⁶

As expected, concentration plays the largest role in determining viability. At low concentrations, light has a negligible effect on cell viability. Above a threshold concentration which varies from compound to compound, light continues to affect viability, but concentration effects are predominant. At intermediate concentrations (5-10 $\mu\text{g}/\text{mL}$ for most compounds), the interplay between light and the light-activated compounds is very important.

Viability trends were consistent across cell types, therefore the mode of action of mammalian cell killing appears to be independent of mammalian cell type, thus related to basal cell function. For applications below cytotoxic concentrations, these compounds are safe for mammalian cells. The

concentrations at which the longer S-OPEs and the DABCO-containing compounds are cytotoxic are much higher than for the shortest S-OPE, PPE-Th, and the remaining two EO-OPEs, thus these compounds have the widest range of concentrations available for potential applications.

CHAPTER 3 - SKIN IRRITATION TESTING

3.1 Introduction

3.1.1 Background

Cytotoxicity testing is useful in identifying which compounds among a library of related compounds are more or less harmful to cellular processes common to all eukaryotic cells. However, once a specific compound has been chosen for a specific biocidal application, further testing is necessary. Because many biocidal applications may produce contact hazards, evaluating skin irritation is an important step in a tiered approach to evaluating risks to human health. ISO 10993-10 provides guidelines for conducting skin and mucosal irritation, eye irritation, and skin sensitization tests.⁷⁰

Traditional means of testing for skin damage involve exposing animals (primarily rabbits and guinea pigs) to test chemicals for a period of time, after which, they are observed for any redness (erythema) or swelling (edema) that occurs as a result of exposure.⁷⁰ Recent European legislation, specifically the Registration, Evaluation, Authorisation, and Restriction of Chemicals (REACH) Regulation of 2006, has called for reducing animal testing for new products.⁷¹ Several *in vitro* alternatives to animal testing have been validated in multi-laboratory studies.⁷² In particular, the European Centre for the Validation of Alternative Methods (ECVAM) has accepted *in vitro* skin irritation tests with EpiSkin™ and EpiDerm™ tissues as valid predictors of *in vivo* irritation.⁷³

EpiSkin™ and EpiDerm™ tissues are human-derived products that model the effect of test substances on skin. Normal human skin consists of three layers:

the dermis, epidermis, and stratum corneum. The uppermost layer, the stratum corneum, consists mostly of keratin and provides a protective barrier for the underlying epidermis and dermis. Structurally, EpiDerm™ is closely parallel to human skin, specifically the stratum corneum and the upper layers of the epidermis.⁷² Figure 3-1 compares the structures of normal human skin and EpiDerm™ tissue.

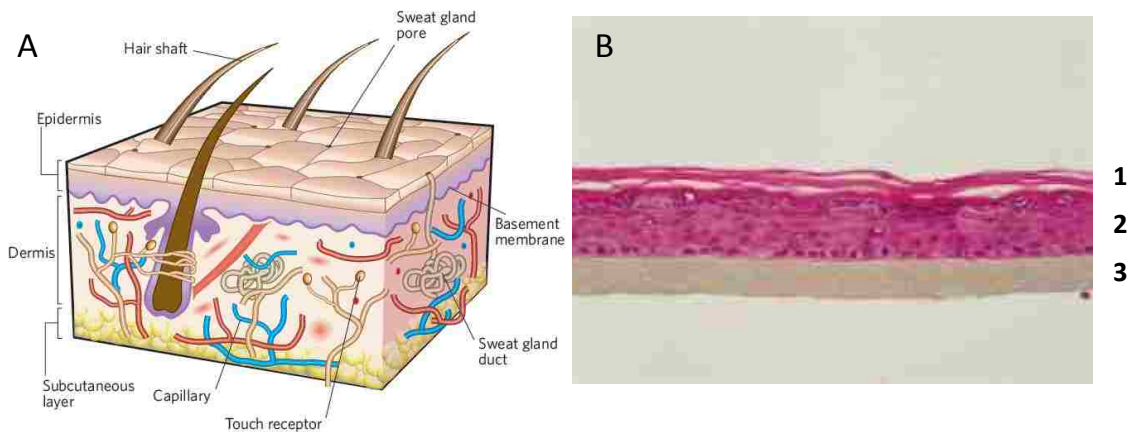


Figure 3-1. A) Cross-sectional diagram of human skin illustrating the epidermis, dermis, and subcutaneous layers. The uppermost layers of the epidermis are the stratum corneum. (MacNeil 2007) B) Cross section of EpiDerm™ tissue, stained with hematoxylin and eosin. 1) stratum corneum, 2) basal layer, and 3) permeable cell culture filter insert. (Perkins 1999)

3.1.2 Description of test methods

Five experimental protocols have been established for EpiDerm™ tissues.⁷⁴⁻⁷⁹ The similarities and differences among these protocols are presented in Table 3-1. One protocol determines skin corrosion, two determine skin irritation, and two determine phototoxicity. *Skin corrosion* is defined as

Table 3-1. Pertinent characteristics of established protocols for EpiDerm™ tissues.

Protocol Name	Irradiation	Sample Configuration	Route of Exposure	Exposure Time	Endpoint(s)	Positive Control
Dermal Corrosivity ⁷⁴	none	4 chemicals (or conc.) x 2 times x 2 + (2 NC + 2 PC) x 2 times	topical	3 min, 1 hr	MTT	potassium hydroxide, 8 N
Skin Irritation Test (SIT) ⁷⁵	none	6 chemicals (or conc.) x 3 + 3 NC + 3 PC	topical	1 hr	MTT, IL-1α	5% SDS
Effective Time-50 (ET-50) ⁷⁷	none	3 chemicals (or conc.) x 3 times x 2 + 2 NC (5 hrs) + PC	topical	2, 15, 18 hrs	MTT, cytokines	1% Triton X-100
Phototoxicity ⁷⁸	6 J/cm ² UVA/none	UVA+: (5 conc. + 1 vehicle) x 2 UVA-: (5 conc. + 1 vehicle) x 2	topical	18-24 hrs (dark) + 1 hr (UVA+/UVA-)	MTT	chlorpromazine
Systemic Phototoxicity ⁷⁹	6 J/cm ² UVA/none	UVA+: (5 conc. + 1 vehicle) x 2 UVA-: (5 conc. + 1 vehicle) x 2	systemic (in medium)	18-24 hrs (dark) + 1 hr (UVA+/UVA-)	MTT	chlorpromazine

IL = interleukin; MTT = (3-(4,5-Dimethylthiazol-2-yl)-2,5-diphenyltetrazolium bromide; NC = negative control; N = normal; PC = positive control; SDS = sodium dodecyl sulfate; UVA = ultraviolet A

irreversible damage to the skin following chemical exposure. *Skin irritation* is defined as reversible damage to the skin following chemical exposure.

Phototoxicity (photoirritation) is reversible damage to the skin following chemical exposure and subsequent irradiation by UVA light.

The Dermal Corrosivity Protocol tests for corrosion,⁷⁴ whereas the Skin Irritation Test and Effective Time-50 Protocols test for irritation.⁷⁵⁻⁷⁷

Experimentally, the only differences between the Dermal Corrosivity Protocol and the Skin Irritation Test are the duration of exposure (3 minutes vs. 60 minutes) and the threshold viability to establish corrosion or irritation (15% vs. 50% at 1 hour). The Effective Time-50 Protocol also tests for irritation, but does so by measuring viability at three exposure times and interpolating or extrapolating the time at which viability is 50%. This time is compared to similar data for known irritants. For example, 1% SDS (moderate skin irritant in vivo) has an ET-50 between 0.5 and 4 hours and baby shampoo (very mild skin irritant in vivo) has an ET-50 of 12 to 24 hours.

The two phototoxicity protocols differ mainly from the others in that they require a specific solar simulator (sunlamp) and have the longest exposure times,⁷⁸⁻⁷⁹ comparable to the longest time point for the ET-50 Protocol. Like the protocols for skin corrosion and irritation, the Phototoxicity Protocol involves applying test substances topically on the skin tissue surface. The Systemic Phototoxicity Protocol is unique in that it involves incorporating test substances into the growth medium. Doing so mimics system exposure to a test substance,

but necessitates that the test substance be soluble in water or dimethyl sulfoxide (DMSO).

The Skin Irritation Test Protocol was chosen for these experiments primarily for the following reasons: skin corrosion is unlikely given 2D in vitro results for 24-hour exposure, the Skin Irritation Test allows for screening more chemicals per EpiDerm™ kit than the ET-50 Protocol, and the two phototoxicity protocols required either extensive calibration with lamps used in 2D in vitro tests (to establish what light exposure damaged untreated EpiDerm™ tissues) or purchase and calibration of a specific solar simulator. The various protocols were discussed with Dr. Joseph Kubilus of MatTek Corporation prior to final selection.⁸⁰ Joseph Kubilus, Ph. D., formerly affiliated with the Department of Dermatology, Harvard Medical School, Massachusetts General Hospital, has more than 50 scientific publications related to keratinocytes and epidermal proteins.⁸¹⁻⁹¹

3.1.3 Description of test system

EpiDerm™ tissues consist of 8-12 cell layers (basal, spinous, and granular layers) beneath 10-15 layers of stratum corneum. The tissues are composed of normal human epidermal keratinocytes from single-donor neonatal foreskin tissue that were cultured in a Dulbecco's modified Eagle's medium (DMEM)-based medium containing 5 µg/mL gentamicin; 0.25 µg/mL amphotericin B; phenol red; lipid precursors to enhance epidermal barrier formation; and epidermal growth factor, insulin, hydrocortisone, and other proprietary stimulators of epidermal differentiation. Tissues are shipped from the

manufacturer at 4° C in medium-supplemented agarose. Tissues are supplied on 9-mm single-well, collagen-coated tissue culture plate inserts, as shown in Figure 3-2.

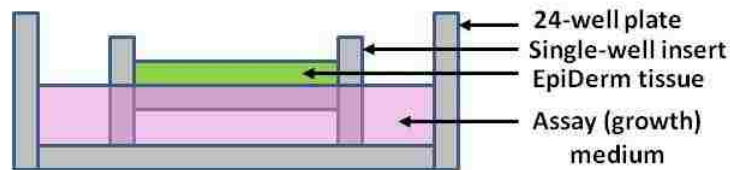


Figure 3-2. Diagram of the side view of one EpiDerm™ tissue in a 24-well plate. The single-well insert situates the lower layers of the tissue (green) in the growth medium (pink), while the upper layers of the tissue remain dry. The insert is permeable to the medium, allowing exchange of nutrients and waste to occur from below.

Each EPI-200-SIT kit (MatTek, Ashland, MA) contains 24 tissues in a 24-well plate, two 24-well plates, eight 6-well plates, 100 mL assay medium, 100 mL Dulbecco's phosphate-buffered saline (DPBS), 1 mL 5% sodium dodecyl sulfate (SDS) solution, and 25 pieces of 8-mm 200- μ m pore nylon mesh. Each MTT-100 kit (MatTek, Ashland, MA), ordered separately, contains 2 mL 3-(4,5-dimethylthiazol-2-yl)-2,5-diphenyl tetrazolium bromide (MTT) concentrate, 8 mL MTT diluent (assay medium), and 60 mL MTT extractant (isopropanol). Because MTT solution (combined concentrate and diluent) is light sensitive and should be used within a day, one MTT-100 kit was ordered to arrive with each EPI-200 SIT. Unless requested otherwise, tissues are shipped from the manufacturer on Monday, arrive Tuesday before 10 am, and should be used prior to Friday at 4 pm for reproducible results.

Interleukin-1 α is a pro-inflammatory cytokine released from keratinocytes in response to irritation. Other frequently studied biomarkers involved in skin irritation are cytokines IL-6 and IL-8 and kinases PGE₂, SKALP, and HSP70.⁹² In irritation produced by surfactants, surfactants disrupt cell membranes and cause release of IL-1 α from the cytoplasm. This released IL-1 α triggers a cascade, which results in expression of IL-6 and IL-8, activation of phospholipase A₂, and ultimately the edema, erythema, itching, and pain associated with contact dermatitis.⁹³ Though not a validated component of in vitro skin irritation testing, the IL-1 α endpoint improves test sensitivity without reducing specificity.⁷⁰ This secondary endpoint is particularly recommended for substances that are non-irritants as determined by the MTT assay, because the MTT assay tends to slightly underestimate irritation.

The IL-1 α assay is based on the double-antibody 'sandwich' technique, shown in Figure 3-3. The plate surface has been coated with a capture antibody for the analyte of interest, in this case, a monoclonal antibody for IL-1 α . The plate surface not covered by the capture antibody has been coated with blocking proteins to prevent non-specific binding. Upon addition of the sample, the analyte binds to the capture antibody. Following introduction of the sample, an acetylcholinesterase:Fab' conjugate (AChE:Fab') is added. The conjugate binds to the opposite side of the analyte (to a different epitope of IL-1 α), thus the analyte is sandwiched by two different antibodies. After an incubation period sufficient to allow specific binding, all unbound molecules are washed away by a buffered detergent solution. The final step involves adding Ellman's reagent,

which contains acetylthiocholine and 5,5'-dithio-bis-(2-nitrobenzoic acid). The acetylcholinesterase already present in the bound conjugate catalyzes the hydrolysis of the acetylthiocholine in the Ellman's reagent. A product of the hydrolysis, thiocholine, reacts with the 5,5'-dithio-bis-(2-nitrobenzoic acid) in the Ellman's reagent to make 5-thio-2-nitrobenzoic acid, which has a strong absorbance at 412 nm readily measured by a plate reader. Therefore, absorbance at 412 nm is proportional to the amount of IL-1 α present.

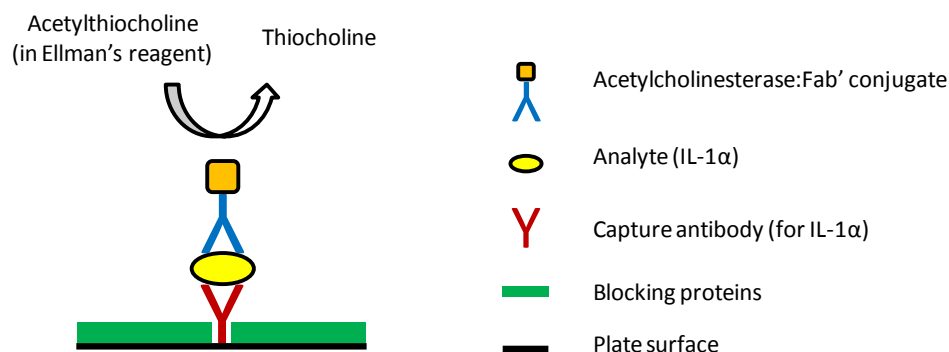


Figure 3-3. Diagram of IL-1 α assay. The analyte (IL-1 α , yellow) is sandwiched between a capture antibody (red Y) and an acetylcholinesterase(AChE):antibody conjugate (blue Y with orange AChE), which catalyzes a reaction that eventually produces a product with strong absorbance at 412 nm.

3.2 Materials and Methods

3.2.1 Sample preparation

Test substances consisted of two polymers, three “end-only” oligomers, three symmetric oligomers, and two types of electrospun mats. The polymers and oligomers were synthesized as previously described.²⁹⁻³⁴ Polymer test solutions were prepared by diluting aqueous stock solutions to the desired test concentration by adding sterile DPBS. Stock solutions of the oligomers were prepared by weighing the oligomers, dissolving them in 100 μ L DMSO (assisted

by vortex mixing), adding 900 μL ultrapure water, and vortex mixing. The oligomer test solutions were prepared by diluting stock solutions to the desired test concentration by adding sterile DPBS. Polymer and oligomer test solutions were prepared fresh on the day of exposure. Electrospun (ES) mats were prepared according to a protocol previously published,⁹⁴ and were cut to size using sterile 6-mm biopsy punches. The polymers, oligomers, and electrospun mats were used “as-is” in the tests (i.e., not sterilized prior to use).

The concentration of polymer and oligomer test solutions used for the first week of testing (10 $\mu\text{g}/\text{mL}$) was chosen because this value correlated to observed biocidal activity in several species of bacteria, and was an intermediate value in mammalian cytotoxicity testing. After analyzing the results obtained from these initial tests (using one EpiDerm™ kit), the concentration of the same polymer and oligomer solutions was increased five-fold (to 50 $\mu\text{g}/\text{mL}$) during the second week of testing. In addition, one of the polymers, PPE-DABCO, was tested at 100 $\mu\text{g}/\text{mL}$ during the second week. Preliminary cytotoxicity testing indicated that PPE-DABCO was more cytotoxic to mammalian endothelial cells than PPE-Th at 100 $\mu\text{g}/\text{mL}$ (see Figure A-4 in Section A.5). Following results obtained during the second week of testing (using a second EpiDerm™ kit), three additional oligomers and a possible product formulation (ES mat described above) were included in the third week of testing (using a third EpiDerm™ kit). As space allowed, higher concentrations of PPE-DABCO and PPE-Th than those tested during the second week (924 $\mu\text{g}/\text{mL}$ vs. 100 $\mu\text{g}/\text{mL}$ for PPE-DABCO; 100 $\mu\text{g}/\text{mL}$ vs. 50 $\mu\text{g}/\text{mL}$ for PPE-Th) were also included in the third week of testing. A PPE-

DABCO concentration of 924 µg/mL corresponds to 2 mM stock solution as received from the University of Florida. Refer to Table 3-2 for a list of substances and concentrations used for testing with each of the three EpiDerm™ kits.

3.2.2 Skin irritation test

Day 0 – Tissue conditioning

Prior to receipt of the EpiDerm™ skin irritation test kit, forceps and blotting paper were sterilized by autoclaving. Contents of the kit were carefully unpacked and placed in the refrigerator or freezer as needed. All lot numbers were recorded and expiration dates checked. Once the assay medium reached room temperature, 0.9 mL of assay medium was pipetted into each well of eight labeled six-well tissue culture polystyrene (TCPS) plates. The 24-well plate containing the tissues in agarose medium was opened under sterile airflow. Using forceps, each tissue insert was removed from the plate, blotted to remove agarose from the bottom and sides of the insert, and placed in a new 24-well TCPS plate. Once all inserts were in the new plate, the tissues were quickly inspected for edge defects and excess moisture (>40% surface coverage). The inserts were then transferred to the upper row of the six-well plates. Any tissues with defects were assigned to be positive controls. The surface of each tissue was very gently blotted with a pre-sterilized cotton swab to remove any moisture. The eight six-well plates were placed into an incubator (37° C, 5% CO₂, ~90% RH) for one hour to allow exchange of waste products accumulated during travel. After

Table 3-2. Experimental design for skin irritation testing, by 24-tissue kit. The design was such that each kit included negative controls and positive controls, and no more than 18 tissues made up a set. Additional interference controls, to ensure the test substances did not discolor the tissues, were necessary for the first two kits tested.

Kit 1			Kit 2			Kit 3		
<i>Chemical name</i>	<i>Concentration (µg/mL)</i>	<i>Number of tissues</i>	<i>Chemical name</i>	<i>Concentration (µg/mL)</i>	<i>Number of tissues</i>	<i>Chemical name</i>	<i>Concentration (µg/mL)</i>	<i>Number of tissues</i>
<i>Set 1</i>			<i>Set 1</i>			<i>Set 1</i>		
NC (DPBS)		3	NC (DPBS)		3	NC (DPBS)		3
PPE-DABCO	10	3	PPE-DABCO	50	3	S-OPE-1(H)	50	3
PPE-Th	10	3	PPE-Th	50	3	S-OPE-2(H)	50	3
EO-OPE-1-DABCO	10	3	EO-OPE-1-DABCO	50	3	S-OPE-3(H)	50	3
EO-OPE-1-Th	10	3						
EO-OPE-1-C2	10	3						
<i>Set 2</i>			<i>Set 2</i>			<i>Set 2</i>		
PC (5% SDS)		2	EO-OPE-1-Th	50	3	PPE-DABCO	924	3
<i>Interference controls:</i>			EO-OPE-1-C2	50	3	PPE-Th	100	3
PPE-DABCO	10	1	PPE-DABCO	100	3	Control ES mat		1
PPE-Th	10	1	PC (5% SDS)		2	EO-OPE-Th ES mat		2
EO-OPE-1-DABCO	10	1	<i>Interference control:</i>			PC (5% SDS)		2
EO-OPE-1-Th	10	1	DPBS		1	1% Triton X-100		1
Totals:		24			24			24

one hour, the inserts were gently swabbed again, transferred from the upper to lower row of the six-well plates (effectively changing the medium), and returned to the incubator for an 18 hour period.

Day 1 – Chemical exposure

Test substances, as described above, were prepared. All negative controls, polymer solutions, and oligomer solutions were tested in triplicate. Positive controls, controls to check for interference with the MTT assay, and electrospun mat samples were tested in duplicate or individually, as space allowed. Each kit was divided in two sets, with no more than 18 tissues per set. 0.9 mL of warm medium was added to the upper row of a sufficient number of six-well plates for Set 1. At the end of the 18-hour incubation period, one set of tissues was removed from the incubator. The tissues were gently swabbed and re-checked for edge defects and excess moisture.

The tissues were then dosed, following slightly different procedures for liquid test substances and solid test substances (e.g. electrospun mats). For liquid test substances, 30 μ L were pipetted on to the skin surface and an 8-mm nylon mesh disc was applied to aid in uniform application. For the electrospun mats, 30 μ L sterile DPBS were pipetted on to the skin surface, the 6-mm mat was placed with sterile tweezers, an 8-mm nylon mesh disc was applied, and 20 μ L sterile DPBS were pipetted on the mesh. The additional 20 μ L DPBS were applied to fully wet the mat surface. See Figure 3-4 for a diagram comparing application of liquid and solid test substances.

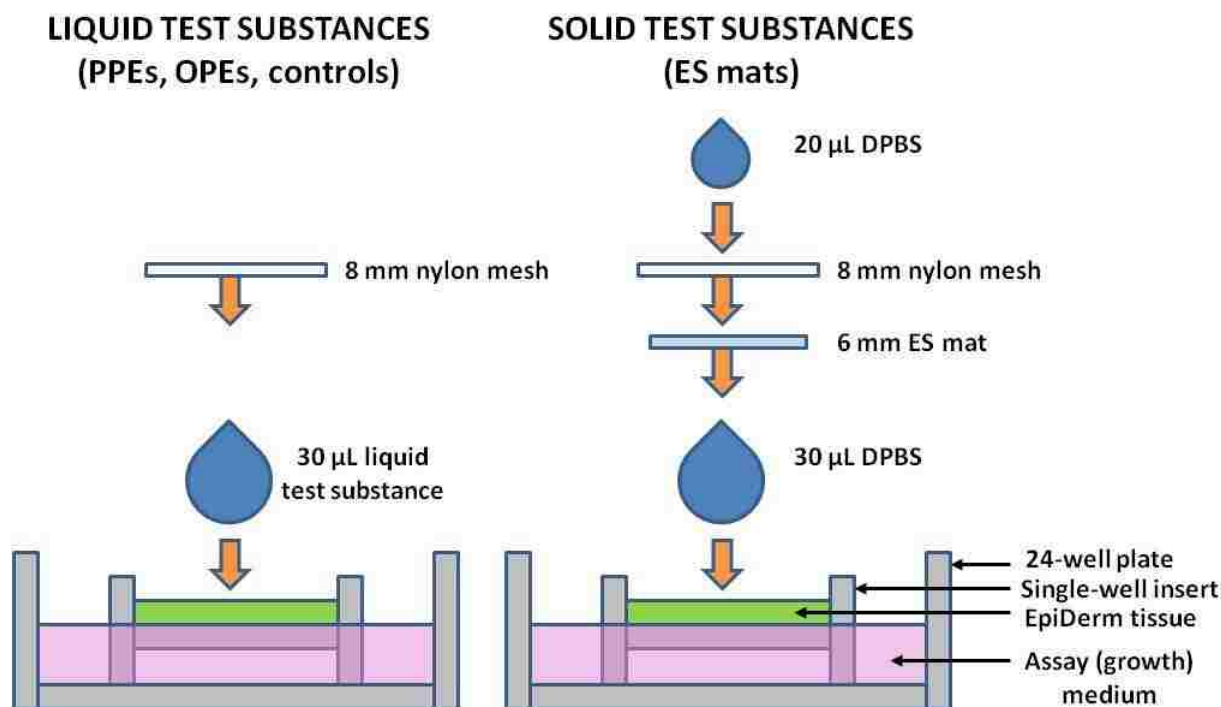


Figure 3-4. Diagram comparing application of liquid and solid test substances to EpiDerm™ tissues. For liquid test substances, 30 µL of liquid were applied to the tissue surface, followed by nylon mesh to promote even wetting. For solid test substances (electrospun mats), 30 µL of DPBS were applied, followed by the mat, nylon mesh, and an additional 20 µL DPBS for complete wetting of the mat.

Following application the last test substance and mesh, a 35-minute timer was started and Set 1 tissues were placed in the incubator. After 35 minutes, the tissues were removed from the incubator, placed in the biosafety cabinet, and a timer was started for 25 minutes. After 25 minutes (1 hour total dose period), the tissues were rinsed 15 times with sterile DPBS. The tissue inserts were blotted on the bottom and sides, gently swabbed on the skin surface, then placed in the medium-filled six-well plates and returned to the incubator. Immediately after

placing Set 1 in the incubator, Set 2 was removed from the incubator and dosing and washing steps were carried out, still within the 18 ± 3 hour period. All dosing was performed in the dark (minimal light) and all washing steps were done in semi-darkness (overhead light on, cabinet light off).

Day 2 – Medium change and collection for cytokine analysis

After 24 hours in the incubator, Set 1 was removed and 0.9 mL of warm assay medium was pipetted into the lower wells of the six-well plates. The inserts were then transferred to the lower wells, effectively changing the medium. The medium in the upper wells was collected in labeled freezer vials for later cytokine analysis. Similarly, medium was added to and collected from the six-well plates for Set 2.

Day 3 – MTT viability test

The 2-mL MTT concentrate (5 mg/mL) and 8-mL pre-measured assay medium were warmed and combined to make a 1 mg/mL MTT solution. 300 μ L of MTT solution were added to a sufficient number of wells for Set 1 in a 24-well plate. Set 1 was removed from the incubator after a 24-hour period. The tissues were blotted and transferred to the MTT-filled 24-well plate. The tissues were returned to the incubator for a 3-hour period. After exactly 3 hours, the MTT solution was aspirated from the wells and the wells were rinsed twice with sterile DPBS, making sure not to overfill the well and wet the skin surface. The inserts were blotted and transferred to a new empty 24-well plate. 2 mL of isopropanol were added to each insert, pipetting directly above the skin surface such that the

first milliliter fills the insert and the second milliliter overflows into the well, thus covering both sides of the tissue. The plate was then covered, wrapped in Parafilm to reduce evaporation, and placed on a plate shaker set at low speed for 2 hours. After 2 hours, the tissue was pierced with sharp tweezers to allow the liquid in the insert to better mix with the liquid in the well. The inserts were then carefully removed from the wells. The 24-well plate was covered and returned to the shaker for 5 minutes of gentle shaking. After 5 minutes, the remaining ~2 mL of MTT/isopropanol solution were transferred in 200 μ L aliquots to a labeled 96-well plate. At least two aliquots for each well were taken. Six blanks (isopropanol) were added to the 96-well plate and the plate was immediately analyzed on a plate reader. After 10 seconds of mixing, absorbance readings were taken every 5 nm between 540 and 595 nm. Set 2 was prepared and analyzed for viability in a similar manner, beginning after the conclusion of its 24-hour incubation period.

3.2.3 Cytokine analysis

An interleukin-1 α (human) EIA kit (Cayman Chemical, Ann Arbor, MI) was stored at -20 $^{\circ}$ C prior to use. The kit consisted of an anti- IL- 1 α ELISA strip plate, an IL- 1 α AChE Fab' conjugate, an IL- 1 α standard, EIA buffer concentrate, wash buffer concentrate, Polysorbate 20, Ellman's reagent, and a plate cover sheet. Reagents were prepared according to manufacturer's instructions.⁹⁵ EIA buffer was prepared by adding 10 mL EIA buffer concentrate to 90 mL ultrapure water. Wash buffer was prepared by adding 2.5 mL wash buffer and 0.5 mL Polysorbate 20 to 1 L ultrapure water. The IL- 1 α standard was reconstituted

with 2 mL EIA buffer to a final concentration of 5 ng/mL. The 5 ng/mL bulk standard was serially diluted with normal maintenance medium (MatTek, Ashland, MA) to make standards at 250, 125, 62.5, 31.3, 15.6, 7.8, and 3.9 pg/mL. The IL- 1 α AChE Fab' conjugate was reconstituted with 10 mL EIA buffer.

Media samples set aside during skin irritation testing were thawed at room temperature and diluted with fresh normal maintenance medium (MatTek, Ashland, MA). All samples (except certain 5% SDS positive controls) were diluted 1:5 per MatTek protocol⁹⁶ by adding 200 μ L of sample medium to 800 μ L of normal maintenance medium. Three assays were performed. As a result of the 5% SDS positive control (diluted 1:5) in the first assay having a measured IL-1 α concentration nearly exceeding the highest standard (250 pg/mL), subsequent positive controls were diluted 1:6. 100 μ L of each of 24 diluted samples were added to the plate in triplicate. 100 μ L of each of the eight standards (0, 3.9-250 pg/mL IL-1 α) were added to the plate in duplicate. 100 μ L of IL- 1 α AChE Fab' conjugate was added to each of the wells containing either samples or standards. Two wells were left empty to serve as blanks. The plate was incubated at 4° C overnight.

Immediately prior to development of the plate, the Ellman's reagent was reconstituted with 20 mL ultrapure water. The plate was removed from the refrigerator and each well (including blanks) was washed five times with previously-prepared wash buffer. Following the last wash, the wells were emptied and 200 μ L of Ellman's reagent were added to each well (including blanks). Upon addition of Ellman's reagent to the last well, a timer was started.

The plate was covered with the provided cover sheet, placed on an orbital shaker (setting =2, Lab-Line Instruments, Melrose Park, IL), and covered with foil. At 15, 30, 60, 120, 180, and 360 minutes, the absorbance at 412 nm (407-417 nm, 1 nm step) was determined for each well on a plate reader (manufacturer here). The plate was re-covered and returned to the shaker between readings.

3.3 Results and Discussion

3.3.1 Skin irritation criteria

The threshold to distinguish an irritant from a non-irritant is 50% relative viability.⁷⁰ If relative viability is greater than 50%, the chemical is considered a non-irritant. Likewise, a relative viability of 50% or less classifies the chemical as an irritant. Though cytokine analysis does not officially categorize a test substance one way or another, guidelines for EpiSkin™ are shown in Table 3-3 below.

Table 3-3. Predictive classification model with two endpoints (MTT and IL-1 α).

Relative Viability	IL-1 α Release	Classification
$\leq 50\%$	> 9 IU/mL	Irritant
$\leq 50\%$	≤ 9 IU/mL	Irritant
$> 50\%$	> 9 IU/mL	Irritant
$> 50\%$	≤ 9 IU/mL	Non-irritant

3.3.2 MTT assay

Relative viability is based on absorbance (optical density, OD) at 570 nm as follows:

$$OD_{570}(\text{test substance or control, raw}) - OD_{570}(\text{blank, raw}) = OD_{570}(\text{test substance or control}) \quad (1)$$

$$\text{Relative viability} = [OD_{570}(\text{test substance})/OD_{570}(\text{mean of negative control})] \times 100\% \quad (2)$$

Relative viabilities are calculated with respect to the mean of the negative control tissues within a kit, as viabilities are expected to vary slightly among EpiDerm™ kits. Table 3-2 describes which test substances were included in testing for each of the three 24-tissue kits used for skin irritation testing. All polymer and oligomer solutions were tested for interference with the MTT assay, and none had a color change (see Section A.6).

Figure 3-5 shows the relative viabilities for both the negative controls (DPBS) and positive controls (5% SDS) for each of the three EpiDerm™ kits tested. Because the mean viability of the negative controls is the basis of the relative viabilities for the positive controls and test substances, the relative viabilities of the negative controls are 100% by definition. The negative controls have increasing standard deviations across subsequent kits. The increasing standard deviations of the negative controls are most likely due to tissue lot number, as each lot is derived from an individual infant. The second and third kits each had isolated examples of tissues that did not uptake the MTT as uniformly as the tissues in the first kit. (See Figure 3-6 for a photograph of an example of such tissues.)

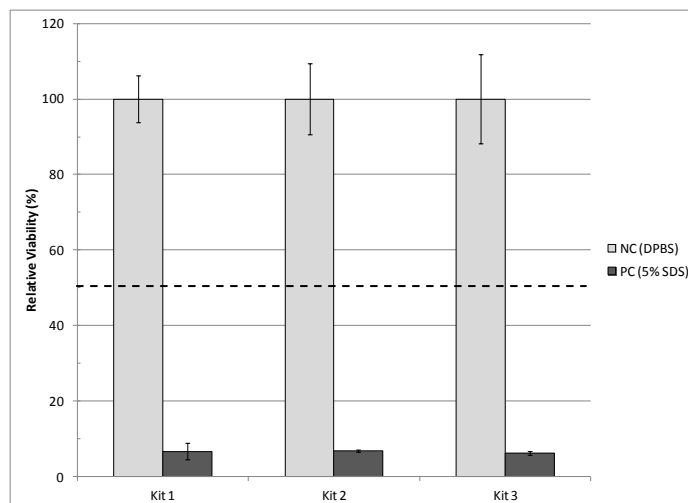


Figure 3-5. Relative viabilities (\pm SD) of negative controls (NC, n=2, DPBS) and positive controls (PC, n=3, 5% SDS) for each of the three EpiDerm™ kits tested, as determined by MTT assays 42 hours after 1-hour exposure. The dashed line indicates 50% relative viability, below which substances are classified as irritants.

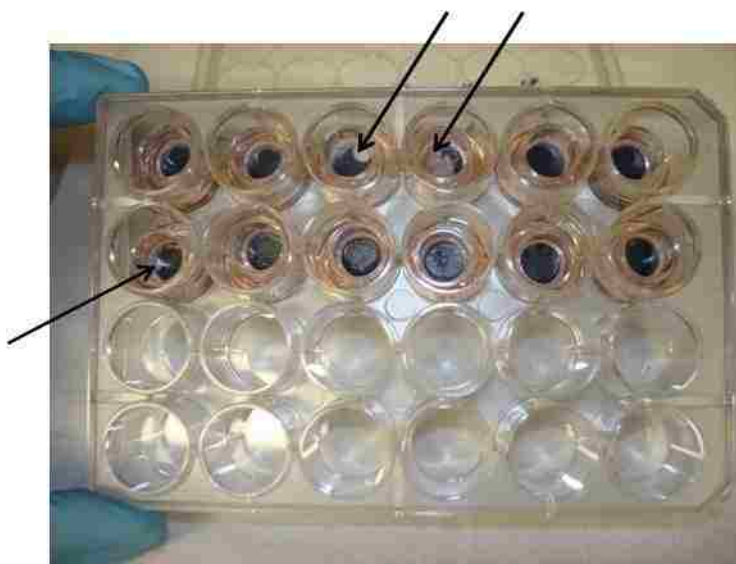


Figure 3-6. Photograph of tissues with non-uniform MTT uptake. The three arrows show areas of tissues that have not changed color after addition of MTT.

Figures 3-7 and 3-8 compare responses of EpiDerm™ tissues to the polymers and the “end-only” oligomers. Figure 3-7 compares the relative viabilities of the tissues exposed to the two polymers at the three concentrations tested for both: 10, 50, and 100 $\mu\text{g}/\text{mL}$. The relative viability of tissues exposed to PPE-DABCO appears to increase with concentration; however, examination of

Table 3-4 reveals that the relative viability for PPE-DABCO at 924 $\mu\text{g}/\text{mL}$ (not shown in Figure 3-7) is comparable to that at 10 $\mu\text{g}/\text{mL}$. Though not statistically significant, the relative viabilities of PPE-DABCO are higher than those of PPE-Th at 10, 50, and 100 $\mu\text{g}/\text{mL}$. Figure 3-8 compares the relative viabilities of the three “end-only” oligomers tested at 10 and 50 $\mu\text{g}/\text{mL}$. Figure 3-8 shows an apparent, though not statistically significant, *increase* in viability with increasing concentration; this increase is, however, most likely due to differences between kits, as all EO-OPEs were tested at 10 $\mu\text{g}/\text{mL}$ with the first kit and 50 $\mu\text{g}/\text{mL}$ with the second kit.

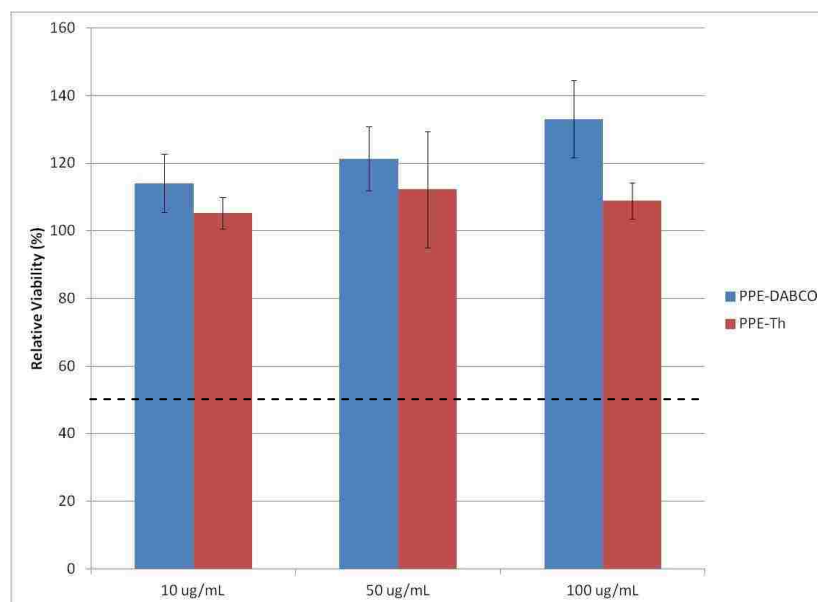


Figure 3-7. Relative viabilities (\pm SD) of two polymers, PPE-DABCO and PPE-Th, at three concentrations tested, as determined by MTT assays of EpiDerm™ tissues 42 hours after 1-hour exposure ($n=3$). The dashed line indicates 50% relative viability, below which substances are classified as irritants.

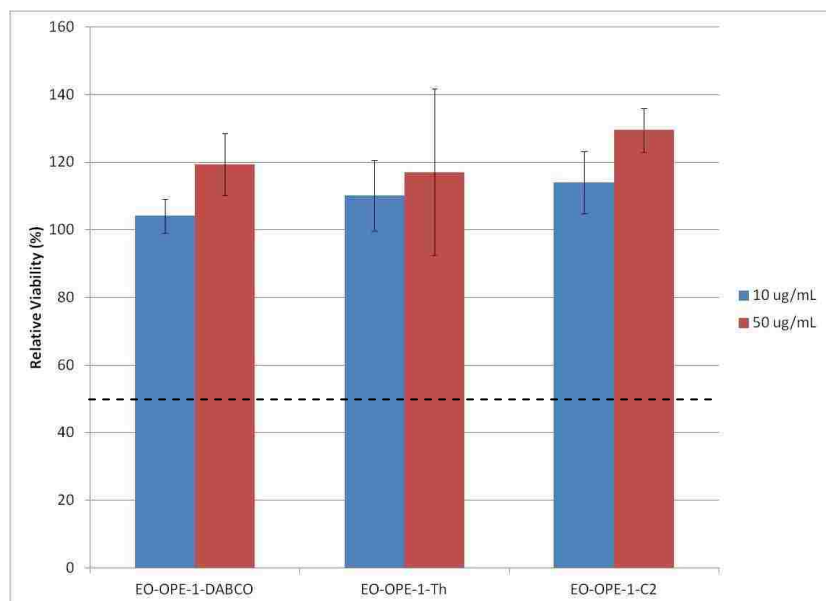


Figure 3-8. Relative viabilities (\pm SD) of three “end-only” oligomers (EO-OPEs) at two concentrations tested, as determined by MTT assays of EpiDerm™ tissues 42 hours after 1-hour exposure (n=3). The dashed line indicates 50% relative viability, below which substances are classified as irritants.

Table 3-4. Relative viabilities (in %) of all substances tested in skin irritation tests.

<i>Chemical Name</i>	<i>10 µg/mL</i>	<i>50 µg/mL</i>	<i>100 µg/mL</i>	<i>924 µg/mL</i>	<i>solid</i>
PPE-DABCO	114.1 ± 8.6	121.3 ± 9.5	133.1 ± 11.4	114.7 ± 4.1	N/A
PPE-Th	105.4 ± 4.7	112.2 ± 17.3	108.9 ± 5.4	N/A	N/A
EO-OPE-1-DABCO	104.2 ± 5.0	119.3 ± 9.2	N/A	N/A	N/A
EO-OPE-1-Th	110.2 ± 10.4	117.1 ± 24.6	N/A	N/A	N/A
EO-OPE-1-C2	114.1 ± 9.1	129.6 ± 6.5	N/A	N/A	N/A
S-OPE-1(H)	N/A	112.5 ± 3.4	N/A	N/A	N/A
S-OPE-2(H)	N/A	112.1 ± 5.9	N/A	N/A	N/A
S-OPE-3(H)	N/A	113.1 ± 2.5	N/A	N/A	N/A
Control ES mat	N/A	N/A	N/A	N/A	133.8 (n=1)
EO-OPE-Th ES mat	N/A	N/A	N/A	N/A	105.2 ± 4.1

Figure 3-9 shows the most comprehensive data in terms of comparing polymers and oligomers: two polymers and six oligomers, all at 50 µg/mL. All compounds have relative viabilities well above 50%, the viability below which the compounds would be skin irritants, therefore none are irritants. The DABCO-containing compounds appear to have slightly higher viabilities than the thiophene-containing compounds, perhaps due to the relatively low number of data points or inherent variability of samples derived from individual infants, but this trend is not statistically significant.

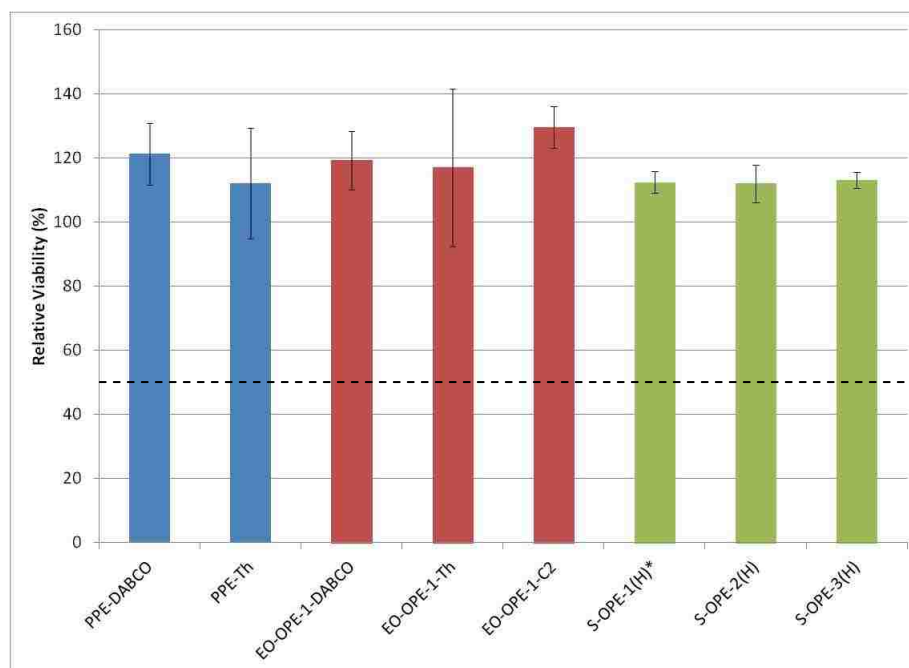


Figure 3-9. Relative viabilities (\pm SD) of two polymers (PPEs, blue) and six oligomers (OPEs, red and green) at 50 µg/mL, as determined by MTT assays of EpiDerm™ tissues 42 hours after 1-hour exposure (n=3). *n=2 (Third tissue had excess moisture between layers). The dashed line indicates 50% relative viability, below which substances are classified as irritants.

3.3.3 Cytokine assay

For each plate development time (15, 30, 60, 120, 180, or 360 minutes), the average absorbance of the two blanks was subtracted from the absorbance values for the rest of the plate. A standard curve was generated for each time by plotting the 16 absorbance values for the eight standards versus concentration and a best-fit line was constructed. The slope and y-intercept of this best-fit line was used to determine sample concentrations as follows:

$$\text{Concentration} \left(\frac{\text{pg}}{\text{mL}} \right) = \frac{[A_{412}(\text{sample}) - b]}{m} \times \text{Dilution} \quad (3)$$

where A_{412} = absorbance at 412 nm,

b = y-intercept of best-line fit of calibration curve, and

m = slope of best-line fit of calibration curve (mL/pg).

Sample concentrations below 3.9 pg/mL (prior to multiplication by dilution factor) are reported as ND (not detected). In some cases, dropping sample concentrations ≤ 3.9 pg/mL resulted in small sample sizes (n=1 vs. n=3), and standard deviations could not be calculated for these samples. Due to its highly-correlated calibration curve ($r^2 \geq 0.975$ for each of three kits) and range of absorption values ($\sim 0-1.6$, blank-corrected), a plate development time of 120 minutes was chosen to provide representative data.

Figure 3-10 shows the cytokine assay results for both the negative controls and positive controls from each kit. As the results for the cytokine assay are derived from the same tissues that generated relative viability data, the controls are the same, tissues treated with DPBS (negative control) and 5% SDS (positive control). Like the viability data, the results for the controls are consistent across

the three kits. Tables 3-5 and 3-6 give IL-1 α values for the negative and positive controls, respectively, by tissue. For the negative controls, IL-1 α concentrations range from 21 to 103 pg/mL, with an overall mean of 77 ± 18 pg/mL. For the positive controls, IL-1 α concentrations range from 206 to 384 pg/mL, with an overall mean of 307 ± 36 pg/mL.

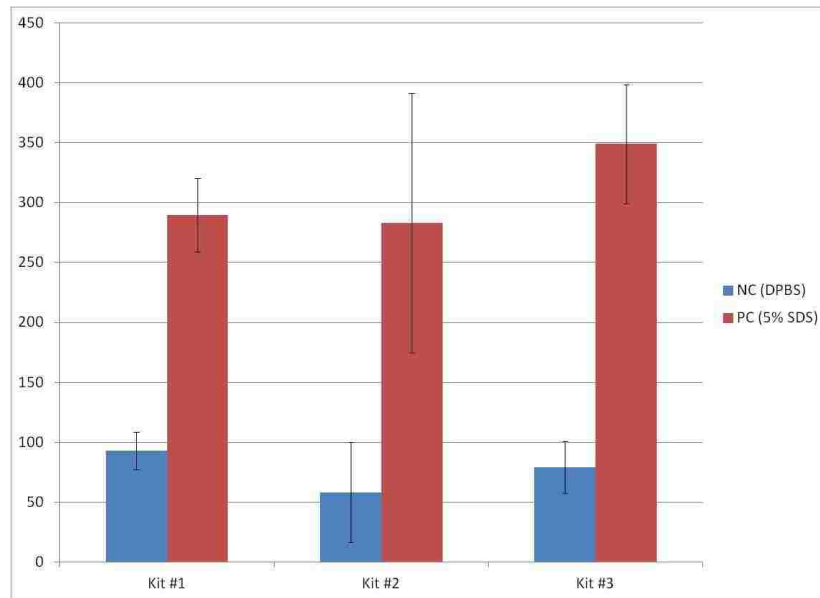


Figure 3-10. Concentration of IL-1 α of negative controls (tissues treated with DPBS) and positive controls (tissues treated with 5% SDS) for each of three EpiDerm™ kits used in skin irritation testing.

Table 3-5. Concentration of IL-1 α of negative controls for each kit.

	Concentration \pm SD (pg/mL)	Concentration \pm SD (pg/mL)	Concentration \pm SD (pg/mL)
	<i>Kit 1</i>	<i>Kit 2</i>	<i>Kit 3</i>
Mean for Tissue 1	75	49	98
Mean for Tissue 2	101	21	85
Mean for Tissue 3	102	103	55
Mean for Tissues 1-3	93 ± 16	58 ± 42	79 ± 22

Table 3-6. Concentration of IL-1 α of positive controls for each kit.

	Concentration \pm SD (pg/mL)	Concentration \pm SD (pg/mL)	Concentration \pm SD (pg/mL)
	<i>Kit 1</i>	<i>Kit 2</i>	<i>Kit 3</i>
Mean for Tissue 1	311	360	384
Mean for Tissue 2	268	206	314
Mean for Tissues 1 and 2	290 ± 31	283 ± 109	349 ± 50

Table 3-7 shows the cytokine assay results for the eight compounds and two electrospun mats assayed. IL-1 α concentrations range from 20 to 105 pg/mL with a median value of 56 pg/mL. All values are below the concentrations for the Kit 1 negative controls (93 ± 16), so it is reasonable to conclude that the test substances produced no more IL-1 α than the negative control (DPBS).

Table 3-7. Concentration of IL-1 α (in pg/mL) from tissues corresponding to test substances.

<i>Chemical Name</i>	<i>10 μg/mL</i>	<i>50 μg/mL</i>	<i>100 μg/mL</i>	<i>924 μg/mL</i>	<i>solid</i>
PPE-DABCO	73 ± 49	ND	ND	44 ± 15	N/A
PPE-Th	97 ± 23	25 (n=1)	49 ± 15	N/A	N/A
EO-OPE-1-DABCO	105 ± 6	20 (n=1)	N/A	N/A	N/A
EO-OPE-1-Th	51 ± 22	ND	N/A	N/A	N/A
EO-OPE-1-C2	80 (n=1)	104 (n=1)	N/A	N/A	N/A
S-OPE-1(H)	N/A	101 ± 40	N/A	N/A	N/A
S-OPE-2(H)	N/A	50 ± 6	N/A	N/A	N/A
S-OPE-3(H)	N/A	56 ± 18	N/A	N/A	N/A
Control ES mat	N/A	N/A	N/A	N/A	56 (n=1)
EO-OPE-Th ES mat	N/A	N/A	N/A	N/A	34 ± 1

ND = Not detected (≤ 3.9 pg/mL in diluted sample)

For compounds tested at multiple concentrations, such as PPE-DABCO, there are no clear trends in cytokine assay results with respect to concentration. Though not statistically significant, the IL-1 α release values of PPE-DABCO are lower than those of PPE-Th at 10, 50, and 100 μ g/mL. However, the IL-1 α release values of EO-OPE-1-DABCO are higher than those of EO-OPE-1-Th, so the trend is not consistent with DABCO and thiophene functional groups. For the S-OPEs, which vary in terms of number of repeat units, S-OPE-2(H) had the lowest IL-1 α release (50 /mL), followed by S-OPE-3(H) (56 pg/mL) and S-OPE-1(H) (101 pg/mL). Based on this limited data, it appears that n=2 is the optimum number of repeat units for S-OPEs in terms of IL-1 α release.

Table 3-8 provides literature values for IL-1 α release for 22 neat chemicals tested for skin irritation following the same protocol using EpiDerm™ tissues.⁹¹ All of these chemicals were non-irritants as determined by MTT assays for relative viability, and IL-1 α release was used as a secondary endpoint to confirm non-irritant status. IL-1 α release values ranged from 25.8 to 130.6 pg/mL, a very similar range to the IL-1 α release values reported here (20-105 pg/mL). Though four of the 22 neat chemicals were irritants in rabbit tests, these four chemicals were non-irritants in human patch tests. These data support the conclusion that the ten test substances (eight compounds and two electrospun mats) assayed in this work are non-irritants as determined by IL-1 α release.

Table 3-8. Comparison of IL-1 α release, in vivo rabbit, and 4-hour human patch tests for chemicals predicted to be non-irritants based on MTT assay results.⁹¹

Chemical	IL-1 α (pg/mL)		In vivo rabbit	Human patch test
	mean	SD		
Diethyl phthalate	77.56	54.32	NI	
Di-propylene glycol	88.38	43.72	NI	NI
Napthalene acetic acid	35.25	7.02	NI	NI
3-Chloronitrobenzene	54.72	15.29	NI	
3,3-Dithiodipropionic acid	33.61	25.73	NI	
4,4-Methylene-bis(2,6-ditertbutyl)phenol	26.77	6.37	NI	
4-Amino-1,2,4-triazole	106.15	51.47	NI	
Benzyl benzoate	47.30	24.81	NI	
Sodium bicarbonate	68.13	10.70	NI	
Allyl phenoxyacetate	38.66	9.34	NI	
Isopropanol	130.60	116.44	NI	NI
Benzyl salicylate	41.23	15.80	NI	
Methyl stearate	25.76	0.50	NI	
Benzyl acetate	99.49	58.80	NI	
Isopropyl myristate	34.27	14.25	NI	NI
Isopropyl palmitate	30.60	16.23	NI	NI
Allyl heptanoate	50.15	15.30	NI	
Heptyl butyrate	97.80	75.94	NI	NI
Hexyl salicylate	106.20	134.30	I	NI
Linalyl acetate	91.25	56.24	I	NI
Terpinyl acetate	53.49	26.96	I	NI
Di-n-propyl disulphide	91.88	20.15	I	NI

I = irritant; NI = non-irritant; SD = standard deviation

3.4 Summary

Two polymers, six oligomers, and two types of electrospun mats were tested for skin irritation using multi-layered tissues based on human epidermal keratinocytes. After receipt, the tissues were conditioned for a day, exposed to the test substances on the second day for one hour, and tested for viability using a colorimetric assay on the fourth day. Media was collected on the third day for cytokine analysis.

Viability (MTT) and cytokine (IL-1 α) assays concluded that all oligomers were non-irritants up to the highest tested concentration (50 $\mu\text{g}/\text{mL}$). PPE-DABCO and PPE-Th were non-irritants up to the highest tested concentrations, 924 $\mu\text{g}/\text{mL}$ and 100 $\mu\text{g}/\text{mL}$, respectively. The poly(caprolactone) (PCL) and PCL/EO-OPE-1-Th ES mats also did not induce skin irritation. Therefore, all test substances can be conservatively classified as non-irritants after the one-hour exposure.

Three MTT assay acceptance criteria have been established by the tissue kit manufacturer to serve as quality control checks for the kits. The three kits received passed all three acceptance criteria, with the exception of one of the eighteen substance/concentration combinations tested failing the third acceptance criterion (see Section A.7). However, failure of the third criterion does not affect the overall classification of the substance. The IL-1 α assay seems to be more prone to variability than the MTT assay, which likely explains its lack of acceptance as a validated secondary endpoint for in vitro skin irritation. However, the IL-1 α results obtained in this work are consistent with literature

values, and support the conclusion that the polymers, oligomers, and electrospun mats do not cause the tissues to produce additional IL-1 α .

In summary, all substances tested did not cause skin irritation after a one-hour exposure time, the chemistry of the viability assay was not affected by the test substances, and the tissues were of sufficient quality to obtain reproducible results. The lack of skin irritation for all substances, as measured by two endpoints, alleviates initial safety concerns for products based on these polymers and oligomers, both in solution and as electrospun mats. Solution-based products could include disinfectant sprays, wipes, and paints. Mat-based products could include wound dressings, fabrics for hospitals and clinics, and filters.

CHAPTER 4 – INTRACELLULAR LOCALIZATION

4.1 Introduction

Eukaryotic cells are different from prokaryotic cells, such as bacteria, in that their deoxyribonucleic acid (DNA) is contained in a distinct membrane-enclosed compartment. Eukaryotic cells contain a number of membrane-enclosed compartments, called organelles, each with a specific function. Organelles common to all animal cells include the nucleus, the endoplasmic reticulum (ER), ribosomes, the Golgi apparatus, mitochondria, endosomes, lysosomes, and peroxisomes.⁹⁷ DNA and ribonucleic acid (RNA) synthesis occur in the nucleus, where the nuclear DNA is located. The ER receives proteins from adjacent ribosomes, produces lipids for the rest of the cell, and serves as a Ca^{2+} store. Ribosomes, both free and ER-bound, synthesize proteins. The Golgi apparatus receives proteins and lipids from the ER and distributes them to various locations in the cell. Mitochondria generate adenosine triphosphate (ATP), an energy source for reactions throughout the cell. Endosomes are compartments for materials taken in from outside the cell. Lysosomes and peroxisomes are enzyme-filled compartments. Lysosomes degrade material from endosomes. Peroxisomes contain enzymes used in oxidation reactions. These compartments comprise approximately half of the cell's volume, and many times the membrane area of the plasma membrane. For example, the endoplasmic reticulum alone is 12-25 times the area of the plasma membrane.⁹⁷ Relative amounts of membrane area by compartment for two types of mammalian cells are presented in Table 4-1 below.

Table 4-1. Relative amounts of membrane types in mammalian cells (from Alberts 2008).

Membrane Type	Percentage of Total Cell Membrane Area	
	<i>Hepatocyte</i>	<i>Pancreatic exocrine cell</i>
Plasma membrane	2	5
ER membrane	51	60
Golgi apparatus membrane	7	10
Mitochondria	39	21
Nucleus (inner membrane)	0.2	0.7
Other	1.2 [†]	3 [‡]

[†]Lysosome, peroxisome, and endosome membranes

[‡]Secretory vesicle membrane

The organelles tend to occupy the same relative locations for many types of mammalian cells (see Figure 4-1). The nucleus is near the center of the cell. The endoplasmic reticulum membrane is contiguous with the nucleus, therefore directly adjacent to the nucleus. The Golgi apparatus lies between the ER and the plasma membrane. The lysosomes and endosomes tend to be closer to the plasma membrane. These organelles are transparent when viewed via optical microscopy, but the addition of fluorescent compartment-specific dyes, stains, or labels allows imaging when viewed via fluorescence microscopy. Compartment-specific dyes have been developed for mitochondria, lysosomes, peroxisomes, vacuoles (in yeast), the ER, and the Golgi apparatus.⁹⁸ A fluorescent molecule may be introduced to the cell and its location within the cell can be determined by its proximity to a fluorescently-labeled intracellular compartment. This co-localization can link a molecule to its target structure, and with knowledge of that structure's function, help determine how the molecule is affecting a cell.

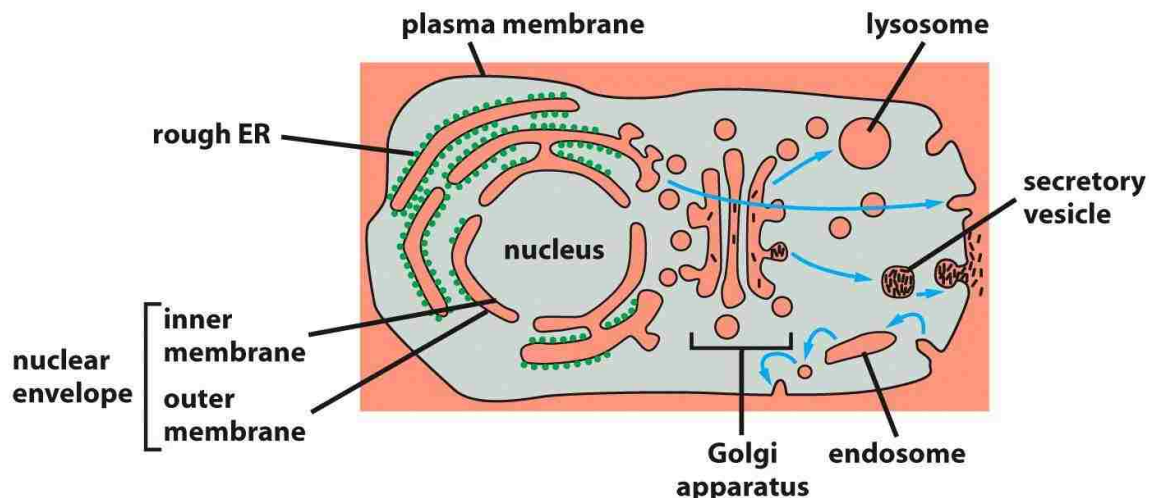


Figure 4-1. Relative locations of organelles within a mammalian cell (from Alberts 2008). The nucleus and ER are near the center of the cell. The Golgi apparatus lies between the ER and the plasma membrane. The lysosomes and endosomes tend to be closer to the plasma membrane.

The majority of antimicrobial peptides have a mode of action that involves disruption of the bacterial cell membrane. However, there are some antimicrobial peptides that have specific intracellular targets. Similarly, some antimicrobial peptides enter mammalian cells and some do not.⁹⁹ The specific properties of antimicrobial peptides that correlate to mammalian cell entry and cytotoxicity are not well understood, but these structure-activity relationships are an active area of research.¹⁰⁰⁻¹⁰² The antimicrobial peptides that enter mammalian cells, but do not exhibit cytotoxicity, are promising in terms of intracellular drug delivery. Another class of peptides, the cell-penetrating peptides, has similarities to this subset of antimicrobial peptides.¹⁰³ Hence, antimicrobial peptides that penetrate mammalian cell membranes have been “re-branded” as cell-penetrating peptides.¹⁰⁴ Cell-penetrating peptides derived from antimicrobial peptides include Bac7, Pyrrocoricin, Human lactoferrin (19-40), Buforin 2, Melittin, Magainin 2, LL-37, SynB1, Crotamine, S4₁₃-PV_{rev}, and L-2.¹⁰⁵

As peptides are subject to degradation by proteases in the body, researchers are also developing antimicrobial peptide mimics and cell-penetrating peptide mimics.¹⁰⁶⁻¹⁰⁷

In this work, epithelial cells were exposed to three phenylene ethynylene-based compounds: one thiophene-substituted polymer, one thiophene-substituted oligomer, and one non-substituted oligomer. The specific structures of these compounds are shown in Figure 4-2. These compounds are antimicrobial peptide mimics, and are similarly effective in killing Gram-positive bacteria, Gram-negative bacteria, and fungi. These phenylene-ethynylene-based compounds are different from antimicrobial peptides, however, in that they exhibit greater antimicrobial activity in visible or UV light, depending on the compound. The polymer strongly absorbs light in the visible region, while the oligomers absorb in the ultraviolet (UV) region of the electromagnetic spectrum. The effects of 1-hour or 4-hour exposures (with and without light) to the polymer and the two oligomers on mammalian cells were observed. Epithelial cells were exposed to each of the three compounds at 10 $\mu\text{g}/\text{mL}$. For comparison, endothelial cells were observed with one of the oligomers, also at 10 $\mu\text{g}/\text{mL}$. Initially imaged with a plasma membrane stain, the cells were later imaged with an organelle-specific stain as needed to identify the location of the polymer or oligomer.

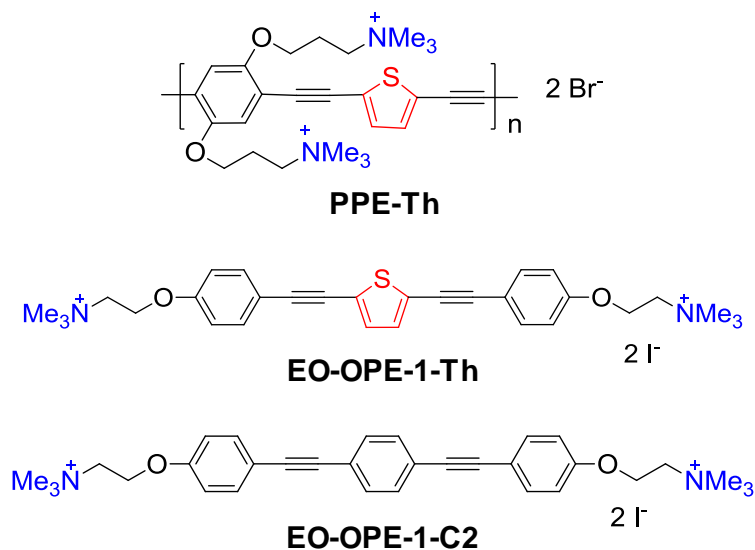


Figure 4-2. Structures of compounds included in localization studies. PPE-Th is a thiophene-substituted phenylene ethynylene polymer. EO-OPE-1-Th is a thiophene-substituted “end-only” phenylene ethynylene oligomer. EO-OPE-1-C2 is a non-substituted “end-only” phenylene ethynylene oligomer. Thiophene substitutions are shown in red. In PPE-Th, the *side chains* are shown in blue. In the two “end-only” oligomers, the *end groups* are shown in blue.

4.2 Materials and Methods

4.2.1 Cell culture

For routine culture, Vero cells and BAECs were grown as previously described (refer to Chapter 2). For microscopy, cells were seeded on Lab-Tek™ chamber slides (Nunc, Rochester, NY) one day prior to polymer/oligomer addition.

4.2.2 Cell treatment with polymer/oligomer solutions

For ‘4 hour’ samples, normal growth media was exchanged for polymer/oligomer-treated media ~4 hours prior to start of imaging and the slide was returned to the incubator. For ‘1 hour’ samples, normal growth medium was exchanged for polymer/oligomer-treated media ~90 minutes prior to imaging. For both time points, slides were removed from the incubator ~75 minutes prior

to imaging, allowed to cool for 10 minutes (to prevent overheating under the light), and placed in visible or UV light (light samples only) for 50 minutes. Slides containing polymer solutions were placed on a light box (Mini Light Box, Bel-Art Products, Pequannock, NJ) emitting visible light. Slides containing oligomer solutions were placed beneath a 365-nm UV lamp (4-Watt Model EA-140, Spectroline, Westbury, NY) supported by two empty tissue culture flasks.

4.2.3 Cell staining

Upon arrival at the microscopy facility, cells were washed in the appropriate buffer, stained, and washed again. Polymer-treated cells (and associated controls) were washed 3 times before and after staining with Tyrode's buffer. Polymer-treated cells were stained with 1:2000 CellMask™ Orange or CellMask™ Deep Red (Molecular Probes, Eugene, OR) in Tyrode's buffer for 5 minutes at room temperature. Oligomer-treated cells (and associated controls) were washed 3 times before and after staining with Hank's Balanced Salt Solution (HBSS). Oligomer-treated cells were stained with 1:500 ER-Tracker™ Red (Molecular Probes, Eugene, OR) in HBSS for 30 minutes at 37° C. Cells were imaged in the final wash buffer.

4.2.4 Microscopy

PPE-Th (Figures 4-2 - 4-4)

Confocal imaging was performed on a Zeiss LSM 510 META system (includes lasers and filters, Carl Zeiss AG, Oberkochen, Germany) with a 63x oil objective. Excitation of PPE-Th was provided by a 488 nm argon laser; emission was collected through 500-530 nm BP or 505 nm LP filters. Cell Mask™ Deep

Red excitation was provided by a 633 nm HeNe2 laser; emission was collected through a 650 nm LP filter.

EO-OPE-1-Th (Figures 4-7 - 4-8)

Confocal imaging was performed on a Zeiss LSM 510 META system (includes lasers and filters, Carl Zeiss AG, Oberkochen, Germany) with a 63x oil objective. Excitation of EO-OPE-1-Th was provided by a 405 nm laser diode; emission was collected through a 420-480 nm BP filter. ER-Tracker™ Red excitation was provided by a 543-nm HeNe1 laser; emission was collected through a 560 nm LP filter.

EO-OPE-1-Th and EO-OPE-1-C2 (Figures 4-9 - 4-10)

Wide-field imaging was performed on an Olympus IX71 inverted microscope (Olympus America, Center Valley, PA) with a 60x H₂O objective. Excitation of EO-OPE-1-Th and EO-OPE-1-C2 was provided by a mercury fluorescence lamp with a 387/11 band pass filter (Semrock, Rochester, NY); emission was collected through a 447/60 band pass filter (Semrock, Rochester, NY). CellMask™ Orange excitation was provided by the same mercury lamp with a 545/30 band pass filter; emission was collected through a 620/30 band pass filter (Chroma Technology, Bellows Falls, VT). Images were acquired with an Andor iXon 887 EmCCD camera (Andor Technology, Belfast, Northern Ireland).

Images were false colored with Zeiss LSM Image Browser software (Carl Zeiss GmbH, Jena, Germany) and merged with SPOT Advanced v4.5 software (Diagnostic Instruments, Sterling Heights, MI). The SPOT Advanced software automatically adjusted image brightness when merging images (overlying images taken with different filters in place). For example, in Figure 4-10, the

image from the red filter (CellMask™ Orange) was overlaid with the image from the blue filter (EO-OPE-1-Th) to compare locations of the CellMask™ plasma membrane stain with the EO-OPE-1-Th.

4.3 Results and Discussion

4.3.1 Co-localization of polymer and plasma membrane

Figure 4-3 compares the effects of a 4-hour exposure to the thiophene polymer, PPE-Th, on epithelial cells with and without the final 50 minutes in visible light. In both light and dark conditions, the polymer has accumulated at the plasma membrane. However, upon the addition of light, the polymer has entered the cell and localized to the nucleus.

Figure 4-4 shows an individual epithelial cell after a 4-hour exposure to the thiophene polymer with the final 50 minutes in visible light. As both the CellMask™ membrane stain and the polymer have entered the cell, the plasma membrane is likely compromised. The bulges in the nuclear membrane (denoted by white arrows) and the presence of polymer within the nucleus indicates that the nuclear membrane integrity has also been compromised.

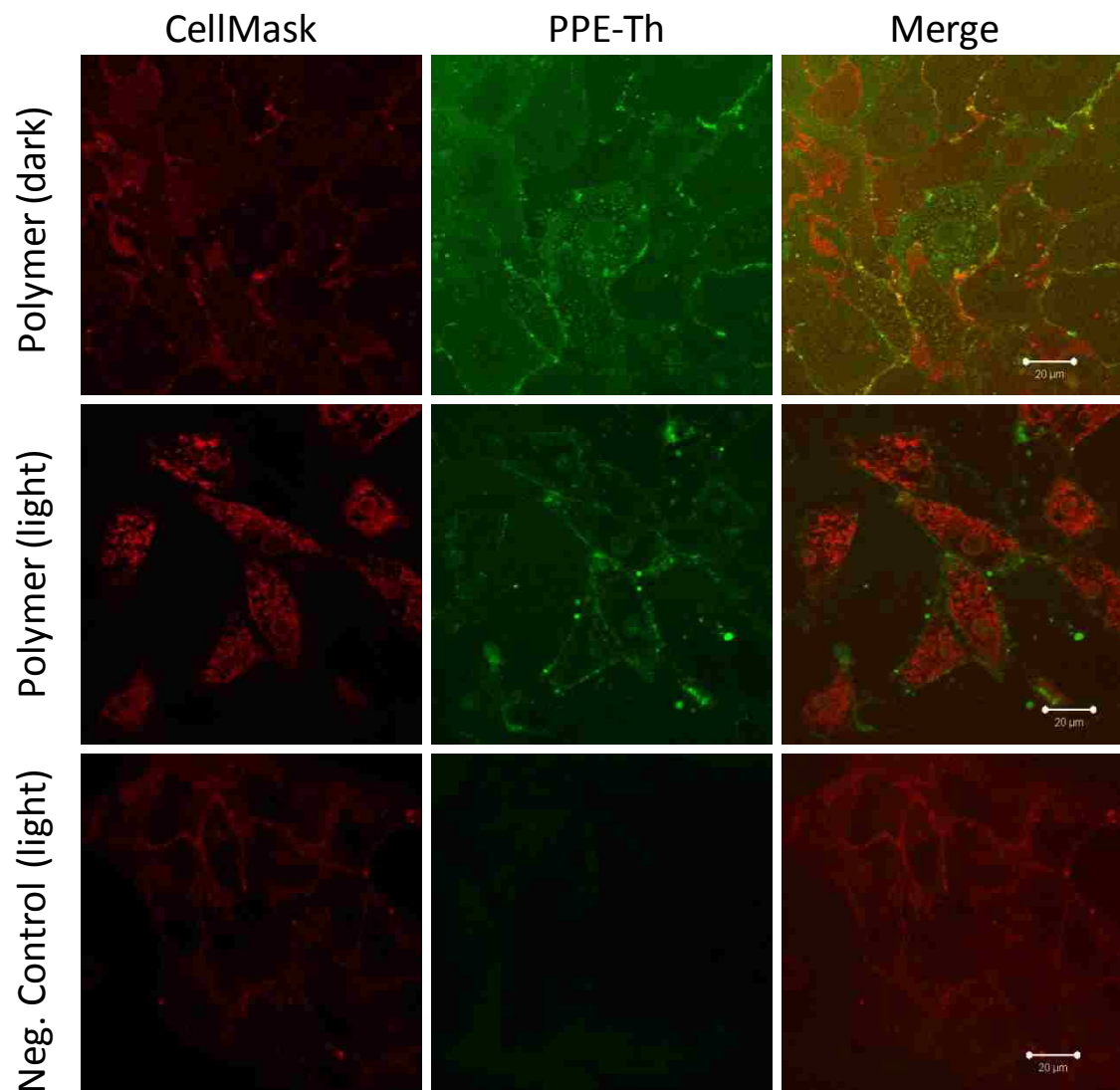


Figure 4-3. Confocal microscope images epithelial cells after a 4-hour exposure to 10 $\mu\text{g}/\text{mL}$ PPE-Th, with the last 50 minutes in the *dark* (top row) or in visible *light* (middle row). The negative control (bottom row) shows the same epithelial cells without polymer exposure after 50 minutes in visible light. The red color (left column) is CellMask™ Deep Red, a plasma membrane stain, and the green color (center column) is fluorescence from PPE-Th. The scale bars in the merged images (right column) are 20 μm .

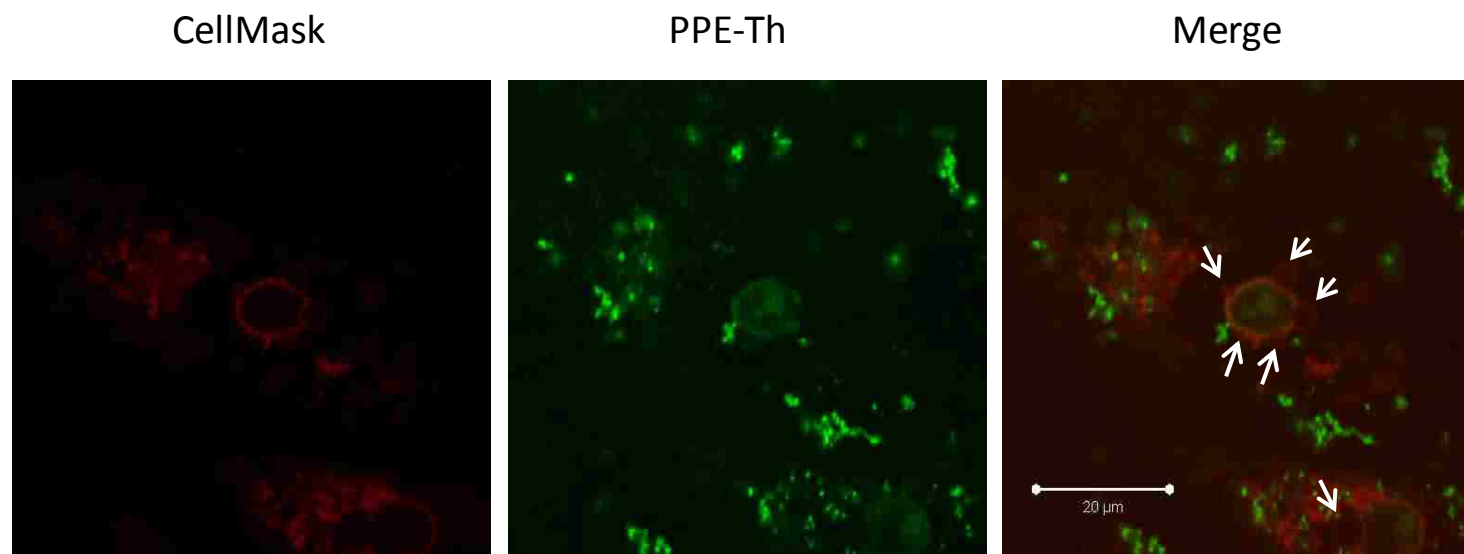


Figure 4-4. Confocal microscope images of an epithelial cell after a 4-hour exposure to 10 $\mu\text{g}/\text{mL}$ PPE-Th with the final 50 minutes in visible *light*. The red color (left) is CellMask™ Deep Red, a plasma membrane stain, and the green color (center) is fluorescence from PPE-Th. The plasma membrane stain within the cell indicates that the plasma membrane has been compromised. The presence of polymer fluorescence within the nucleus and the bulges in the nuclear membrane (denoted by white arrows) indicate that the integrity of the nuclear membrane is also compromised. The scale bar in the merged image (right) is 20 μm .

Figure 4-5 shows an epithelial cell after a 1-hour exposure to the thiophene polymer. This particular cell is undergoing mitosis, and the polymer has localized to the chromosomes lined up at the center of the cell. The cell is in metaphase, when the chromosomes are aligned at the equator of the spindle. The breakdown of the nuclear envelope occurred in the previous phase of mitosis (prometaphase). As shown in Figure 4-6, mammalian cells spend the majority of the time in interphase, when the chromosomes are within the nuclear membrane. Together, Figures 4-3 and 4-4 suggest that the polymer is bound to the plasma membrane in the dark, and upon the addition of light, the polymer disrupts the plasma membrane and the nuclear membrane. Further, the polymer appears to preferentially bind to DNA.

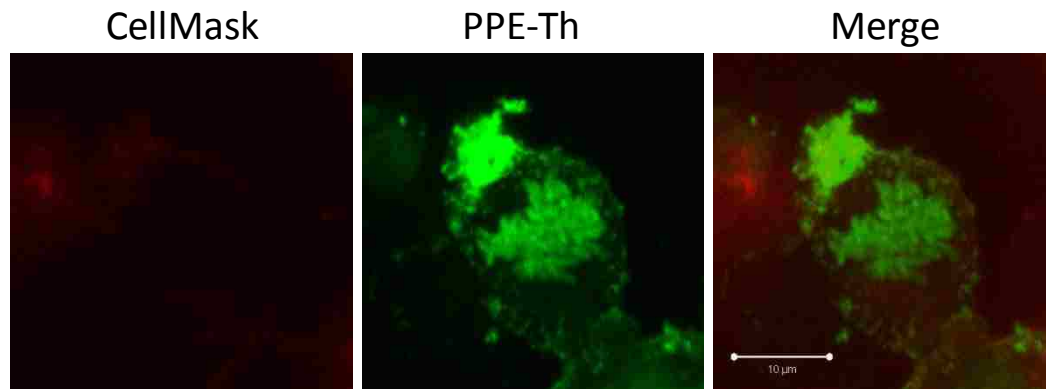


Figure 4-5. This maximum intensity projection of a 3D confocal microscope image stack shows an epithelial cell after a 1-hour exposure to 10 $\mu\text{g}/\text{mL}$ PPE-Th with the final 50 minutes in visible *light*. The red color (left) is CellMask™ Deep Red, a plasma membrane stain, and the green color (center) is fluorescence from PPE-Th. This cell is undergoing mitosis, as indicated by the chromosomes aligned at the equator of the spindle. The scale bar in the merged image (right) is 10 μm .

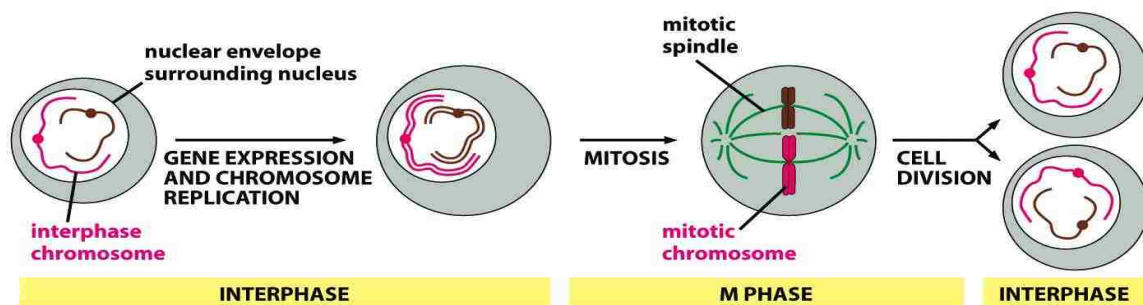


Figure 4-6. Comparison of chromosome location in M phase and interphase (Alberts 2008). The majority of a mammalian cell's lifetime is spent in interphase. Chromosomes are within the nuclear envelope unless the cell is undergoing mitosis.

4.3.2 Co-localization of oligomers and endoplasmic reticulum

Figure 4-7 shows epithelial cells after a 4-hour exposure to the thiophene-substituted oligomer, with and without the final 50 minutes in ultraviolet light. In both light and dark conditions, the oligomer has entered the cell and localized to the endoplasmic reticulum (ER), as evidenced by the co-localization of oligomer and ER-Tracker dye. However, the addition of light results in detergent-like action on the ER. The ER appears to be dissolved into numerous membrane-bound structures. The detergent-like action of light and the oligomer favors dissolution of the ER membrane over the plasma membrane, as the dissolved ER is retained, at least initially, within the plasma membrane. Figure 4-8 shows similar effects of EO-OPE-1-Th on epithelial cells after only a 1-hour exposure, with and without the final 50 minutes in ultraviolet light. Figure 4-9 compares epithelial cells after exposure to the non-substituted oligomer, EO-OPE-1-C2, and cells after exposure to the thiophene-substituted oligomer, EO-OPE-1-Th. Initial results indicate that EO-OPE-1-Th and EO-OPE-1-C2 act by a similar mode of action, localization to the ER and subsequent detergent-like action upon the addition of light.

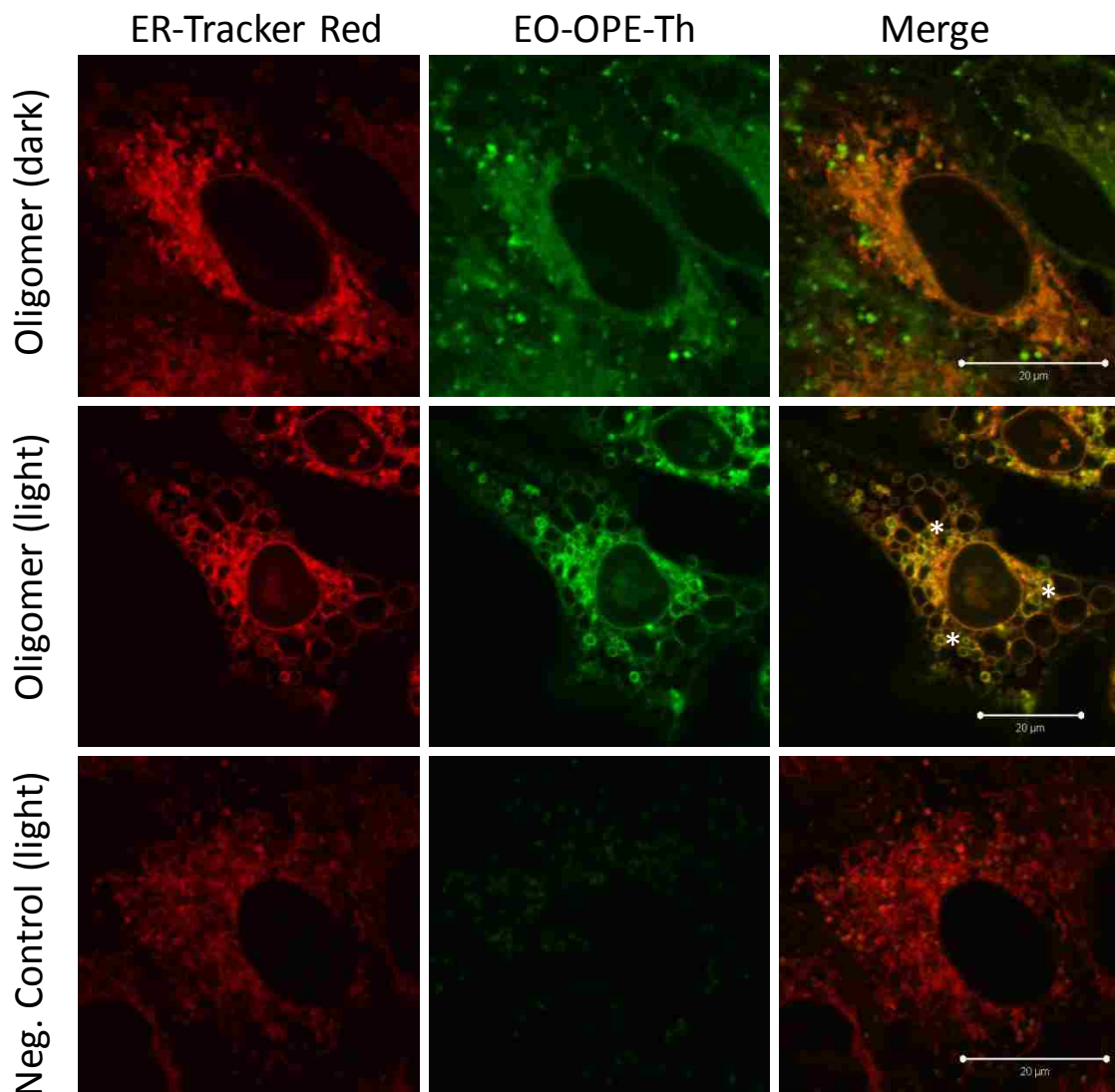


Figure 4-7. Confocal microscope images of epithelial cells after a 4-hour exposure to 10 $\mu\text{g}/\text{mL}$ EO-OPE-1-Th with the last 50 minutes in the *dark* (top row) or *UV light* (middle row). The negative control (bottom row) shows the same epithelial cells without polymer exposure after 50 minutes in visible light. The red color (left column) is ER-Tracker™ Red, an endoplasmic reticulum dye, and the green color (center column) is fluorescence from EO-OPE-1-Th. In both the dark and light, the oligomer is co-localized with the ER. The addition of light results in numerous membrane-bound structures, as indicated by the white asterisks, consistent with detergent-like action on the ER. The scale bars in the merged images (right column) are 20 μm .

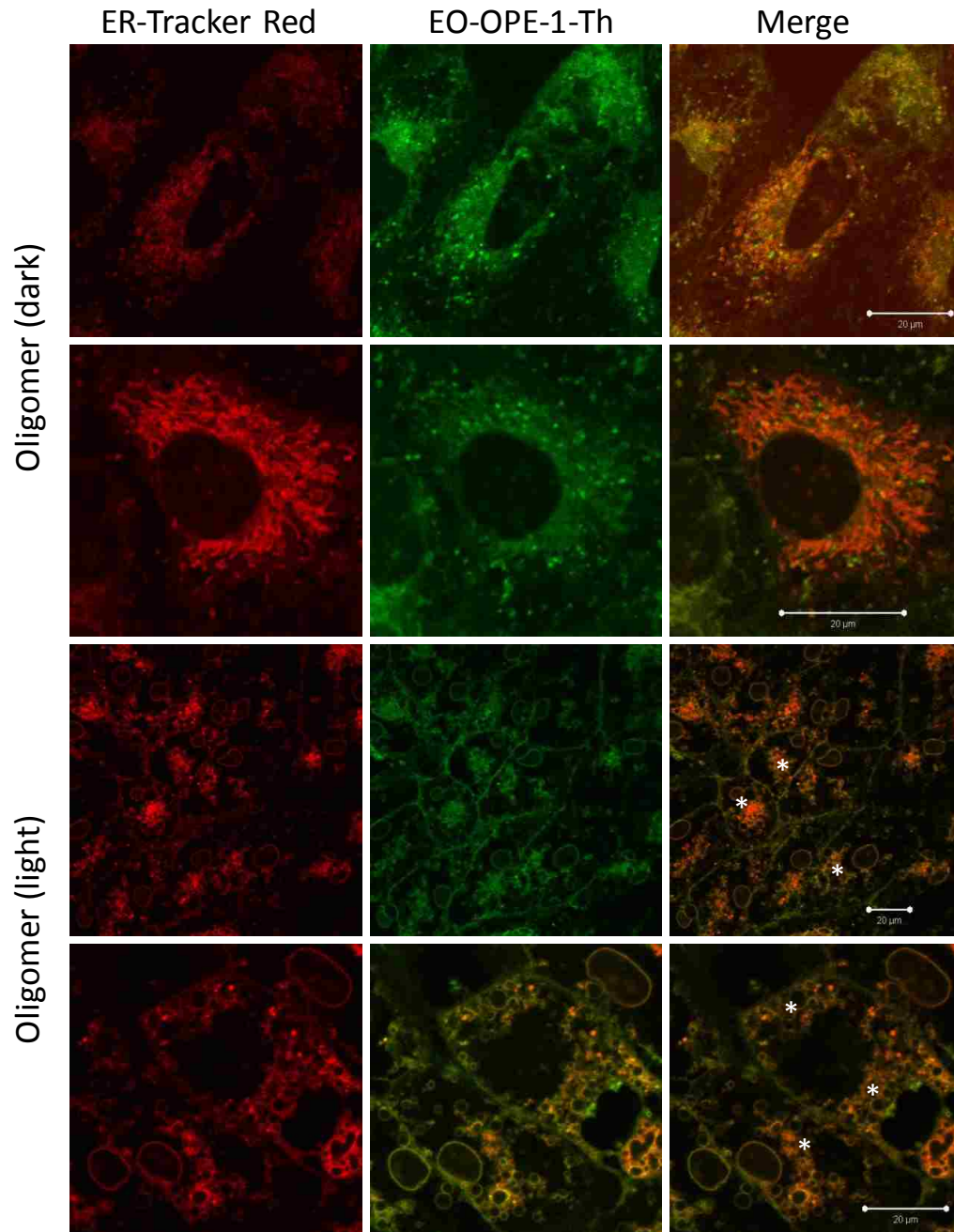


Figure 4-8. Confocal microscope images of epithelial cells after a 1-hour exposure to 10 $\mu\text{g}/\text{mL}$ EO-OPE-1-Th with the last 50 minutes in the *dark* (upper two rows) or UV *light* (lower two rows). The red color (left column) is ER-Tracker™ Red, an endoplasmic reticulum dye, and the green color (center column) is fluorescence from EO-OPE-1-Th. As in Figure 4-7, the oligomer is co-localized with the ER and the ER is dissolved into numerous membrane-bound structures (indicated by white asterisks). The plasma membrane remains intact enough to contain the dissolved ER. The scale bars in the merged images (right column) are 20 μm .

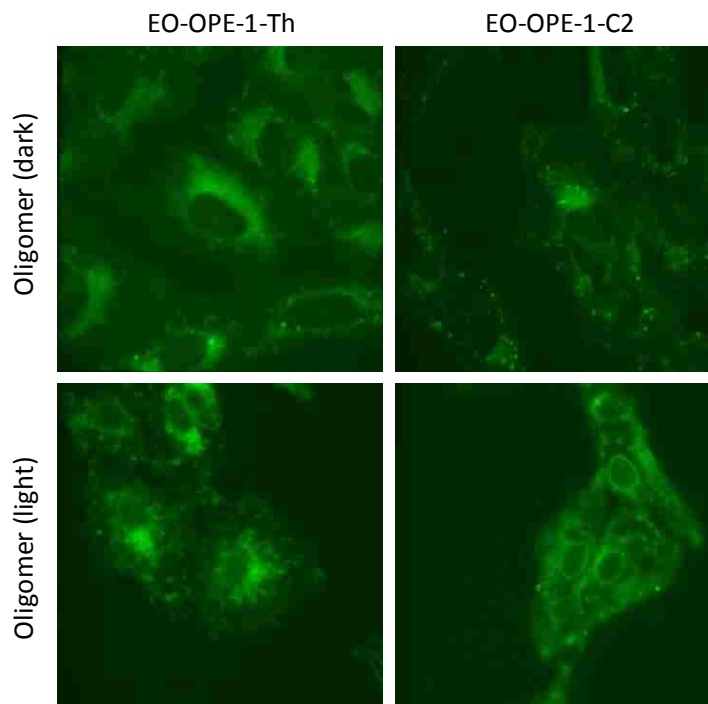


Figure 4-9. Wide-field images of epithelial cells after a 4-hour exposure to EO-OPE-1-Th (left column) or EO-OPE-1-C2 (right column), with the last 50 minutes in the *dark* (top row) or *UV light* (bottom row). The green color is fluorescence from the oligomers. The cells exposed to EO-OPE-1-C2 have structures similar to those exposed to EO-OPE-1-Th. EO-OPE-1-C2 appears to affect epithelial cells by the same mode of action as EO-OPE-1-Th, which localizes to the ER and dissolves it upon the addition of light.

4.3.3 Comparison of different cell types

Figure 4-10 compares epithelial cells and endothelial cells after a 4-hour exposure to EO-OPE-1-Th in dark and light conditions. In the dark, EO-OPE-1-Th has localized to the ER of both cell types. In the light, EO-OPE-1-Th has begun to dissolve the ER in the endothelial cells, but the damage appears to be less extensive than that observed in the epithelial cells under the same conditions. The mode of action of EO-OPE-1-Th is the same in both epithelial and endothelial cells, therefore, independent of cell type.

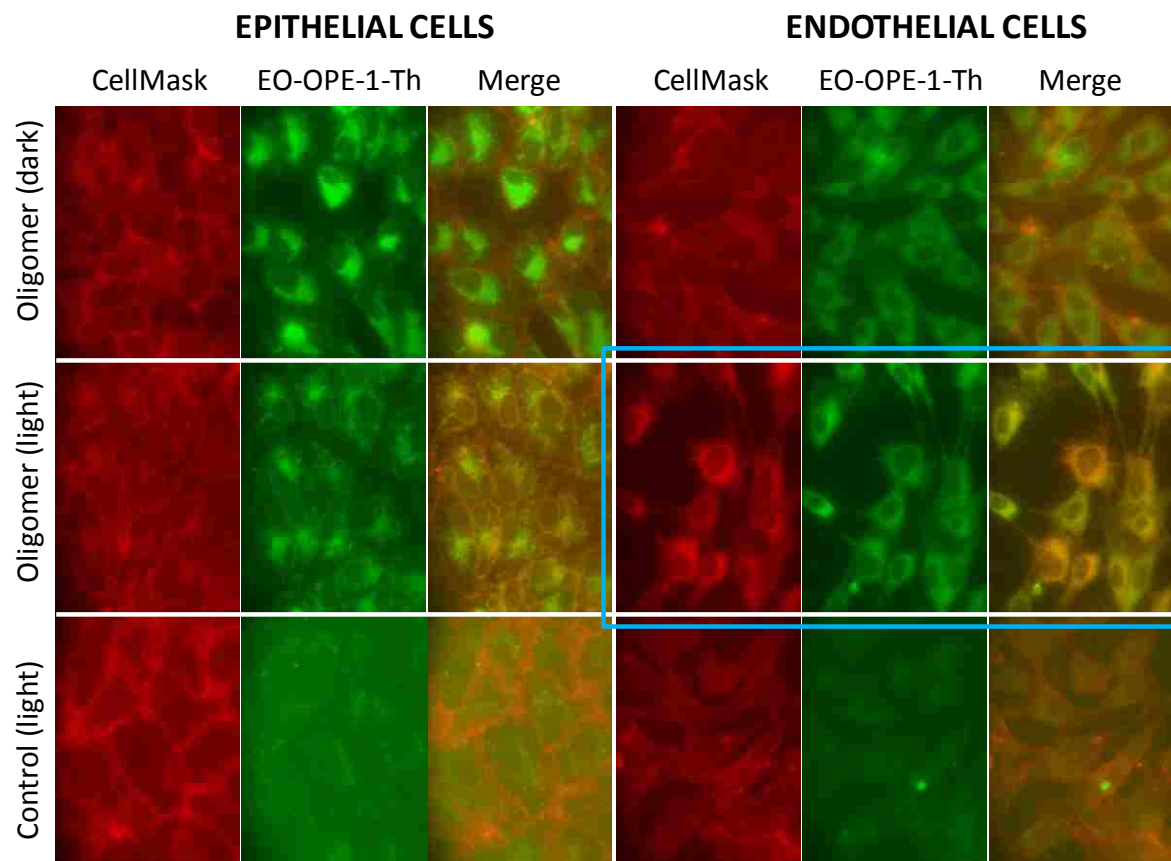


Figure 4-10. Wide-field images of epithelial and endothelial cells after a 4-hour exposure to 10 $\mu\text{g}/\text{mL}$ EO-OPE-1-Th with the last 50 minutes in the *dark* (top row) or UV *light* (middle row). The negative control (bottom row) shows the same epithelial cells without polymer exposure after 50 minutes in visible light. The red color (left column) is ER-Tracker™ Red, an endoplasmic reticulum dye, and the green color (center column) is fluorescence from EO-OPE-1-Th. In both cell types, the oligomer is localized to the ER and the ER is dissolved to some extent with the addition of light. The endothelial cells exhibit less ER damage with light (see images in blue box) and appear to be more robust than the epithelial cells under the same conditions.

4.4 Summary

In summary, epithelial cells were closely examined after exposure to three phenylene-ethynylene compounds: PPE-Th, EO-OPE-1-Th, and EO-OPE-1-C2. In the dark, the PPE-Th polymer accumulates at the cell membrane, but no cellular damage is apparent. After the addition of light, the PPE-Th polymer enters the cell, including the nucleus, but the morphology is largely intact. In the dark, the two oligomers studied here, EO-OPE-1-Th and EO-OPE-1-C2, localize to the ER. However, the addition of light after oligomer exposure dramatically changed the internal cellular structure, as evidenced by widespread detergent-like action on the ER. In all cases, the addition of light changed the effects of the compounds on the mammalian cells.

The modes of action of these compounds appear to be governed primarily by length. Both PPE-Th and EO-OPE-1-Th have thiophene substitutions and quaternary ammonium groups (refer to Figure 4-2), yet affect mammalian cells very differently. The key difference between PPE-Th and EO-OPE-1-Th is the number of phenylene ethynylene repeat units. Further, the oligomers, which each have three aryl rings, act via the same mode of action despite one having a thiophene substitution and one not.

The observed modes of action do not necessarily limit applications where the polymers or oligomers contact mammalian cells. In fact, the DNA localization observed for PPE-Th and the ER localization observed for EO-OPE-1-Th and EO-OPE-1-C2 hold promise in terms of using these compounds for live-cell imaging. For example, the oligomers could be used in the same types of

applications as the ER-Tracker™ dyes are currently used. The structure of EO-OPE-1-Th is remarkably similar to one of the ER-Tracker™ dyes, ER-Tracker™ Blue-White, shown in Figure 4-10. Both EO-OPE-1-Th have two phenyl rings with a five-sided ring in between, and one or more end groups containing nitrogen and methyl groups.

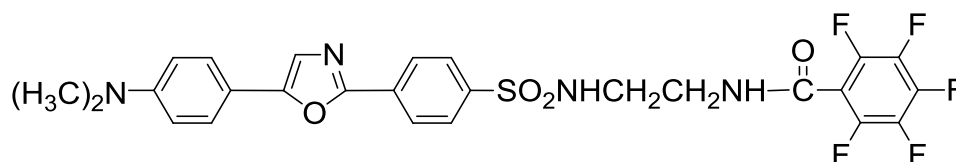


Figure 4-11. Structure of ER-Tracker™ Blue-White.¹⁰⁸ This dye has a chemical structure similar to EO-OPE-1-Th. Like the ER-Tracker™ Red shown in Figures 4-7 and 4-8, it is used to label the endoplasmic reticulum for live cell imaging.

Interestingly, ER-Tracker™ Red and ER-Tracker™ Green are drug conjugates glibenclamide BODIPY® FL and glibenclamide BODIPY® TR, respectively. Glibenclamide (glyburide), is a drug taken by diabetic patients to correct hyperglycemia.¹⁰⁹ Intracellular drug delivery is another possible application for these compounds, particularly the EO-OPEs. Cell-penetrating peptides and mimics, introduced in Section 4.1, are being developed for applications in drug delivery.¹¹⁰ Because most drugs with intracellular targets enter the cell via endocytosis, these drugs are subject to degradation by the acidic environment of the lysosomes.¹¹¹ Circumventing the endocytotic pathway provides new applications for pH-sensitive drugs. Cell-penetrating peptides and mimics facilitate entry of drugs into the cell, either by directly attaching drug ‘cargo’ to the peptide¹¹² or by causing non-cytotoxic membrane disruption.

CHAPTER 5 – CONCLUSIONS AND FUTURE DIRECTIONS

5.1 Conclusions

5.1.1 Review of experimental methods

This work examined toxicity of phenylene ethynylene compounds to mammalian cells at three levels. The three studies span distances from hundreds of nanometers at the intracellular level to multi-layered tissue constructs almost 10 mm in size consisting of more than a million cells. An overview of the three studies, cytotoxicity testing of cell monolayers, skin irritation testing of tissues, and intracellular co-localization is shown in Figure 5-1 below.

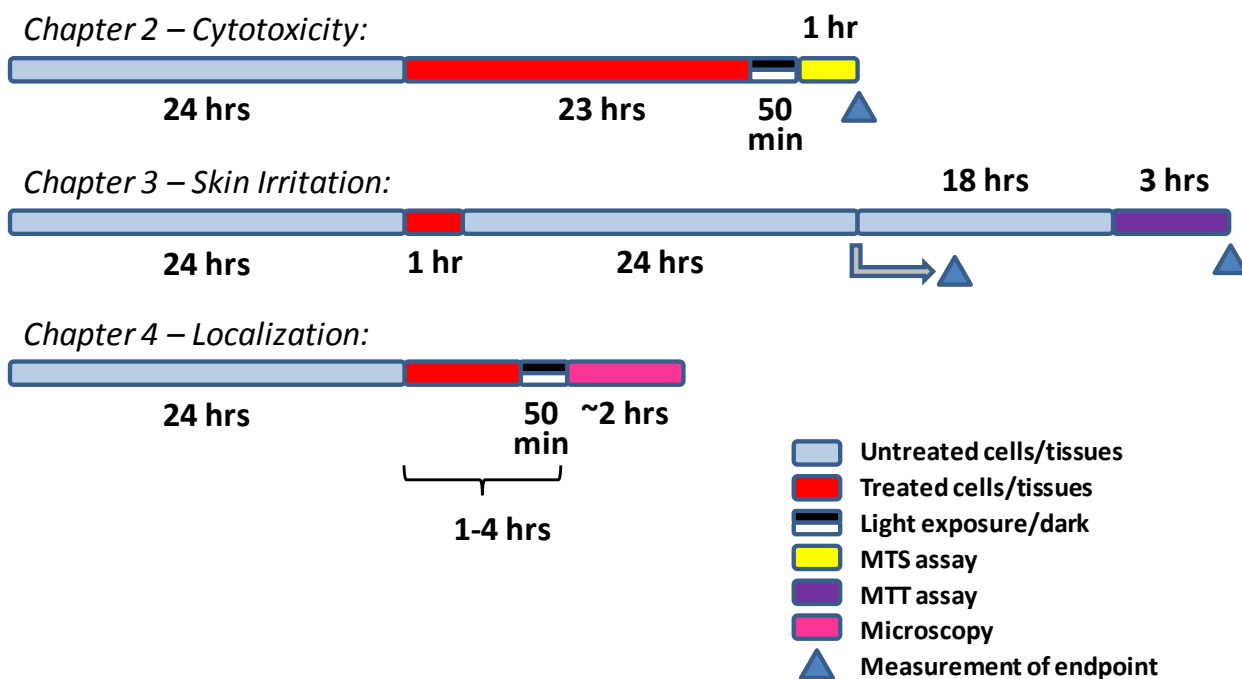


Figure 5-1. Comparison of experimental techniques described in the three previous chapters.

Eight phenylene ethynylene compounds, two polymers and six oligomers, were selected for initial studies based on biocidal activity and diversity of repeat unit number and functional groups. In the initial cytotoxicity studies, *endothelial* cells were exposed to these polymers and oligomers at concentrations from 1-100 $\mu\text{g}/\text{mL}$ for 24 hours. During the last 50 minutes of the 24-hour exposure period, half of the cells were irradiated with either visible or ultraviolet light, depending on the compound. Following irradiation, the cells were assayed for viability relative to untreated cells. To better approximate external (e.g. skin) exposure, *epithelial* cells were assayed for cytotoxicity in the same manner.

To further mimic skin exposure in the closest possible manner *in vitro*, eight compounds (two polymers and six oligomers) and two types of electrospun mats were selected for skin irritation testing using tissues derived from human epidermal keratinocytes. The test substances were applied directly to the tissue surface for a one-hour period. Based on the results of the cytotoxicity studies, skin irritation testing, and complementary techniques, three of the eight compounds, one polymer and two oligomers, were chosen for additional study with co-localization. The three compounds were included in growth media above epithelial cell monolayers for one to four hours, stained with membrane- or organelle-specific dyes to co-localize the polymer/oligomer and the nearest membrane/organelle, and viewed using fluorescence microscopy.

5.1.2 Conclusions from cytotoxicity testing of cell monolayers

Relative viabilities of two cell types were compared among eight compounds with respect to light or dark conditions and five concentrations (160

subsets of data). As expected, concentration plays the largest role in determining viability. At low concentrations, light has a negligible effect on cell viability. Above a threshold concentration which varies from compound to compound, light continues to affect viability, but concentration effects are predominant. At intermediate concentrations (5-10 µg/mL for most compounds), the interplay between light and the light-activated compounds is very important.

Viability trends were consistent across cell types, therefore the mode of action of mammalian cell killing appears to be independent of mammalian cell type, thus related to basal cell function. For applications below cytotoxic concentrations, these compounds are safe for mammalian cells. The concentrations at which the longer S-OPEs and the DABCO-containing compounds are cytotoxic are much higher than for the shortest S-OPE, PPE-Th, and the remaining two EO-OPEs, thus these compounds have the widest range of concentrations available for potential applications.

5.1.3 Conclusions from skin irritation testing of tissues

Following an established protocol for skin irritation testing, growth media samples were taken from the tissues 24 hours following exposure and viability of the tissues was assayed 42 hours following exposure. The media samples were later tested for cytokines, proteins produced in response to tissue irritation. Viability (MTT) and cytokine (IL-1α) assays concluded that all oligomers were non-irritants up to the highest tested concentration, 50 µg/mL. PPE-DABCO and PPE-Th were non-irritants up to the highest tested concentrations, 924 µg/mL

and 100 µg/mL, respectively. The poly(caprolactone) (PCL) and PCL/EO-OPE-1-Th ES mats also did not induce skin irritation.

The lack of skin irritation for all substances, as measured by two endpoints, alleviates initial safety concerns for products based on these polymers and oligomers, both in solution and as electrospun mats. Solution-based products could include disinfectant sprays, wipes, and paints. Mat-based products could include wound dressings, fabrics for hospitals and clinics, and filters.

5.1.4 Conclusions from intracellular co-localization studies

Using fluorescence microscopy, epithelial cells were closely examined after exposure to three phenylene ethynylene compounds: PPE-Th, EO-OPE-1-Th, and EO-OPE-1-C2. In the dark, the PPE-Th polymer accumulates at the cell membrane, but no cellular damage is apparent. After the addition of light, the PPE-Th polymer enters the cell, including the nucleus, but the morphology is largely intact. In the dark, the two oligomers studied here, EO-OPE-1-Th and EO-OPE-1-C2, localize to the ER. However, the addition of light after oligomer exposure dramatically changed the internal cellular structure, as evidenced by widespread detergent-like action on the ER. In all cases, the addition of light changed the effects of the compounds on the mammalian cells.

The three compounds were successfully localized to two distinct locations within the cell, indicating that at least two modes of action are possible for these compounds. The modes of action of these compounds appear to be governed primarily by length. Both PPE-Th and EO-OPE-1-Th have thiophene

substitutions and quaternary ammonium groups, yet affect mammalian cells very differently. The key difference between PPE-Th and EO-OPE-1-Th is the number of phenylene ethynylene repeat units. The observed modes of action do not necessarily limit applications where the polymers or oligomers contact mammalian cells. In fact, the DNA localization observed for PPE-Th and the ER localization observed for EO-OPE-1-Th and EO-OPE-1-C2 hold promise in terms of using these compounds for live-cell imaging. Intracellular drug delivery is another possible application for these compounds. Cell-penetrating peptides and mimics, some of which are also antimicrobial peptides and mimics, are being developed to facilitate entry of pH-sensitive drugs into the cell. The next sections will suggest possible future directions for these interesting and unique antimicrobial compounds, including a new drug-based application.

5.2 Future Directions

5.2.1 Refining the mode of action

Co-localization

Co-localization experiments have been conducted for the thiophene-substituted polymer, PPE-Th, and two “end-only” oligomers, EO-OPE-1-Th and EO-OPE-1-C2. Five other compounds have been discussed within this dissertation, and could be tested similarly. These compounds include one additional “end-only” oligomer, EO-OPE-1-DABCO; three symmetric oligomers, S-OPE-1(H), S-OPE-2(H), and S-OPE-3(H); and one DABCO-functionalized polymer, PPE-DABCO.

The intent of initial co-localization studies was to locate the test compound in relation to the cell membrane. However, having established that the polymer and oligomers are entering mammalian cells, the time scale of entry and specific route to the localized membrane or organelle (e.g. via endocytosis or a non-endocytotic pathway) are the next research questions to address. Endocytosis is an energy-dependent process, thus energy dependence of oligomer entry into the cell could be established by comparing experiments at 37° C and 4° C, as done by Tezgel et al. for a protein transduction domain mimic.⁵³

Flow Cytometry

Co-localization experiments have established that the “end-only” thiophene-substituted oligomer penetrates the plasma membrane of bovine aortic endothelial cells and Vero cells after a 4-hour exposure in dark or light conditions. Viability assays conducted on monolayers of the same cell types confirm that the majority of cells are dying under the same conditions. Co-localization experiments visualize cells at the organelle layer and include perhaps ten cells in a given image. Viability assays provide information for tens of thousands of cells,⁶⁶ but provide no specific information about why viability has been affected. Flow cytometry combines the advantages of both techniques. By utilizing the same fluorescent dyes employed in co-localization, flow cytometry could provide correlated data for as many or more cells queried by viability assays.⁵³ Some advanced flow cytometers are even capable of imaging each cell as it passes through the system. Further, flow cytometry results for mammalian

cells would allow for directly comparison of live/dead percentages to previously published results for bacteria.^{53, 59, 113}

Molecular Dynamics

While localization studies have indentified relative polymer-membrane locations, the mechanism of entry (or lack of) cannot be visualized on any practical level. Therefore, simulated membrane insertion studies could be performed using a PC-based molecular dynamics software package, such as NAMD. To facilitate comparison with experimental conditions, MD simulations should utilize a constant number of molecules (within each run), constant 37 °C temperature, and constant 1 atm pressure. The volume element would contain a hydrated lipid bilayer, and one or more of the same oligomer molecules. The hydrated bilayer should have physiologically relevant molecular spacing and composition. Oligomers (rather than polymers) should be simulated, because they have far fewer atoms than the polymers. The oligomer should be given an initial orientation with respect to the membrane and an initial velocity toward the membrane.

Two sets of studies could be undertaken – constant orientation (with relative energies as the output) and minimum energy (with relative orientations as the output). Understanding preferred oligomer orientation with respect to the bilayer may give insight into the mechanism of action. For antimicrobial peptides, peptide orientation – perpendicular to the membrane bilayer, parallel to the bilayer, or somewhere in between perpendicular and parallel – is directly related to models of membrane disruption. See Figure 5-2 for a visual

explanation of four models of membrane disruption: barrel-stave pore, carpet (detergent-like) mechanism, toroidal pore, and disordered toroidal pore.

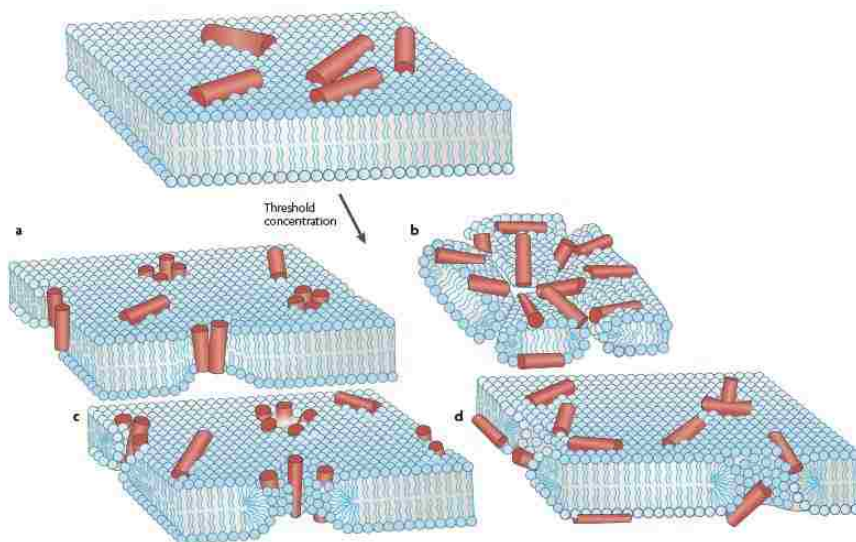


Figure 5-2. Four proposed models of antimicrobial peptide membrane disruption: (a) barrel-stave pore, (b) carpet mechanism, (c) toroidal pore, and (d) disordered toroidal pore models.¹¹⁴

For the constant orientation studies, there are three possible oligomer orientations for symmetric oligomers: end first (phenyl rings are normal to bilayer), side first-parallel (phenyl rings are parallel to bilayer), and side first-perpendicular (phenyl rings are perpendicular to the bilayer). Asymmetric oligomers have an additional possible ‘end first’ orientation because they have two different end groups. Initial simulations on a computer cluster are currently underway in the Whitten Group (Eric Hill, unpublished results).

Depending on the outcome of initial simulations, more complex studies may be undertaken. The more complex studies could be more complex in terms of testing longer-chain polymers (vs. only testing oligomers), longer time periods

(e.g. 10 ns vs. 100 ps), smaller time steps, and/or more molecules per volume element. Running simulations for longer time periods may be useful if the oligomer embeds in the membrane. Smaller time steps could provide additional information if the oligomer appears to undergo a very rapid conformation change in close proximity to the lipid bilayer. Adding more oligomer molecules per volume element would provide information about concentration effects.

5.2.2 Product safety

Phototoxicity

In terms of experimental set-up, the cytotoxicity studies conducted in both light and dark conditions are similar to phototoxicity assays. The intent of the cytotoxicity studies was to explore the test compounds' effects on mammalian cells under conditions correlating to maximum and minimum biocidal activity, which in turn correlate to particular wavelengths of light. However, neither the cell types (bovine aortic endothelial cells, Vero cells) nor light sources (mini light box, UV lamp) used in our studies to date match protocols widely found in the literature.¹¹⁵⁻¹¹⁷ Therefore, our studies cannot be directly compared to published phototoxicity results for other compounds. Published results commonly employ Balb/c 3T3 cells (mouse fibroblasts) and a solar simulator with a specific irradiance (~ 1.7 mW/cm²) as described in OECD Test No. 432.¹¹⁸ The effects of light on cells are widely known for established protocols. Phototoxicity studies should be conducted, particularly for the polymers – which have maximum biocidal activity in visible light, using Balb/c 3T3 cells, a solar simulator, and the neutral red uptake assay.⁶⁹

Skin and Eye Irritation Tests

As discussed in Chapter 3, EpiDerm™ tissues were used to test for skin irritation. EpiDerm™ models the upper layers of human skin. As skin is a common route of exposure for many products, testing for skin irritation is a logical first step in product formulation. However, testing for eye irritation and repeating skin irritation testing with final product formulation are also important. MatTek offers additional 3D tissue models, including models based on ocular, airway, vaginal, oral and gingival tissues.¹¹⁹

Animal Testing

A tiered approach should be taken in testing new antimicrobial products, testing at the cell or tissue level prior to whole animals whenever possible.¹²⁰⁻¹²¹ However, should product development proceed, testing on a small number of animals becomes a necessary part of the regulatory approval process. In the United States, drugs and biomedical devices, including devices as simple as bandages, are regulated by the Food and Drug Administration. The responsibility for regulating pesticides is shared among the Food and Drug Administration, Department of Agriculture, and Environmental Protection Agency. Consumer products are regulated by the Consumer Product Safety Commission. Involving such regulatory agencies early in the product development cycle will minimize animal testing and facilitate approval.

Acquired Bacterial Resistance

The chief advantage of antimicrobial polymers is that they tend to act via a non-specific mechanism and can therefore effectively kill a wide variety of organisms including Gram-positive bacteria, Gram-negative bacteria, viruses, and fungi. However, if microorganisms are able to defeat this non-specific killing mechanism, antibiotic-resistant, biocide-resistant microbes could feasibly exist, making these microbes virtually impossible to kill. Long-term studies should be undertaken to ensure bacteria are not resistant to biocides incorporated into future products.

Bacterial resistance to biocides can be either innate or acquired. Innate resistance refers to how difficult it is to kill certain microorganisms over others. For example, Gram-negative bacteria and mycoplasma are generally harder to kill than Gram-positive bacteria due to their outer cell membrane and waxy coating, respectively. Acquired resistance refers to phenotypic or genotypic differences acquired by bacteria after exposure to biocides. Phenotypic resistance (e.g., adaptation to nutrient limitation) is generally not stable¹²²⁻¹²³, so it is less of a concern long term. However, genotypic differences, acquired by mutation or gene transfer, persist and become a threat to biocide effectiveness. Innate resistance is addressed by initial product design.

Biocide testing against biofilms, which are notoriously resistant to biocides, is currently underway in the Whitten Group.¹²⁴ Acquired resistance due to mutation can sometimes be induced by growing bacteria in sub-MIC (minimum inhibitory concentration) biocide concentrations, then gradually

increasing biocide concentration.¹²⁵ Acquired resistance due to gene transfer is more difficult to create in a laboratory setting. Exposing susceptible bacteria to bacteria resistant to biocides that have the same mode of action as those under test could create bacteria resistant to both biocides. Bacterial strains resistant to quaternary ammonium compounds (QACs) have been isolated,¹²⁶ and could be used to test for co-resistance.

5.2.3 New application

Several antimicrobial peptides (AMPs) have shown promising anti-cancer activity.¹²⁷⁻¹³⁰ The AMPs that have anti-cancer activity generally fall into two groups: those that preferentially kill cancer cells versus normal mammalian cells, and those that are equally toxic to both cancer and non-cancer cells. The preferential activity is linked to differences between cancer cells and normal cells. Cancer cell membranes have a net negative charge,¹²⁷⁻¹³⁰ a negative membrane potential,^{127, 129} greater membrane fluidity,¹²⁹⁻¹³⁰ and many microvilli¹²⁷⁻¹³⁰ (effectively increasing the surface area available to interact with AMPs).

Antimicrobial peptides tend to be cationic and amphiphilic. However, not all AMPs have a well-defined amphiphilic structure; some short cationic peptides also exhibit antimicrobial activity.¹³⁰ As the phenylene-ethynylene polymers and oligomers are both cationic and antimicrobial, they hold promise in treating cancer and should be tested against various cancer cells. For example, Lee et al. tested buforin IIb for toxicity against 62 human tumor cell lines.¹³¹ Viability of Jurkat and HeLa cells was tested via MTT assay, and the viability of the remaining 60 cell lines was tested via sulforhodamine B assay as part of the Developmental Therapeutics Program of the U.S. National Cancer Institute

(NCI).¹³² The 60 cell lines represent leukemia, melanoma, and cancers of the breast, lung, kidney, colon, ovary, prostate, and central nervous system. The study by Lee et al. includes an exceptionally large number of cell lines. A reasonable preliminary study would be to test the cytotoxicity of one or two of the tumor cell lines in the NCI screen after exposure to the phenylene ethynylene polymers and oligomers, and compare the results to those for normal mammalian cells. If the polymers or oligomers show promising anti-cancer activity in the preliminary study, then a multi-drug resistant tumor cell line should be included in subsequent testing. Testing the multi-drug resistant cell line would ascertain effectiveness against cancer cells that are harder to kill with traditional chemotherapies.

If the phenylene ethynylene compounds selectively kill cancer cells over normal mammalian cells, then it becomes important to understand the mode or modes of action for anti-cancer activity. Including a tumor cell line with elevated levels of cholesterol-rich lipid rafts¹³³ in cytotoxicity testing would help determine if the observed anti-cancer activity is dependent on membrane fluidity (or lack thereof). Microscopy, flow cytometry, and/or apoptosis assays could be used to postulate a mode of action for any observed anti-cancer activity. Previously observed modes of action for anti-cancer activity include cell membrane lysis, mitochondrial membrane lysis (resulting in release of cytochrome c and subsequent apoptosis), and altered gene expression.¹³⁰

APPENDIX

A.1 Terminology

Before discussing the wide variety of chemicals that kill microorganisms, it is helpful to understand the terminology widely used in the relevant literature.¹³⁴⁻
¹³⁵ The terms ‘antimicrobial’ and ‘antibacterial’ are used interchangeably, and generally refer to a chemical that kills bacteria. Biocides kill bacteria, but may also act against fungi, viruses, and mammalian cells, depending on the context. ‘Selective’ biocides preferentially kill bacteria, fungi, and/or viruses over mammalian cells.⁴¹ Disinfectants attack the same types of microorganisms as biocides. Sterilants are unique in that they are effective against bacterial spores. Antimicrobial agents, antibacterial agents, biocides, sterilants, and disinfectants are used on inanimate surfaces. Antiseptics are biocides for external human use, either for hand hygiene or for topical treatment/prevention of infection. Antibiotics are for internal human use and are generally not termed biocides.

A.2 Development of Antibiotics

Penicillin, the first modern antibiotic, was discovered by Fleming in the late 1920s, and was in widespread use to treat bacterial infections by the 1940s, largely due to the war effort. The sulfonamides, or sulfa drugs, were the first synthetic antibiotics and preceded penicillin in clinical use. See Figure A-1 for a timeline of antibiotic development. Several new classes were developed in the early 1950s: phenypropanoids (e.g. chloramphenicol), tetracyclines, aminoglycosides (e.g. streptomycin), and macrolides (e.g. erythromycin).

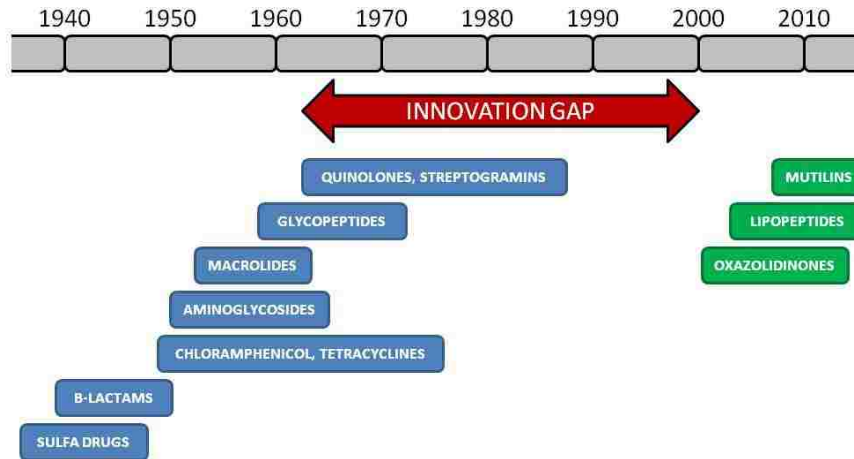

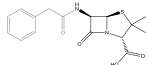
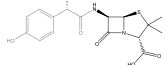
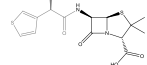
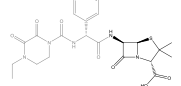
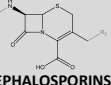
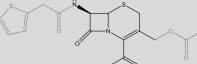
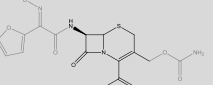
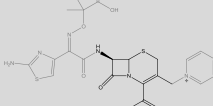
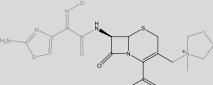
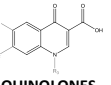
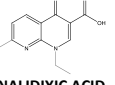
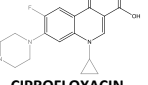
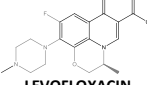
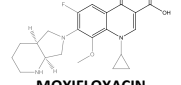
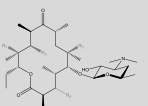
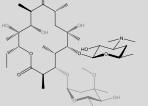
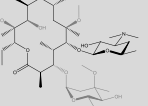
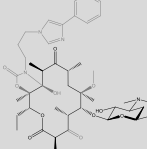
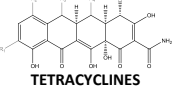
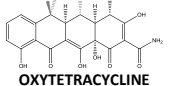
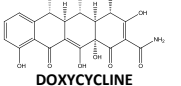
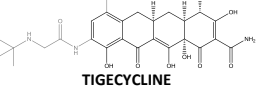


Figure A-1. Timeline of antibiotic development.¹ No new classes of antibiotics were developed between the early 1960s and the introduction of the oxazolidinones in 2000.

Between 1955 and 1962, development of new classes of antibiotics slowed significantly. Only glycopeptides (e.g. vancomycin), quinolones, and streptogramins were developed during this seven-year period. However, the period that followed was even worse in terms of antibiotic innovation. No new classes of drugs entered the clinic between 1962 and the introduction of the oxazolidinines in 2000. In the mid-2000s, two new classes, the lipopeptides and mutilins, were made available for clinical use.

Of the 12 classes of antibiotics discussed above, only three are synthetic: sulfonamides, quinolones, and oxazolidinones. The remaining classes have natural origins and are synthetically modified as needed. The resulting drugs are termed ‘semi-synthetic.’ Table A-1 below illustrates how successive generations of antibiotics have been modified as bacteria defeat the initial drug. Antibiotic resistance will be covered in more detail in the next section.

Table A-1. Successive generations of antibiotics based on initial scaffolds.¹

ANTIBIOTIC CLASS	GENERATION 1 ----->	GENERATION 2 ----->	GENERATION 3 ----->	GENERATION 4
 PENICILLINS (B-LACTAMS)	 PENICILLIN G	 AMOXICILLIN	 TICARCILLIN	 PIPERACILLIN
 CEPHALOSPORINS (B-LACTAMS)	 CEFALOTIN	 CEFUROXIME	 CEFTAZIDIME	 CEFEPIME
 QUINOLONES	 NALIDIXIC ACID	 CIPROFLOXACIN	 LEVOFLOXACIN	 MOXIFLOXACIN
 MACROLIDES	 ERYTHROMYCIN	 CLARITHROMYCIN	 TELITHROMYCIN	
 TETRACYCLINES	 OXYTETRACYCLINE	 DOXYCYCLINE	 TIGECYCLINE	

A.3 Antibiotic Resistance

Antibiotics are targeted to internal processes specific to bacteria. Figure A-2 shows antibiotic targets in a bacterium and antibiotics or classes of antibiotics that act on these targets. More than half of the antibiotic classes discussed above inhibit protein synthesis. The phenylpropanoids, macrolides, streptogramins, oxazolidinones, and mutilins target the 50s (large) ribosomal subunit. Within the 50s subunit, the drugs target either the decoding center or the protein exit tunnel. Tetracyclines and aminoglycosides interfere with the catalytic site on the 30s (small) ribosomal subunit. The β -lactams (i.e. penicillins and cephalosporins) and glycopeptides affect cell wall biosynthesis. A minority of drugs interacts with other targets: the cell membrane, folic acid biosynthesis, DNA gyrase, and RNA polymerase.

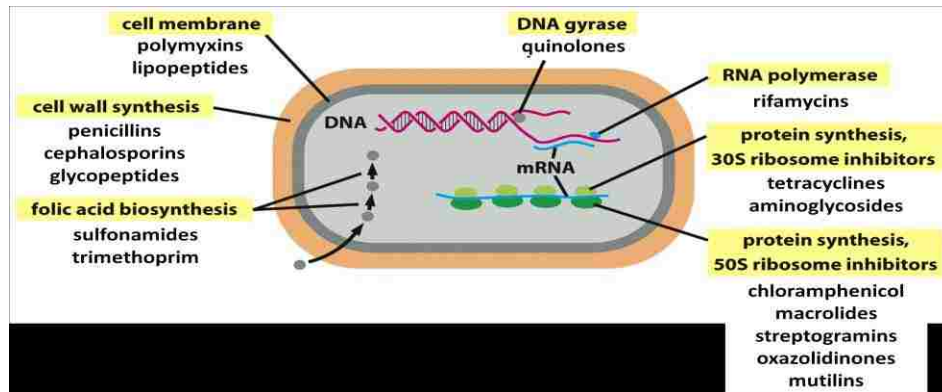


Figure A-2. Antibiotic targets and corresponding drug classes (adapted from 97). Nearly every antibiotic in use today falls into one of the classes depicted above; most target either protein synthesis or cell wall synthesis.

Because antibiotics are so targeted, bacteria have been able to develop new strains that circumvent the desired antibiotic action. As shown in Figure A-3 below, bacteria have three means of becoming drug-resistant: by altering the target enzyme, by expressing a product that binds to the drug, and by up-regulating efflux pumps that lower the drug concentration within the bacteria.

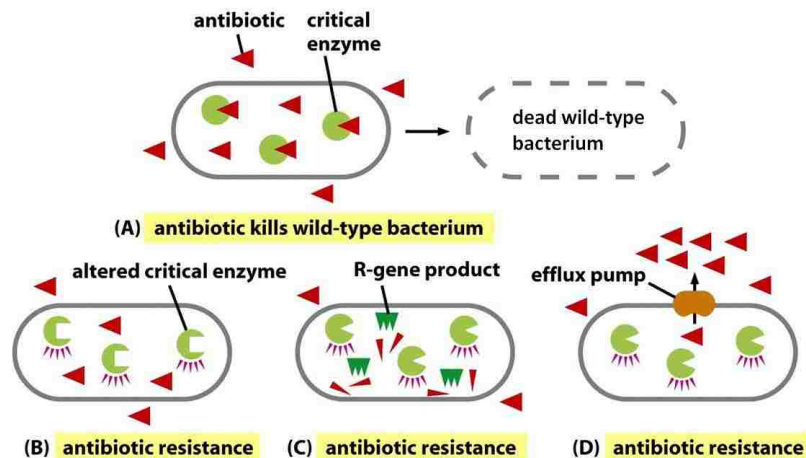


Figure A-3. Mechanisms of antibiotic resistance.⁹⁷ Drug-susceptible bacteria (A) acquire drug resistance in three ways: (B) by altering the enzyme on which the drug acts, (C) by expressing an enzyme that degrades or modifies the drug, and (D) by up-regulating efflux pumps that expel the drug from the cytoplasm.

A.4 Conventional Biocides

Because biocides within the health care setting represent a wide variety of applications (from metals to plastics to fabrics), common biocides in the U.S. clinical setting will be covered here. Further, these biocides tend to be better studied than those in consumer markets and, therefore, are more likely to have a known mechanism for biocide action.

Patient care items and environmental surfaces are sterilized or disinfected based on the nature of the item and the nature of patient contact. Patient care items that contact sterile tissue (e.g. surgical instruments) are critical and must be sterilized prior to use. If an item contact mucous membranes (e.g. gastrointestinal endoscope), then an item is considered semi-critical and must be disinfected with a “high-level” disinfectant. Items that contact intact skin (e.g. blood pressure cuff) are non-critical and are disinfected with “intermediate-level” or “low-level” disinfectants, depending on the presence or absence of visible blood. As outlined in Table A-2 below, all sterilants and disinfectants are effective against Gram-positive and Gram-negative bacteria, but have varying degrees of effectiveness against mycobacteria, bacterial spores, fungi, and viruses.¹³⁴⁻¹³⁵

These sterilants and disinfectants can be classified by general chemical structure into eight types: alcohols, aldehydes, biguanides, chlorine-releasing agents, heavy metals, peroxygens, phenolics, and quaternary ammonium compounds (QACs). Each of these biocide types targets one or more of the following sites: outer layers (cell wall or outer membrane), cytoplasmic

membrane, cytoplasmic constituents, and specific groups.¹³⁶ Mechanisms at these sites include cross-linking; coagulation; increased permeability (of outer or cytoplasmic membranes); decreased proton motive force, electron transport, ATP synthesis, or enzyme activity; and interaction with specific cytoplasmic constituents or groups. Specific mechanisms of biocidal action are identified for each of the eight sterilant and disinfectant types in Table A-3 below. Similar information is presented for antiseptics in Table A-4 below. Where a sterilant or disinfectant may also be used as an antiseptic, its mechanism of action is presented in Table A-3.

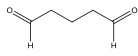
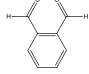
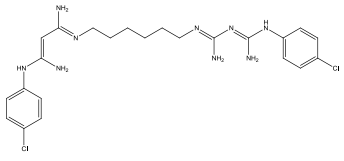
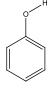
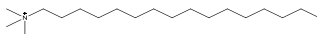
Table A-2. Methods for sterilization and disinfection of patient-care items and environmental surfaces (adapted from ¹³⁴ and ¹³⁵).

Process, method	Activity against ^a						Example(s) (processing time)	Application
	Gram-positive	Gram-negative	Mycobacteria	Bacterial spores	Fungi	Viruses		
<i>Sterilization</i>								
High temperature	+++	+++	+++	+++	+++	+++	Steam (~40 min) and dry heat (1-6 h)	<i>Heat-tolerant critical and semicritical patient-care items (e.g. surgical instruments)</i>
Low temperature	+++	+++	+++	+++	+++	+++	Ethylene oxide gas (~15 h) or hydrogen peroxide gas plasma (~50 min)	<i>Heat-sensitive critical and semicritical patient-care items</i>
Liquid immersion	+++	+++	+++	+++	+++	+++	Chemical sterilants (~50 min-12 h)	<i>Heat-sensitive critical and semicritical patient-care items that can be immersed</i>
<i>High-level disinfection</i>								
Heat automated	+++	+++	+++	++	+++	+++	Pasteurization (~50 min)	<i>Heat-sensitive semicritical patient-care items (e.g. respiratory-therapy equipment)</i>
Liquid immersion	+++	+++	+++	++	+++	+++	Chemical sterilants or high-level disinfectants (10-45 min)	<i>Heat-sensitive semicritical patient-care items that can be immersed (e.g. GI endoscopes)</i>
<i>Intermediate-level disinfection</i>								
Liquid contact	+++	+++	+++	-	++	++	EPA-registered hospital disinfectants with TB label (≥60 s)	<i>Noncritical patient-care items with visible blood (e.g. blood pressure cuff)</i>
<i>Low-level disinfection</i>								
Liquid contact	+++	+++	-	-	+	+	EPA-registered hospital disinfectants without TB label (≥60 s)	<i>Noncritical patient-care items without visible blood (e.g. blood pressure cuff)</i>

EPA, Environmental Protection Agency; GI, gastrointestinal; TB, tuberculocidal.

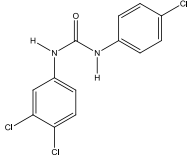
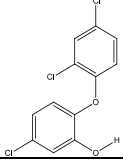
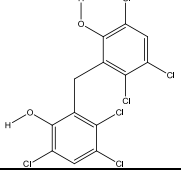
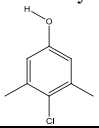
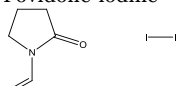
^a+++ , excellent; ++, good (most species); +, fair (some species); -, insufficient or no activity.

Table A-3. Bacterial target sites and mechanisms of chemical sterilants and disinfectants (adapted from ¹³⁶).

Biocide Type	Example(s)	Target Site(s)	Mechanism(s)	Application(s)
Alcohols	Ethanol, CH ₃ CH ₂ OH Isopropyl alcohol, (CH ₃) ₂ CHOH	Cytoplasmic membrane	Increased permeability	Low-level disinfectant, Antiseptic
Aldehydes	Glutaraldehyde 	Outer layers	Cross-linking of cell wall	Sterilant
		Cytoplasmic constituents	General coagulation, nucleic acids	
	Ortho-phthalaldehyde 	Outer layers	Cross-linking of cell wall	High-level disinfectant
		Interaction with specific groups	Amino groups	
Biguanides	Chlorhexidine 	Outer layers	Increased permeability of outer membrane*	Disinfectant, Antiseptic
		Cytoplasmic membrane	Increased permeability, ATP synthesis, inhibition of enzyme activity	
		Cytoplasmic constituents	General coagulation	
Chlorine-releasing agents	OCl ₂ , HOCl, Cl ₂	Outer layers	Increased permeability of outer membrane*	Intermediate-level disinfectant
		Cytoplasmic constituents	Nucleic acids	
		Interaction with specific groups	Thiol, sulfhydryl groups	
Heavy metals	Silver nitrate, AgNO ₃	Cytoplasmic constituents	General coagulation	Disinfectant, Antiseptic
		Interaction with specific groups	Thiol groups	
Peroxygens	Hydrogen peroxide, H ₂ O ₂	Cytoplasmic constituents	Ribosomes	Sterilant, High-level disinfectant
		Interaction with specific groups	Thiol, sulfhydryl groups	
Phenolics	Phenol 	Outer layers	Increased permeability of outer membrane*	Intermediate-level disinfectant
		Cytoplasmic membrane	Increased permeability, PMF and e ⁻ transport chain, inhibition of enzyme activity	
		Cytoplasmic constituents	General coagulation	
QACs	General: [NR ₁ R ₂ R ₃ R ₄] ⁺ X ⁻ Cetrimonium bromide 	Outer layers	Increased permeability of outer membrane*	Low-level disinfectant, Antiseptic
		Cytoplasmic membrane	Increased permeability, PMF and e ⁻ transport chain, inhibition of enzyme activity	
		Cytoplasmic constituents	General coagulation	

PMF, proton motive force; QACs, quaternary ammonium compounds.

Table A-4. Bacterial target sites and mechanisms of antiseptics (adapted from ¹³⁶).

Biocide Type	Example(s)	Target Site(s)	Mechanism(s)
Anilides	General: C ₆ H ₅ NHCOR Triclocarban 	Cytoplasmic membrane	Increased permeability, PMF and e ⁻ transport chain
Bisphenols	Triclosan 	Unknown	Possibly similar to hexachlorophene
	Hexachlorophene 	Cytoplasmic membrane Cytoplasmic constituents	Increased permeability, PMF and e ⁻ transport chain General coagulation
Halophenols	Chloroxylenol 	Unknown	Similar to phenols?
Iodine/iodophors	Iodine (tincture) Povidone-iodine 	Interaction with specific groups	Thiol groups

PMF, proton motive force

A.5 Preliminary Results

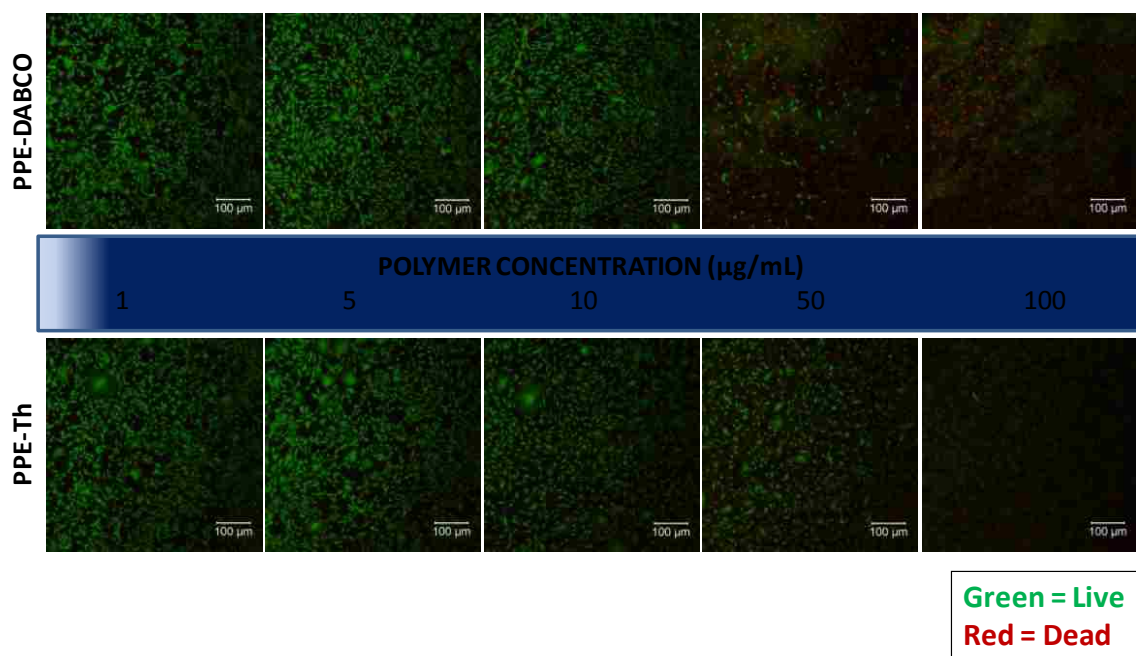


Figure A-4. Merged fluorescence microscopy images of endothelial cells: (top row) after 24-hour exposure to PPE-DABCO in serum-free medium, and (bottom row) after 24-hour exposure to PPE-Th in serum-free medium. More cells are red in the upper row than in the lower row at concentrations $\geq 50 \mu\text{g/mL}$, indicating that PPE-DABCO is more cytotoxic than PPE-Th at these concentrations. The cells have been stained with calcein AM (green, live cells) and ethidium homodimer-1 (red, dead cells). All scale bars are $100 \mu\text{m}$.

A.6 Interference with MTT Assay

Colorimetric assays based on optical measurements, such as the MTT assay, are prone to interference from colored test substances *and* substances that affect the chemical reaction that causes the color change. Specifically, in this case of assessing skin irritation with EpiDerm™ tissues, test substances that stain the tissues *and* test substances that directly reduce MTT can cause interference with the MTT assay.⁷⁵ As discussed in Section 3.2, the MTT assay occurs 42 hours after exposure (and subsequent washing), so having residual test substances present during the assay is unlikely. However, there were two test substances that appeared to discolor the tissues after washing. Tissues exposed to PPE-DABCO stock solution (924 µg/mL) and PPE-Th at 100 µg/mL had a yellowish cast immediately following the wash steps. Two days later, when the MTT assays were performed, these tissues did not have any obvious discoloration. Furthermore, the isopropanol leachate did not appear to be a different color than that of the other tissues exposed to test substances.

To assess for direct MTT reduction, 30 µL of the highest concentration of all liquid test substances was added to 270 µL MTT medium and placed in an incubator (37° C, 5% CO₂, ~90% RH) for one hour. After one hour, the colors of the eight solutions were compared to MTT medium (added at the same time). No change in color was evident in any of the solutions. See Figure A-5 for a photograph of the solutions and the MTT medium after 1 hour incubation.

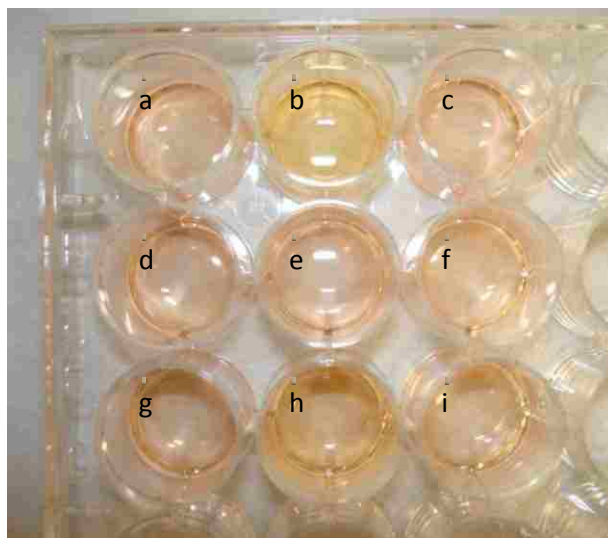


Figure A-5. Colorimetric test for direct MTT reduction by polymer and oligomer solutions. Solutions shown are: a) EO-OPE-1-DABCO, b) EO-OPE-1-Th, c) EO-OPE-1-C2, d) PPE-DABCO stock, e) negative control (media only), f) PPE-Th (100 $\mu\text{g}/\text{mL}$), g) S-OPE-1(H), h) S-OPE-2(H), and i) S-OPE-3(H). The lack of purple color in all solutions indicates that the polymer and oligomer solutions do not reduce MTT. Absorbance readings confirmed visual observations.

Absorbance readings at 570 nm were taken to confirm the lack of color change. Despite initial discoloration of tissues exposed to very high polymer concentrations, no evidence of interference could be seen and the MTT assay is believed to be valid for this particular set of test substances.

The two solid substances were not assessed for interference with the assay. The control electrospun mat was made from poly(caprolactone) (PCL). PCL is a widely-used biomaterial,¹³⁷ and relatively inert in DPBS and assay medium. It is therefore unlikely to interfere with viability assays. The second mat was made from PCL and EO-OPE-1-Th. EO-OPE-1-Th solution was evaluated at a higher concentration than that expected to leach from an electrospun mat.

A.7 MTT Assay Acceptance Criteria

Based on historical manufacturing data, the EpiDerm™ kit manufacturer has established three assay acceptance criteria to serve as quality control checks for the components of the EpiDerm™ Skin Irritation Test Kit. The first criterion is based on the negative controls, the second criterion is based on the negative controls, and the third is based on statistical variability among replicates.

Assay Acceptance Criterion 1

To pass Acceptance Criterion 1, the mean of the absolute optical density at 570 nm of the negative control tissues should be ≥ 1.0 and ≤ 2.5 . As shown in Table A-5 below, all three EpiDerm™ kits used passed this criterion.

Table A-5. Optical densities and relative viabilities of negative controls for each kit.

	<i>Kit 1</i>		<i>Kit 2</i>		<i>Kit 3</i>	
	OD₅₇₀ (NC, raw)	Relative viability \pm SD (%)	OD₅₇₀ (NC, raw)	Relative viability \pm SD (%)	OD₅₇₀ (NC, raw)	Relative viability \pm SD (%)
Mean for Tissue 1	1.9053	106.0	1.7560	89.1	1.3848	104.8
Mean for Tissue 2	1.8035	100.2	1.8198	105.8	1.6377	108.7
Mean for Tissue 3	1.6905	93.8	1.4549	105.1	1.6274	86.5
Mean for Tissues 1-3	1.7977	100.0 \pm 6.1	1.6769	100.0 \pm 9.5	1.5499	100.0 \pm 11.9

Assay Acceptance Criterion 2

To pass Acceptance Criterion 2, the mean of the relative viabilities of the positive control tissues (those exposed to 5% SDS) should be $\leq 20\%$. As shown in Table A-6, the means for the three kits range from 6.2-6.9%, well under 20%.

Table A-6. Relative viabilities of positive controls for each kit.

	<i>Kit 1</i>	<i>Kit 2</i>	<i>Kit 3</i>
	Relative viability ± SD (%)	Relative viability ± SD (%)	Relative viability ± SD (%)
Mean for Tissue 1	8.3	7.2	6.5
Mean for Tissue 2	5.2	6.7	5.9
Mean for Tissues 1 and 2	6.7 ± 2.2	6.9 ± 0.3	6.2 ± 0.4

Assay Acceptance Criterion 3

To pass Acceptance Criterion 3, the standard deviation of the relative viabilities of three replicates should be less than 18%. As shown in Table 3-4 and Table A-6, relative viabilities for all positive controls and all test substances had standard deviations of less than 18% with the exception of EO-OPE-1-Th at 50 µg/mL, which had a standard deviation of 25%. However, even with the large standard deviation, EO-OPE-1-Th at 50 µg/mL had a relative viability so far above the non-irritant/irritant threshold of 50% that the large standard deviation does not risk changing its classification as a non-irritant.

REFERENCES

1. Fischbach, M. A.; Walsh, C. T., Antibiotics for Emerging Pathogens. *Science* **2009**, *325* (5944), 1089-1093.
2. Page, K.; Wilson, M.; Parkin, I. P., Antimicrobial surfaces and their potential in reducing the role of the inanimate environment in the incidence of hospital-acquired infections. *J. Mater. Chem.* **2009**, *19* (23), 3819-3831.
3. Delcour, A. H., Outer membrane permeability and antibiotic resistance. *BBA-Proteins Proteomics* **2009**, *1794* (5), 808-816.
4. Matsuzaki, K., Why and how are peptide-lipid interactions utilized for self-defense? Magainins and tachyplesins as archetypes. *Biochim. Biophys. Acta-Biomembr.* **1999**, *1462* (1-2), 1-10.
5. Hancock, R. E. W.; Sahl, H. G., Antimicrobial and host-defense peptides as new anti-infective therapeutic strategies. *Nat. Biotechnol.* **2006**, *24* (12), 1551-1557.
6. Guani-Guerra, E.; Santos-Mendoza, T.; Lugo-Reyes, S. O.; Teran, L. M., Antimicrobial peptides: General overview and clinical implications in human health and disease. *Clin. Immunol.* **2010**, *135* (1), 1-11.
7. Rivas, L.; Luque-Ortega, J. R.; Fernandez-Reyes, M.; Andreu, D., Membrane-active peptides as anti-infectious agents. *J. Appl. Biomed.* **2010**, *8* (3), 159-167.
8. Trieste, U. d. S. d. <http://www.bbcm.univ.trieste.it/~tossi/amsdb.html> (accessed April 1).
9. Tang, H.; Doerksen, R. J.; Jones, T. V.; Klein, M. L.; Tew, G. N., Biomimetic facially amphiphilic antibacterial oligomers with conformationally stiff backbones. *Chem. Biol.* **2006**, *13* (4), 427-435.
10. Gabriel, G. J.; Maegerlein, J. A.; Nelson, C. E.; Dabkowski, J. M.; Eren, T.; Nusslein, K.; Tew, G. N., Comparison of Facially Amphiphilic versus Segregated Monomers in the Design of Antibacterial Copolymers. *Chem.-Eur. J.* **2009**, *15* (2), 433-439.
11. Breitenkamp, R. B.; Arnt, L.; Tew, G. N., Facially amphiphilic phenylene ethynylenes. *Polym. Adv. Technol.* **2005**, *16* (2-3), 189-194.
12. Arnt, L.; Tew, G. N., New poly(phenyleneethynylene)s with cationic, facially amphiphilic structures. *J. Am. Chem. Soc.* **2002**, *124* (26), 7664-7665.
13. Arnt, L.; Tew, G. N., Cationic facially amphiphilic poly(phenylene ethynylene)s studied at the air-water interface. *Langmuir* **2003**, *19* (6), 2404-2408.
14. Arnt, L.; Tew, G. N., Conformational changes of facially amphiphilic meta-poly(phenylene ethynylene)s in aqueous solution. *Macromolecules* **2004**, *37* (4), 1283-1288.
15. Arnt, L.; Nusslein, K.; Tew, G. N., Nonhemolytic abiogenic polymers as antimicrobial peptide mimics. *J. Polym. Sci. Pol. Chem.* **2004**, *42* (15), 3860-3864.
16. Yang, L. H.; Gordon, V. D.; Mishra, A.; Sorn, A.; Purdy, K. R.; Davis, M. A.; Tew, G. N.; Wong, G. C. L., Synthetic antimicrobial oligomers induce a

- composition-dependent topological transition in membranes. *J. Am. Chem. Soc.* **2007**, *129* (40), 12141-12147.
17. Rennie, J.; Arnt, L.; Tang, H. Z.; Nusslein, K.; Tew, G. N., Simple oligomers as antimicrobial peptide mimics. *J. Ind. Microbiol. Biotechnol.* **2005**, *32* (7), 296-300.
 18. Arnt, L.; Rennie, J. R.; Linser, S.; Willumeit, R.; Tew, G. N., Membrane activity of biomimetic facially amphiphilic antibiotics. *J. Phys. Chem. B* **2006**, *110* (8), 3527-3532.
 19. Tew, G. N.; Clements, D.; Tang, H. Z.; Arnt, L.; Scott, R. W., Antimicrobial activity of an abiotic host defense peptide mimic. *Biochim. Biophys. Acta-Biomembr.* **2006**, *1758* (9), 1387-1392.
 20. Oren, Z.; Shai, Y., A class of highly potent antibacterial peptides derived from pardaxin, a pore-forming peptide isolated from Moses sole fish *Pardachirus marmoratus*. *Eur. J. Biochem.* **1996**, *237* (1), 303-310.
 21. Baker, M. A.; Maloy, W. L.; Zasloff, M.; Jacob, L. S., Anticancer efficacy of magainin2 and analog peptides. *Cancer Res.* **1993**, *53* (13), 3052-3057.
 22. Hamuro, Y.; Schneider, J. P.; DeGrado, W. F., De novo design of antibacterial beta-peptides. *J. Am. Chem. Soc.* **1999**, *121* (51), 12200-12201.
 23. Porter, E. A.; Wang, X. F.; Lee, H. S.; Weisblum, B.; Gellman, S. H., Antibiotics - Non-haemolytic beta-amino-acid oligomers. *Nature* **2000**, *404* (6778), 565-565.
 24. Arvidsson, P. I.; Frackenpohl, J.; Ryder, N. S.; Liechty, B.; Petersen, F.; Zimmermann, H.; Camenisch, G. P.; Woessner, R.; Seebach, D., On the antimicrobial and hemolytic activities of amphiphilic beta-peptides. *Chem. Bio. Chem.* **2001**, *2* (10), 771-773.
 25. Patch, J. A.; Barron, A. E., Helical peptoid mimics of magainin-2 amide. *J. Am. Chem. Soc.* **2003**, *125* (40), 12092-12093.
 26. Ng, S.; Goodson, B.; Ehrhardt, A.; Moos, W. H.; Siani, M.; Winter, J., Combinatorial discovery process yields antimicrobial peptoids. *Bioorg. Med. Chem.* **1999**, *7* (9), 1781-1785.
 27. Fernandez-Lopez, S.; Kim, H. S.; Choi, E. C.; Delgado, M.; Granja, J. R.; Khasanov, A.; Kraehenbuehl, K.; Long, G.; Weinberger, D. A.; Wilcoxon, K. M.; Ghadiri, M. R., Antibacterial agents based on the cyclic D,L-alpha-peptide architecture. *Nature* **2001**, *412* (6845), 452-455.
 28. Liu, D. H.; Choi, S.; Chen, B.; Doerksen, R. J.; Clements, D. J.; Winkler, J. D.; Klein, M. L.; DeGrado, W. F., Nontoxic membrane-active antimicrobial arylamide oligomers. *Angew. Chem.-Int. Edit.* **2004**, *43* (9), 1158-1162.
 29. Zhao, X. Y.; Pinto, M. R.; Hardison, L. M.; Mwaura, J.; Muller, J.; Jiang, H.; Witker, D.; Kleiman, V. D.; Reynolds, J. R.; Schanze, K. S., Variable band gap poly(arylene ethynylene) conjugated polyelectrolytes. *Macromolecules* **2006**, *39* (19), 6355-6366.
 30. Chemburu, S.; Ji, E.; Casana, Y.; Wu, Y.; Buranda, T.; Schanze, K. S.; Lopez, G. P.; Whitten, D. G., Conjugated Polyelectrolyte Supported Bead Based Assays for Phospholipase A(2) Activity. *J. Phys. Chem. B* **2008**, *112* (46), 14492-14499.
 31. Zhou, Z. J.; Corbitt, T. S.; Parthasarathy, A.; Tang, Y. L.; Ista, L. F.; Schanze, K. S.; Whitten, D. G., "End-Only" Functionalized Oligo(phenylene

- ethynylene)s: Synthesis, Photophysical and Biocidal Activity. *J. Phys. Chem. Lett.* **2010**, *1* (21), 3207-3212.
32. Tang, Y. L.; Zhou, Z. J.; Ogawa, K.; Lopez, G. P.; Schanze, K. S.; Whitten, D. G., Photophysics and self-assembly of symmetrical and unsymmetrical cationic oligophenylene ethynylenes. *J. Photochem. Photobiol. A-Chem.* **2009**, *207* (1), 4-6.
33. Tang, Y. L.; Zhou, Z. J.; Ogawa, K.; Lopez, G. P.; Schanze, K. S.; Whitten, D. G., Synthesis, Self-Assembly, and Photophysical Behavior of Oligo Phenylene Ethynylenes: From Molecular to Supramolecular Properties. *Langmuir* **2009**, *25* (1), 21-25.
34. Tang, Y. L.; Hill, E. H.; Zhou, Z. J.; Evans, D. G.; Schanze, K. S.; Whitten, D. G., Synthesis, Self-Assembly, and Photophysical Properties of Cationic Oligo(p-phenyleneethynylene)s. *Langmuir* **2011**, *27* (8), 4945-4955.
35. Ilker, M. F.; Nusslein, K.; Tew, G. N.; Coughlin, E. B., Tuning the hemolytic and antibacterial activities of amphiphilic polynorbornene derivatives. *J. Am. Chem. Soc.* **2004**, *126* (48), 15870-15875.
36. Kuroda, K.; DeGrado, W. F., Amphiphilic polymethacrylate derivatives as antimicrobial agents. *J. Am. Chem. Soc.* **2005**, *127* (12), 4128-4129.
37. Ikeda, T.; Yamaguchi, H.; Tazuke, S., New Polymeric Biocides - Synthesis and Antibacterial Activities of Polycations with Pendant Biguanide Groups. *Antimicrob. Agents Chemother.* **1984**, *26* (2), 139-144.
38. Zhang, Y. M.; Jiang, J. M.; Chen, Y. M., Synthesis and antimicrobial activity of polymeric guanidine and biguanidine salts. *Polymer* **1999**, *40* (22), 6189-6198.
39. Feiertag, P.; Albert, M.; Ecker-Eckhofen, E. M.; Hayn, G.; Honig, H.; Oberwalder, H. W.; Saf, R.; Schmidt, A.; Schmidt, O.; Topchiev, D., Structural characterization of biocidal oligoguanidines. *Macromol. Rapid Commun.* **2003**, *24* (9), 567-570.
40. Dizman, B.; Elasri, M. O.; Mathias, L. J., Synthesis and antimicrobial activities of new water-soluble bis-quaternary ammonium methacrylate polymers. *J. Appl. Polym. Sci.* **2004**, *94* (2), 635-642.
41. Gabriel, G. J.; Som, A.; Madkour, A. E.; Eren, T.; Tew, G. N., Infectious disease: Connecting innate immunity to biocidal polymers. *Mater. Sci. Eng. R-Rep.* **2007**, *57* (1-6), 28-64.
42. Lu, L. D.; Rininsland, F. H.; Wittenburg, S. K.; Achyuthan, K. E.; McBranch, D. W.; Whitten, D. G., Biocidal activity of a light-absorbing fluorescent conjugated polyelectrolyte. *Langmuir* **2005**, *21* (22), 10154-10159.
43. Ogawa, K.; Chemburu, S.; Lopez, G. P.; Whitten, D. G.; Schanze, K. S., Conjugated polyelectrolyte-grafted silica microspheres. *Langmuir* **2007**, *23* (8), 4541-4548.
44. Chemburu, S.; Corbitt, T. S.; Ista, L. K.; Ji, E.; Fulghum, J.; Lopez, G. P.; Ogawa, K.; Schanze, K. S.; Whitten, D. G., Light-induced biocidal action of conjugated polyelectrolytes supported on colloids. *Langmuir* **2008**, *24* (19), 11053-11062.
45. Corbitt, T. S.; Sommer, J. R.; Chemburu, S.; Ogawa, K.; Ista, L. K.; Lopez, G. P.; Whitten, D. G.; Schanze, K. S., Conjugated Polyelectrolyte Capsules: Light-

- Activated Antimicrobial Micro "Roach Motels". *ACS Appl. Mater. Interfaces* **2009**, *1* (1), 48-52.
46. Corbitt, T. S.; Ding, L. P.; Ji, E. Y.; Ista, L. K.; Ogawa, K.; Lopez, G. P.; Schanze, K. S.; Whitten, D. G., Light and dark biocidal activity of cationic poly(arylene ethynylene) conjugated polyelectrolytes. *Photochem. Photobiol. Sci.* **2009**, *8* (7), 998-1005.
47. Ding, L. P.; Chi, E. Y.; Chemburu, S.; Ji, E.; Schanze, K. S.; Lopez, G. P.; Whitten, D. G., Insight into the Mechanism of Antimicrobial Poly(phenylene ethynylene) Polyelectrolytes: Interactions with Phosphatidylglycerol Lipid Membranes. *Langmuir* **2009**, *25* (24), 13742-13751.
48. Ding, L. P.; Chi, E. Y.; Schanze, K. S.; Lopez, G. P.; Whitten, D. G., Insight into the Mechanism of Antimicrobial Conjugated Polyelectrolytes: Lipid Headgroup Charge and Membrane Fluidity Effects. *Langmuir* **2010**, *26* (8), 5544-5550.
49. Tang, Y. L.; Achyuthan, K. E.; Whitten, D. G., Label-free and Real-Time Sequence Specific DNA Detection Based on Supramolecular Self-assembly. *Langmuir* **2010**, *26* (9), 6832-6837.
50. Wang, Y.; Tang, Y. L.; Zhou, Z. J.; Ji, E.; Lopez, G. P.; Chi, E. Y.; Schanze, K. S.; Whitten, D. G., Membrane Perturbation Activity of Cationic Phenylene Ethynylene Oligomers and Polymers: Selectivity against Model Bacterial and Mammalian Membranes. *Langmuir* **2010**, *26* (15), 12509-12514.
51. Ji, E.; Whitten, D. G.; Schanze, K. S., pH-Dependent Optical Properties of a Poly(phenylene ethynylene) Conjugated Polyampholyte. *Langmuir* **2011**, *27* (5), 1565-1568.
52. Tang, Y. L.; Corbitt, T. S.; Parthasarathy, A.; Zhou, Z. J.; Schanze, K. S.; Whitten, D. G., Light-Induced Antibacterial Activity of Symmetrical and Asymmetrical Oligophenylene Ethynylenes. *Langmuir* **2011**, *27* (8), 4956-4962.
53. Corbitt, T. S.; Zhou, Z. J.; Tang, Y. L.; Graves, S. W.; Whitten, D. G., Rapid Evaluation of the Antibacterial Activity of Arylene-Ethynylene Compounds. *ACS Appl. Mater. Interfaces* **2011**, *3* (8), 2938-2943.
54. Ji, E. K.; Parthasarathy, A.; Corbitt, T. S.; Schanze, K. S.; Whitten, D. G., Antibacterial Activity of Conjugated Polyelectrolytes with Variable Chain Lengths. *Langmuir* **2011**, *27* (17), 10763-10769.
55. Wang, Y.; Jones, E. M.; Tang, Y. L.; Ji, E. K.; Lopez, G. P.; Chi, E. Y.; Schanze, K. S.; Whitten, D. G., Effect of Polymer Chain Length on Membrane Perturbation Activity of Cationic Phenylene Ethynylene Oligomers and Polymers. *Langmuir* **2011**, *27* (17), 10770-10775.
56. Wang, Y.; Canady, T. D.; Zhou, Z. J.; Tang, Y. L.; Price, D. N.; Bear, D. G.; Chi, E. Y.; Schanze, K. S.; Whitten, D. G., Cationic Phenylene Ethynylene Polymers and Oligomers Exhibit Efficient Antiviral Activity. *ACS Appl. Mater. Interfaces* **2011**, *3* (7), 2209-2214.
57. Ista, L. K.; Dascier, D.; Ji, E.; Parthasarathy, A.; Corbitt, T. S.; Schanze, K. S.; Whitten, D. G., Conjugated-Polyelectrolyte-Grafted Cotton Fibers Act as "Micro Flypaper" for the Removal and Destruction of Bacteria. *ACS Appl. Mater. Interfaces* **2011**, *3* (8), 2932-2937.

58. Wang, Y.; Corbitt, T. S.; Jett, S. D.; Tang, Y. L.; Schanze, K. S.; Chi, E. Y.; Whitten, D. G., Direct Visualization of Bactericidal Action of Cationic Conjugated Polyelectrolytes and Oligomers. *Langmuir* **2012**, *28* (1), 65-70.
59. Ji, E.; Corbitt, T. S.; Parthasarathy, A.; Schanzes, K. S.; Whitten, D. G., Light and Dark-Activated Biocidal Activity of Conjugated Polyelectrolytes. *ACS Appl. Mater. Interfaces* **2011**, *3* (8), 2820-2829.
60. Pooler, J. P.; Valenzeno, D. P., Dye-sensitized photodynamic inactivation of cells. *Med. Phys.* **1981**, *8* (5), 614-628.
61. Valenzeno, D. P.; Pooler, J. P., Cell-membrane photo-modification - relative effectiveness of halogenated fluoresceins for photo-hemolysis. *Photochem. Photobiol.* **1982**, *35* (3), 343-350.
62. Lamberts, J. J. M.; Schumacher, D. R.; Neckers, D. C., Novel rose-bengal derivatives - synthesis and quantum yield studies. *J. Am. Chem. Soc.* **1984**, *106* (20), 5879-5883.
63. ISO, 10993 Biological evaluation of medical devices. In *Parts 1-20*.
64. Freshney, R. I., *Culture of animal cells: a manual of basic techniques*. 5th ed.; John Wiley & Sons, Inc.: Hoboken, New Jersey, 2005.
65. Bodnar, A. G.; Ouellette, M.; Frolkis, M.; Holt, S. E.; Chiu, C. P.; Morin, G. B.; Harley, C. B.; Shay, J. W.; Lichtsteiner, S.; Wright, W. E., Extension of life-span by introduction of telomerase into normal human cells. *Science* **1998**, *279* (5349), 349-352.
66. ISO, 10993 Biological evaluation of medical devices. In *Part 5: Tests for in vitro cytotoxicity*, 2009; pp 1-34.
67. Mosmann, T., Rapid colorimetric assay for cellular growth and survival - application to proliferation and cyto-toxicity assays. *J. Immunol. Methods* **1983**, *65* (1-2), 55-63.
68. Scudiero, D. A.; Shoemaker, R. H.; Paull, K. D.; Monks, A.; Tierney, S.; Nofziger, T. H.; Currens, M. J.; Seniff, D.; Boyd, M. R., Evaluation of a soluble tetrazolium/formazan assay for cell growth and drug sensitivity in culture using human and other tumor cell lines. *Cancer Res.* **1988**, *48* (17), 4827-4833.
69. Borenfreund, E.; Puerner, J. A., Toxicity determined *in vitro* by morphological alterations and neutral red absorption. *Toxicol. Lett.* **1985**, *24* (2-3), 119-124.
70. ISO, 10993 Biological evaluation of medical devices. In *Part 10: Tests for irritation and skin sensitization*, 2010.
71. Lilienblum, W.; Dekant, W.; Foth, H.; Gebel, T.; Hengstler, J. G.; Kahl, R.; Kramer, P. J.; Schweinfurth, H.; Wollin, K. M., Alternative methods to safety studies in experimental animals: role in the risk assessment of chemicals under the new European Chemicals Legislation (REACH). *Arch. Toxicol.* **2008**, *82* (4), 211-236.
72. Vinardell, M. P.; Mitjans, M., Alternative methods for eye and skin irritation tests: An overview. *J. Pharm. Sci.* **2008**, *97* (1), 46-59.
73. Spielmann, H.; Hoffmann, S.; Liebsch, M.; Botham, P.; Fentem, J. H.; Eskes, C.; Roguet, R.; Cotovio, J.; Cole, T.; Worth, A.; Heylings, J.; Jones, P.; Robles, C.; Kandarova, H.; Gamer, A.; Remmele, M.; Curren, R.; Raabe, H.; Cockshott, A.; Gerner, I.; Zuang, V., The ECVAM international validation study on *in vitro* tests for acute skin irritation: Report on the validity of the EPISKIN

- and EpiDerm assays and on the Skin Integrity Function Test. *ATLA-Altern. Lab. Anim.* **2007**, 35 (6), 559-601.
74. MatTek Corporation *In Vitro Skin Corrosion: Human Skin Model Test*; Ashland, MA, January 15, 2009, pp 1-31.
 75. MatTek Corporation *Protocol for: In Vitro EpiDerm Skin Irritation Test (EPI-200-SIT)*; Ashland, MA, March 25, 2010, pp 1-37.
 76. Kandarova, H.; Hayden, P.; Klausner, M.; Kubilus, J.; Sheasgreen, J., An In Vitro Skin Irritation Test (SIT) using the EpiDerm Reconstructed Human Epidermal (RHE) Model. *J Vis Exp* **2009**, (29), e1366.
 77. MatTek Corporation *MTT Effective Time-50 (ET-50) Protocol*; Ashland, MA, April 14, 2009, pp 1-5.
 78. MatTek Corporation *Phototoxicity Protocol*; Ashland, MA, November 5, 1997, pp 1-22.
 79. MatTek Corporation *Systemic Phototoxicity Protocol*; Ashland, MA, March 1, 2006, pp 1-14.
 80. Wilde, K., Phone conversation and subsequent e-mail exchange regarding four MatTek protocols. ed.; Kubilus, J., Ed. Ashland, MA.
 81. Kubilus, J.; Macdonald, M. J.; Baden, H. P., Epidermal proteins of cultured human and bovine keratinocytes. *Biochimica Et Biophysica Acta* **1979**, 578 (2), 484-492.
 82. Kubilus, J.; Waitkus, R. W.; Baden, H. P., Presence of citrulline in epidermal proteins. *Biochimica Et Biophysica Acta* **1979**, 581 (1), 114-121.
 83. Kubilus, J.; Baden, H. P.; McGilvray, N., Filamentous protein of basal-cell epithelioma - characteristics in vivo and in vitro. *Journal of the National Cancer Institute* **1980**, 65 (5), 869-875.
 84. Kubilus, J.; Rand, R.; Baden, H. P., Effects of retinoic acid and other retinoids on the growth and differentiation of 3T3 supported human keratinocytes. *In Vitro-Journal of the Tissue Culture Association* **1981**, 17 (9), 786-795.
 85. Baden, H. P.; Kubilus, J.; Macdonald, M. J., Normal and psoriatic keratinocytes and fibroblasts compared in culture. *Journal of Investigative Dermatology* **1981**, 76 (1), 53-55.
 86. Kubilus, J.; Baden, H. P., Isolation of 2 immunologically related transglutaminase substrates from cultured human keratinocytes. *In Vitro-Journal of the Tissue Culture Association* **1982**, 18 (5), 447-455.
 87. Baden, H. P.; Kubilus, J., Effect of minoxidil on cultured keratinocytes. *Journal of Investigative Dermatology* **1983**, 81 (6), 558-560.
 88. Kubilus, J.; Baden, H. P., Isopeptide bond formation in epidermis. *Molecular and Cellular Biochemistry* **1984**, 58 (1-2), 129-137.
 89. Kubilus, J.; Kvedar, J. C.; Baden, H. P., Effect of minoxidil on preconfluent and postconfluent keratinocytes. *Journal of the American Academy of Dermatology* **1987**, 16 (3), 648-652.
 90. Kubilus, J.; Kvedar, J.; Baden, H. P., Identification of new components of the cornified envelope of human and bovine epidermis. *Journal of Investigative Dermatology* **1987**, 89 (1), 44-50.
 91. Kandarova, H.; Hayden, P.; Klausner, M.; Kubilus, J.; Kearney, P.; Sheasgreen, J., In Vitro Skin Irritation Testing: Improving the Sensitivity of the

- EpiDerm Skin Irritation Test Protocol. *ATLA-Altern. Lab. Anim.* **2009**, *37* (6), 671-689.
92. Gibbs, S., In vitro Irritation Models and Immune Reactions. *Skin Pharmacol. Physiol.* **2009**, *22* (2), 103-113.
 93. Welss, T.; Basketter, D. A.; Schroder, K. R., In vitro skin irritation: facts and future. State of the art review of mechanisms and models. *Toxicol. Vitro* **2004**, *18* (3), 231-243.
 94. Cicotte, K. N.; Hedberg-Dirk, E. L.; Dirk, S. M., Synthesis and Electrospun Fiber Mats of Low T(g) Poly(propylene fumarate-co-propylene maleate). *J. Appl. Polym. Sci.* **2010**, *117* (4), 1984-1991.
 95. Cayman Chemical Company, Interleukin-1alpha (human) EIA kit, Item No. 583301. **2011**.
 96. MatTek Corporation, Interleukin-1alpha Assay Protocol, For use with EpiDerm Toxicology Kit (EPI-200). **2006**.
 97. Alberts, B.; Johnson, A.; Lewis, J.; Raff, M.; Roberts, K.; Walter, P., *Molecular Biology of the Cell*. 5th ed.; Garland Science: New York, 2008.
 98. Life Technologies The Molecular Probes Handbook, Probes for Organelles - Chapter 12.
<http://www.invitrogen.com/site/us/en/home/References/Molecular-Probes-The-Handbook/Probes-for-Organelles.html> (accessed April 24, 2012).
 99. Matsuzaki, K., Control of cell selectivity of antimicrobial peptides. *Biochim. Biophys. Acta-Biomembr.* **2009**, *1788* (8), 1687-1692.
 100. Mason, A. J.; Moussaoui, W.; Abdelrahman, T.; Boukhari, A.; Bertani, P.; Marquette, A.; Shooshtarizadeh, P.; Moulay, G.; Boehm, N.; Guerold, B.; Sawers, R. J. H.; Kichler, A.; Metz-Boutigue, M. H.; Candolfi, E.; Prevost, G.; Bechinger, B., Structural Determinants of Antimicrobial and Antiplasmodial Activity and Selectivity in Histidine-rich Amphipathic Cationic Peptides. *J. Biol. Chem.* **2009**, *284* (1), 119-133.
 101. Won, H. S.; Kang, S. J.; Lee, B. J., Action mechanism and structural requirements of the antimicrobial peptides, gaegurins. *Biochim. Biophys. Acta-Biomembr.* **2009**, *1788* (8), 1620-1629.
 102. Takahashi, D.; Shukla, S. K.; Prakash, O.; Zhang, G. L., Structural determinants of host defense peptides for antimicrobial activity and target cell selectivity. *Biochimie* **2010**, *92* (9), 1236-1241.
 103. Lindgren, M.; Hallbrink, M.; Prochiantz, A.; Langel, U., Cell-penetrating peptides. *Trends Pharmacol. Sci.* **2000**, *21* (3), 99-103.
 104. Splith, K.; Neundorff, I., Antimicrobial peptides with cell-penetrating peptide properties and vice versa. *Eur. Biophys. J. Biophys. Lett.* **2011**, *40* (4), 387-397.
 105. Milletti, F., Cell-penetrating peptides: classes, origin, and current landscape. *Drug Discov. Today* (doi:10.1016/j.drudis.2012.03.002).
 106. Mason, J. M., Design and development of peptides and peptide mimetics as antagonists for therapeutic intervention. *Future Med. Chem.* **2010**, *2* (12), 1813-1822.
 107. Goda, T.; Goto, Y.; Ishihara, K., Cell-penetrating macromolecules: Direct penetration of amphipathic phospholipid polymers across plasma membrane of living cells. *Biomaterials* **2010**, *31* (8), 2380-2387.

108. Invitrogen Corp., The Handbook: A Guide to Fluorescent Probes and Labeling Technologies, Tenth Edition. **2005**, 589.
109. Molecular Probes Product Information, ER-Tracker Dyes for Live-Cell Endoplasmic Reticulum Labeling.
<http://probes.invitrogen.com/media/pis/mp12353.pdf>.
110. Vives, E.; Schmidt, J.; Pelegrin, A., Cell-penetrating and cell-targeting peptides in drug delivery. *Biochim. Biophys. Acta-Rev. Cancer* **2008**, 1786 (2), 126-138.
111. Tarrago-Trani, M. T.; Storrie, B., Alternate routes for drug delivery to the cell interior: Pathways to the Golgi apparatus and endoplasmic reticulum. *Adv. Drug Deliv. Rev.* **2007**, 59 (8), 782-797.
112. Zorko, M.; Langel, U., Cell-penetrating peptides: mechanism and kinetics of cargo delivery. *Adv. Drug Deliv. Rev.* **2005**, 57 (4), 529-545.
113. Corbitt, T. S. Antibacterial Activity of Conjugated Electrolytes. University of New Mexico, Albuquerque, New Mexico, 2010.
114. Melo, M. N.; Ferre, R.; Castanho, M., OPINION Antimicrobial peptides: linking partition, activity and high membrane-bound concentrations. *Nat. Rev. Microbiol.* **2009**, 7 (3), 245-250.
115. Spielmann, H.; Lovell, W. W.; Holzle, E.; Johnson, B. E.; Maurer, T.; Miranda, M. A.; Pape, W. J. W.; Sapor, O.; Sladowski, D., In Vitro Phototoxicity Testing - The Report and Recommendations of ECVAM Workshop 2. *ATLA-Altern. Lab. Anim.* **1994**, 22 (5), 314-348.
116. Kleinman, M. H.; Smith, M. D.; Kurali, E.; Kleinpeter, S.; Jiang, K. N.; Zhang, Y. X.; Kennedy-Gabb, S. A.; Lynch, A. M.; Geddes, C. D., An evaluation of chemical photoreactivity and the relationship to phototoxicity. *Regul. Toxicol. Pharmacol.* **2010**, 58 (2), 224-232.
117. Kejlova, K.; Jirova, D.; Bendova, H.; Gajdos, P.; Kolarova, H., Phototoxicity of essential oils intended for cosmetic use. *Toxicol. Vitro* **2010**, 24 (8), 2084-2089.
118. OECD, OECD Guidelines for the Testing of Chemicals Test No. 432: In Vitro 3T3 NRU Phototoxicity Test. Paris, France, 2004.
119. MatTek Corporation <http://www.mattek.com/pages/products/> (accessed March 14, 2012).
120. Macfarlane, M.; Jones, P.; Goebel, C.; Dufour, E.; Rowland, J.; Araki, D.; Costabel-Farkas, M.; Hewitt, N. J.; Hibatallah, J.; Kirst, A.; McNamee, P.; Schellauf, F.; Scheel, J., A tiered approach to the use of alternatives to animal testing for the safety assessment of cosmetics: Skin irritation. *Regul. Toxicol. Pharmacol.* **2009**, 54 (2), 188-196.
121. Knight, A., Non-animal methodologies within biomedical research and toxicity testing. *Altex Altern. Tierexp.* **2008**, 25 (3), 213-231.
122. Russell, A. D., Mechanisms of bacterial insusceptibility to biocides. *Am. J. Infect. Control* **2001**, 29 (4), 259-261.
123. Cloete, T. E., Resistance mechanisms of bacteria to antimicrobial compounds. *Int. Biodeterior. Biodegrad.* **2003**, 51 (4), 277-282.
124. Dascier, D.; Ji, E., Group meeting presentation of biocide testing against biofilms, measuring MIC and MBEC using XTT assays. 2011.

125. Tumah, H. N., Bacterial Biocide Resistance. *J. Chemother.* **2009**, *21* (1), 5-15.
126. Bay, D. C.; Rommens, K. L.; Turner, R. J., Small multidrug resistance proteins: A multidrug transporter family that continues to grow. *Biochim. Biophys. Acta-Biomembr.* **2008**, *1778* (9), 1814-1838.
127. Papo, N.; Shai, Y., Host defense peptides as new weapons in cancer treatment. *Cell. Mol. Life Sci.* **2005**, *62* (7-8), 784-790.
128. Mader, J. S.; Hoskin, D. W., Cationic antimicrobial peptides as novel cytotoxic agents for cancer treatment. *Expert Opin. Investig. Drugs* **2006**, *15* (8), 933-946.
129. Hoskin, D. W.; Ramamoorthy, A., Studies on anticancer activities of antimicrobial peptides. *Biochim. Biophys. Acta-Biomembr.* **2008**, *1778* (2), 357-375.
130. Schweizer, F., Cationic amphiphilic peptides with cancer-selective toxicity. *Eur. J. Pharmacol.* **2009**, *625* (1-3), 190-194.
131. Lee, H. S.; Park, C. B.; Kim, J. M.; Jang, S. A.; Park, I. Y.; Kim, M. S.; Cho, J. H.; Kim, S. C., Mechanism of anticancer activity of buforin IIb, a histone H2A-derived peptide. *Cancer Lett.* **2008**, *271* (1), 47-55.
132. NCI/NIH, D. T. P. NCI-60 DTP Human Tumor Cell Line Screen. <http://dtp.nci.nih.gov/branches/btb/ivclsp.html> (accessed May 2, 2012).
133. Li, Y. C.; Park, M. J.; Ye, S. K.; Kim, C. W.; Kim, Y. N., Elevated levels of cholesterol-rich lipid rafts in cancer cells are correlated with apoptosis sensitivity induced by cholesterol-depleting agents. *Am. J. Pathol.* **2006**, *168* (4), 1107-1118.
134. Rutala, W. A.; Weber, D. J., Disinfection and sterilization in health care facilities: What clinicians need to know. *Clin. Infect. Dis.* **2004**, *39* (5), 702-709.
135. Weber, D. J.; Rutala, W. A.; Sickbert-Bennett, E. E., Outbreaks associated with contaminated antiseptics and disinfectants. *Antimicrob. Agents Chemother.* **2007**, *51* (12), 4217-4224.
136. Maillard, J. Y., Bacterial target sites for biocide action. *J. Appl. Microbiol.* **2002**, *92*, 16S-27S.
137. Woodruff, M. A.; Hutmacher, D. W., The return of a forgotten polymer-Polycaprolactone in the 21st century. *Prog. Polym. Sci.* **2010**, *35* (10), 1217-1256.